THE DESIGN OF A ROTARY COAXIAL CYLINDERS MEMBRANE BLOOD OXYGENATOR

by

THOMAS ALFRED RUESS

Thesis Submitted for the Degree of

Doctor of Philosophy.

University of Edinburgh

March 1975.

Dedicated to my Parents

Gerhard and Gertrud Ruess.

Acknowledgements

I would like to thank Dr. Norman Macleod for his guidance, help and encouragement throughout this research program, as well as for many helpful discussions about areas of engineering not directly related to this project.

I am also indebted to Professor D.G. Melrose of the Royal Postgraduate Medical School, London, for his useful comments on the state of development of oxygenators.

Thanks are also due to Mr. D. Ketchin and the staff of the Chemical Engineering workshop, in particular Mr. K. Fee and Mr. W. Young who built the experimental apparatus.

I am grateful to Mr. Riahd Mirza for drawing the figures appearing in this thesis, and to Mrs. Jane Gorrie for typing the manuscript.

Finally, I would like to thank the University of Edinburgh for financial support during the academic years 1972-73 and 1973-74, in the form of an Edinburgh University Postgraduate Studentship.

Table of Contents

Page

Appendices

Page

Appendix 4

SUMMARY

The present work reviews the development of oxygenators, in particular membrane oxygenators which are accepted as being less traumatic to blood than direct blood-gas interface "lungs". Most existing membrane oxygenators require large mass transfer areas to ensure sufficient arterialization of blood, due to the resistance to oxygen uptake in the concentration boundary layer in blood, where the fluid is essentially in laminar flow.

To improve the rate of oxygen uptake by blood, and thus to reduce the area of contact of blood with noncompatible materials, a gentle form of blood mixing is required. Such a regular, controllable pattern of blood mixing can be obtained when blood flows in the annulus between two coaxial cylinders, where the inner cylinder rotates above a certain critical speed. The resulting hydrodynamic instability is expressed in the formation of regular laminar vortices which substantially enhance the rate of mass transfer.

Since the blood-oxygen system is characterized by a Sc number several orders of magnitude greater than that for previously studied systems, it was decided to measure the overall rates of mass transfer from the surfaces of rotating and stationary concentric cylinders to an axial stream of water in laminar + vortex flow in the annulus. The system chosen was the elution of ethyl salicylate from coatings of silicone rubber applied to one or both surfaces, and initially swollen to equilibrium with the ester. The transfer rate was then measured by ultraviolet absorption of the effluent liquid. The physical data required to present the data in dimensionless form were also determined and the limitations of the experimental technique were investigated.

The influence of rotor speed on transfer rate from either surface was found to be significantly greater in this system (Sc = 1260), than in previous dynamically similar experiments with air at much lower Sc numbers (≃ 2). The axial flow rate was found to have little effect over the axial Reynolds number range studied; it therefore appears legitimate to compare the present results with available data on transfer from rotating cylinders into a stagnant fluid with similar high Sc numbers. The influence of rotor speed on mass transfer rate was found to be the same in both cases; furthermore, the correlation previously reported for mass transfer to a stagnant fluid fits closely the absolute values of the present experimental mass transfer data.

The blood oxygenator design was then optimized, using the available mass transfer correlation and some design guidelines and limitations, and a working prototype blood oxygenator was built to this design.

The estimated mass transfer characteristics of the oxygenator were tested by oxygenating water and sucrose solutions over a Sc range of 419-1962. The incorporation of a thin longitudinal strip into the rotor surface, protruding slightly into the annular gap, was found to greatly enhance the mass transfer rate from the rotor, particularly at low rotor velocity; mass transfer rates up to 50 per cent higher than those predicted from the design mass transfer correlation were obtained. These findings were confirmed by adding a similar thin longitudinal rib to the rotor of the ester apparatus used in the preliminary experiments. Further experiments in which blood was oxygenated, were in general agreement with the experiments with the oxygen-water system in the same apparatus, and up to the oxygen transfer rates studied (≃ 150 cc/min m^2), the rate of oxygen uptake by blood increased with rotor speed.

These results are of great significance for the construction of a rotary coaxial cylinders membrane blood oxygenator, in that they show:

a) that blood oxygenation rate follows the physical mass transfer rate over the range of conditions studied; and

b) that the physical mass transfer rate can be significantly increased in a coaxial cylinders oxygenator by adding longitudinal "ribs" of smooth outline to the rotor.

High rates of oxygen uptake can therefore be obtained at lower rotor speeds than hereto considered; with the reduction of rotor velocity, operational and mechanical difficulties are lessened, and possibly there would also be decreased blood trauma.

List of Figures Page

Page

Page

Nomenclature

A - Mass transfer area.

a - Width of parallel plates.

A_N - Crossectional area of annulus.

A_R - Effective mass transfer area.

b - Annular gap or spacing between parallel plates.

Ci - Inlet concentration.

Co - Outlet concentration.

Cs - Concentration at saturation.

D_{AB} - Diffusion coefficient.

D_R - Diffusivity in the rubber phase.

dh - Hydraulic diameter.

f_1 - A function of χ and ϕ.

Fs - Mass flux.

G - Torque.

H - Hematocrit.

h_D - Mass transfer coefficient.

L - Length of transfer area.

OT - Oxygen transfer rate.

P - Pressure.

PM - Membrane permeability.

Q - Volumetric flow rate.

Ri - Inner radius of annulus.

Ro - Outer radius of annulus.

RPM - Revolutions per minute.

T' - "Constant Rate" period.

V_S - Volume of swelling agent.

V_Z - Axial velocity.

V_ϕ - Azimuthal velocity.

Z - Length of parallel plates or tubes.

δ - Membrane thickness.

δ_1 - Initial thickness of swollen coating.

δ' - Thickness of polymer coating.

μ - Viscosity.

ν - Kinematic viscosity.

ρ - Density.

ϕ - Volume fraction of swelling agent in rubber.

T - Shear stress.

χ - Constant for polymer-swelling agent system.

Re_z - Axial Reynolds number.

$Re\phi$ - Azimuthal Reynolds number.

Sc - Schmidt number.

Sh - Sherwood number.

Ta - Taylor number.

CHAPTER 1

1.1 Introduction

Artificial oxygenators find applications when it is necessary to bypass the heart and lungs during open-chest surgery. They are used, for instance, during valve replacement, vein grafts, and repairs of defects in the cardiovascular system. Furthermore, the superior and improving reliability and blood-handling characteristics of membrane oxygenators in particular, is allowing their introduction into the areas of total and partial long-term respiratory support; for example, in the case of cardiac or respiratory failure, pneumonia, and embolism. As a research tool there are applications for the relatively atraumatic membrane oxygenators in the perfusion and preservation of isolated organs, in regional perfusion in chemotherapy, and in studies of aenesthesia and blood oxygen uptake.

In open-heart surgery, blood bypasses the cardiovascular system, providing the surgeon with a dry, bloodless operating field; the duties of the heart and the lungs are then carried out in an extra-corporeal circuit. The oxygenator replaces or supports the lungs, supplying the body with the oxygen necessary to support the metabolic functions, and remove the main metabolic product, carbon dioxide.

In the earliest attempts at artificial oxygenation, blood was exposed directly to the gas phase, either by bubbling O_2 through blood in an appropriate chamber, or by exposing a thin film of blood directly to oxygen. These oxygenators, though still widely used for short-term surgical applications, introduce the risk of air embolism and have been proved to be traumatic to blood in long-term perfusions. Attempts have therefore been made over a considerable

period to overcome these problems by interposing a thin permeable membrane, in a system analogous to the lungs, between the blood and gas phases.

Despite the additional resistance of the membrane, and the necessarily greater complexity, such arrangements have, as well as the prospect of relatively atraumatic operation, the additional advantage that the blood volume in the closed system is more nearly constant than in an open blood-gas interface oxygenator.

Recently, it has been shown that membrane oxygenation can give significantly reduced blood trauma, including decreased hemolysis (1) and reduced plasma protein denaturation, as demonstrated by the work of Lee et al. (2). The chemical and physical reasons for plasma protein denaturation at the blood-gas interface are not fully understood, nevertheless, it does seem to be clear that the complications arising from long-term use of oxygenators with such interfaces, namely, the release of lipids, and the formation of cell and denatured protein aggregates, with the considerable risk of embolism, are considerably less marked when membrane oxygenators are used (3).

The most widely accepted hypothesis proposes that the main difference between blood-gas interfaces, and blood-solid (membrane) interfaces, as present in oxygenators, lies essentially in the mechanical instability of the former. Plasma proteins are denatured at the interface and continuously mixed back into the blood bulk, while undamaged protein is presented at the interface (4,5). At the blood-solid interface, a layer of protein is quickly absorbed at the interface (7,6,8) and removed from the blood bulk. Furthermore, the absorbed protein forms a protective coating preventing further damage

to protein reaching the interface. Consequently, blood-gas interface oxygenators are suitable only for perfusions lasting a limited time, currently believed to be about two hours (9). Beyond this period of time, the cumulative blood trauma becomes potentially dangerous. This implies that developments in long-term bypass or cardiopulmonary support are subject to the availability of a practical membrane blood oxygenator.

1.2. Blood

Blood can be described as a suspension of cells in a dense fluid medium, plasma. Blood acts as a communications path to the body tissues, supplying them with oxygen and food, and removing the waste products. The latter are subsequently removed through the lungs (CO_2) and kidneys.

Plasma itself carries the dissolved minerals necessary to the tissues, as well as dissolved proteins having various functions. For example, the protein fibrin plays an important part in blood clotting and therefore, wound healing.

There are three types of blood cells (10); red blood cells or erythrocytes, white blood cells or leukocytes, and platelets or thrombocytes. The red blood cells are the principal oxygen carrying agents; these are biconcave disks 7μ in diameter, enclosing within a membrane the iron-based porphyrin, hemoglobin.

The oxygen-hemoglobin reaction to form oxyhemoglobin.

$$Hb + O_2 \rightleftharpoons HbO_2$$

is extremely fast, and it is in the form of oxyhemoglobin that approximately 99% of the body's oxygen requirement is carried. As blood enters the tissues, the equilibrium of the reaction is shifted to the left, and the blood gives up oxygen required by the metabolic processes.

Break-up or deformation of the red cell (hemolysis or sublethal damage) results in the removal of free hemoglobin, cell fragments, and deformed cells by the kidneys. The resulting loss of hemoglobin can lead to the condition of anemia.

Leukocytes are nucleated cells having an active metabolism, and are the main line of defence against sickness. Platelets are the smallest blood cells and are essential in the mechanism of blood clotting and wound healing.

Finally, blood can be considered to behave as a Newtonian fluid in extracorporeal circuits (11); nonetheless, non-Newtonian characteristics are displayed at very low shear rates ($<20\ sec^{-1}$), or in ducts where the erythrocyte diameter is significant compared with the duct diameter; for example, in the lung alveoli.

1.2.1. Blood-O_2 and Blood CO_2 Equilibria

The relationship between the partial pressure of oxygen dissolved in plasma, and the percent saturation of red cell hemoglobin, is given by the sigmoid oxyhemoglobin dissociation curve (Fig.1.1). At low plasma oxygen partial pressures, the percent hemoglobin saturation increases rapidly with oxygen tension up to values of 90% saturation and an approximate O_2 partial pressure of 80 mm Hg.

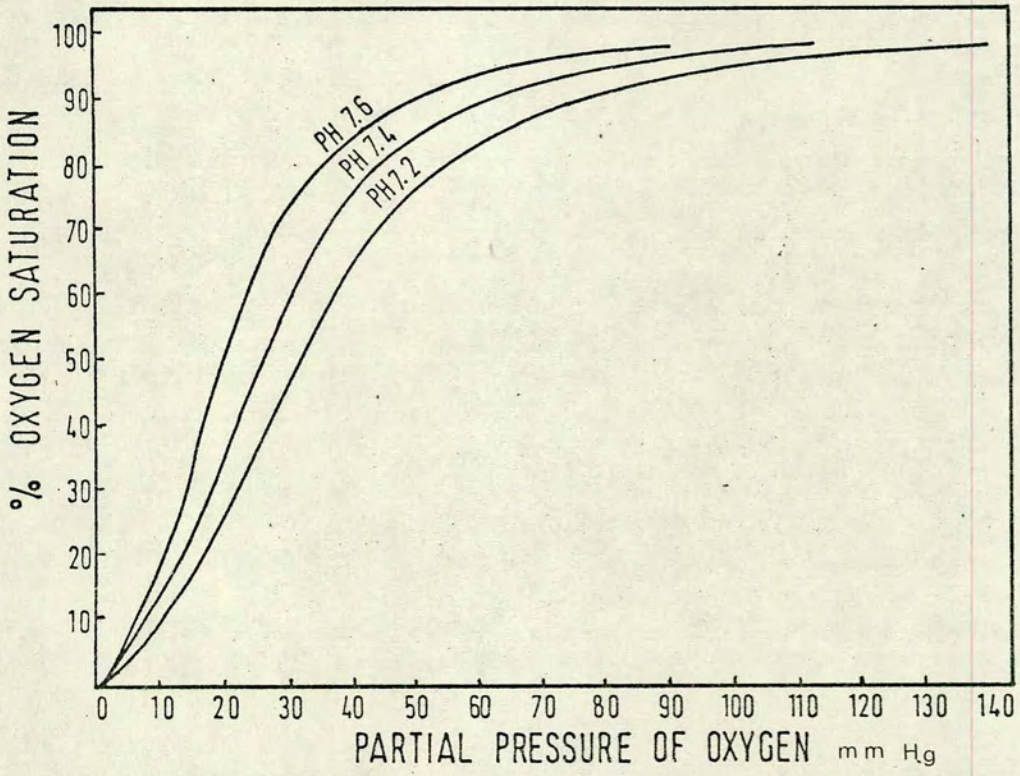

Fig. (1.1): Oxygen Dissociation Curve.

Afterwards, the slope of the curve flattens considerably, and blood hemoglobin becomes fully saturated when the plasma oxygen partial pressure exceeds 150 mm Hg. The shape of the oxyhemoglobin dissociation curve is of great importance physiologically, since the increasing difficulty in oxygenating hemoglobin above 95% saturation hinders excessive, and damaging oxygen supply to the body as a result of abnormally high oxygen tensions; similarly, the rapid rise in saturation values at low plasma oxygen tensions, ensures an adequate supply of oxygen to the tissues, despite low surrounding oxygen pressures.

For humans, the normal venous oxygen saturation level is 70% (40 mm Hg), while arterial blood is 95% saturated (90 mm Hg). Temperature, pH, CO_2 content, and ionic concentrations affect the shape of the equilibrium curve; an increase in temperature shifts the curve to the right, and oxygen is more readily released, for example, in the metabolically active, and therefore, warmer tissues. Decrease in pH has the same effect, and is partly due to increased CO_2 concentration. In fact, oxygen release to the tissues is facilitated by the high local concentration of the metabolic product CO_2; this leads to a decreased blood pH, and the formation of CO_2-hemoglobin compounds like carbamino hemoglobin, which have a decreased oxygen affinity. This process is reversed in the lungs, and as oxygenation proceeds, the curve representing the equilibrium between dissolved CO_2 partial pressure in plasma, and the chemically bound forms of CO_2 i.e. carbamino hemoglobin, bicarbonates and carbonic acid (Fig. 1.2), is shifted to the right, and the release of CO_2 is facilitated.

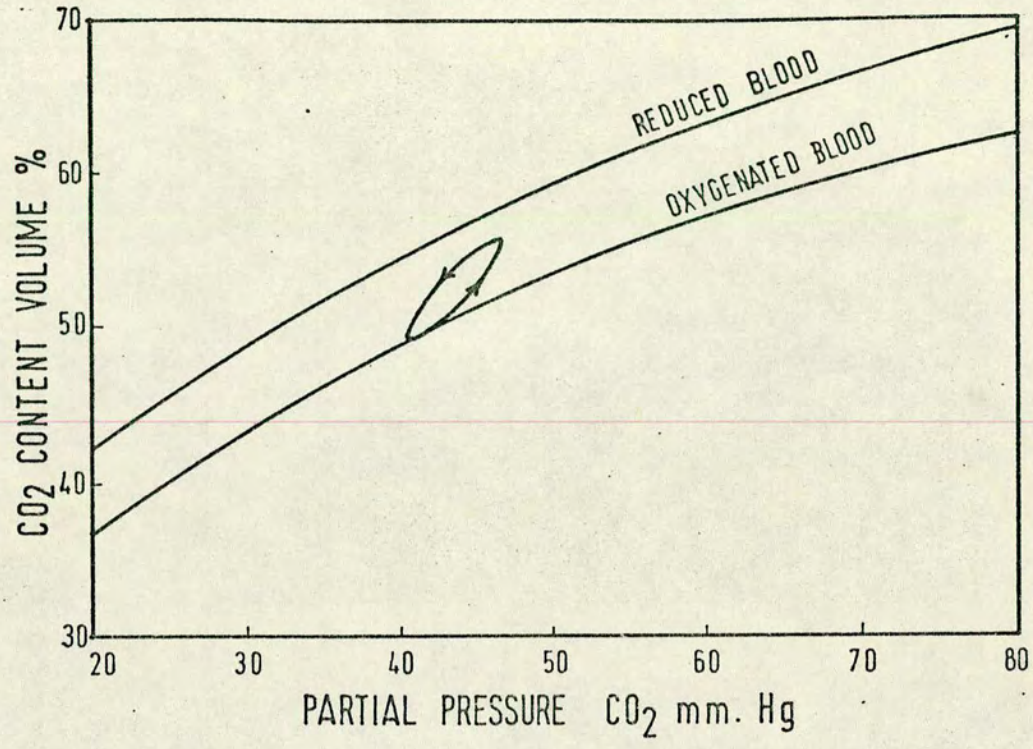

Fig.(1.2): Relationship Between the Partial Pressure of Dissolved CO_2 in Plasma and the Total CO_2 Content in Blood.

1.3. Design Requirements for a Membrane Oxygenator

A successful oxygenator has to meet the required a) O_2 duty, b) CO_2 duty, keeping c) blood trauma to a minimum. This last requirement is most easily met if d) the pressure drop across the oxygenator, e) the mass transfer area, and f) the surface to volume ratio are as small as possible. Furthermore,it is desirable to meet these requirements keeping g) priming volume, and h) overall dimensions minimal. Clinical acceptability depends strongly on i) a simple and reliable construction, ease of assembly and operation, and preferably, fully disposable blood-handling components. Finally, commercial acceptability depends partially on j) cost.

1.3.1. O_2 Duty

Extracorporeal circulation usually takes place with the body at rest under the conditions of general aenesthesia; therefore, the oxygen requirements approach those of the basal metabolic rate. The actual oxygen requirements and blood flow vary considerably from individual to individual, and can deviate considerably from average values; as a guide, a nomogram to estimate O_2 requirements as a function of body weight and size is reproduced in figure 1.3 (14). As a design parameter, the maximum likely oxygen requirement should be adopted, provided enough flexibility is incorporated into the design to handle lower requirements in a practical manner.

Keeping the maximum requirements in mind, it is desirable that a blood oxygenator will raise venous saturation levels of 70% to an arterial saturation of 95% for blood flowing at a rate of 5 litres/ minute (14). Human hematocrit (red cell volume fraction in whole blood)

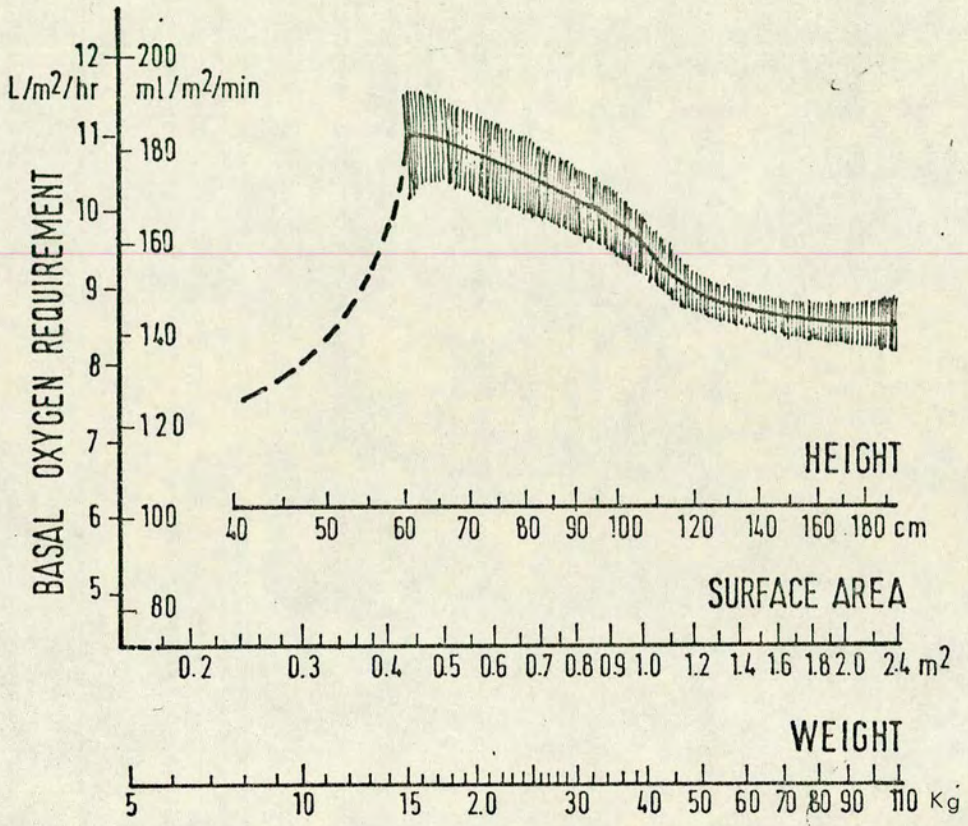

Fig.(1.3): Chart for Estimating the Basal Oxygen Requirement from the Body Surface Area in Man. The O_2 Requirements can be Estimated by Using the Surface Area, Height, and Weight Scales as a Nomogram.

levels seldom rise above 45% (15 gm Hb/100cc) (15), at which the oxygen carrying capacity of blood is 9.1 millimoles O_2 per litre, of this .15 millimoles are carried as dissolved O_2 in plasma. Therefore, it is necessary to supply 2.27 millimoles O_2 per litre - minute to raise from 70% to 95% the oxygen saturation level of blood, or 50cc O_2 STP/min-litre of blood. Consequently, a blood flow rate of 5 litres/min, would require the supply of 250 cc O_2 STP/min.

Since it is possible that in long term perfusions, O_2 requirements as well as flow rates may vary, it is desirable to be able to regulate oxygenation rate instantaneously, in this manner, the hazards connected with prolonged over, or under supply of oxygen could be avoided.

1.3.2. CO_2 Duty

Carbon dioxide is produced as a metabolic waste product and is carried by blood, either physically dissolved in plasma or bonded in the forms of carbonic acid, carbamino hemoglobin, and most important, as bicarbonates. In the lungs, carbon dioxide dissociates from the bicarbonates when the equilibrium of the reaction.

$$H_2O + CO_2 \rightleftarrows H^+ + HCO_3^-$$

is shifted to the left as blood oxygenation proceeds (Haldane Effect). This is caused by the greater acidity of oxyhemoglobin; therefore, it is undesirable to allow venous O_2 saturations to drift to low values as this makes CO_2 elimination more difficult.

Venous CO_2 partial pressure is usually about 50 mm Hg, while arterial CO_2 partial pressure is about 40 mm Hg (15). The partial pressure of carbon dioxide at the gas side of the membrane is usually zero, since pure oxygen at high flow rates (sweep gas) is used. As the design parameter, it is desirable to expel the molar equivalent of the oxygen transferred into the blood, using the available partial pressure driving force. Actually, this represents a somewhat high value for CO_2 transfer requirements, and is appropriate only when the respiratory quotient is 1; this value would be attained if only glucose were consumed. In a balanced diet the respiratory quotient CO_2/O_2 is only about 0.8, as the oxydation of fats and proteins produces fewer moles of CO_2 than moles O_2 burned (15).

Excessive CO_2 removal can easily be compensated by perfusing the membrane lung with 96%:4% - O_2:CO_2 mixture, thereby reducing the CO_2 pressure driving force. In membrane oxygenators, however, the problem is usually insufficient CO_2 elimination due to membrane resistance (Section 1.6.).

1.3.3. Blood Trauma

A certain amount of blood trauma cannot be avoided in extra-corporeal circuits; nevertheless, it should be kept within the limits at which its effects can be compensated by the capacity of the body to regenerate blood. Blood trauma can be categorized under these headings;

1) Damage to the formed elements of blood.
2) Plasma protein absorption and denaturation.
3) Clotting and thrombus formation.

There is a considerable evidence that these are interdependent to a large extent; for example, protein absorbed at a man-made surface offers positions of attachment to platelets and red blood cells if the local shear rate is too low, (16,17). Similarily, substances released from erythrocytes and platelets as a result of lysis, are prominent in the mechanism of clotting and thrombus formation (17,18).

Hemolysis (break-up of red cells) is the most easily and reliably measured kind of blood trauma. Blackshear (19) reviewed the literature on the subject and estimated the critical shear stress for hemolysis to be between 10^4-10^5 dynes/cm^2. Nevaril (20) gives the value of 3000 dynes/cm^2 for the threshold of subhemolytic damage, (deformation of the red cell) and 1500 dynes/cm^2 for bulk hemolytic damage; while Croce (21) gives a value of 1000 dynes/cm^2. Leverett (22) correlated critical shear stress values vs. time taking data from several workers and found that bulk hemolysis is essentially independent of time, although eventual shortened lifespan of the red blood cell is not taken into account (23). It may also be desirable to avoid low shear stresses in the neighbourhood of man-made surfaces (24,25); furthermore, hemolysis is strongly dependent on the nature of the surface and suitable materials must be used if blood trauma is to be minimized (26). Therefore, in order to reduce hemolysis, it is of advantage to use materials compatible with blood, and reduce the wall-cell interaction by reducing the surface to volume ratio (21).

Platelet damage, and their removal from the blood phase, occurs when they adhere to a foreign surface; platelet and cell aggregates are formed in regions of hemostasis and low shear rate. A good oxygenator design should therefore avoid such local regions of flow stagnation.

In an extracorporeal circuit blood trauma is strongly related to the pumping duty necessary to overcome the flow resistance in the circuit. This total flow resistance in the extracorporeal circuit, is in turn, the sum of the pressure drop across the individual elements of the circuit, e.g. heat exchangers, bubble trap, blood lines, and resistance in the return vessel.

The oxygenator represents the single most important resistance in the circuit; therefore, it is particularily desirable to reduce its head loss. Most extracorporeal circuits at present are designed to incorporate two pumps. The first overcomes the pressure loss in the oxygenator but no more, since high inlet blood pressures may damage the membrane or distend the blood passages. The arterial pump then overcomes the remaining resistances of the circuit and return vessel. If it were possible to do away altogether with the venous pump, relying on the hydrostatic head of the venous reservoir to drive blood through the oxygenator; there should be reduced blood trauma due to pumping, and possibly a reduced circuit priming volume. It is therefore desirable to limit the maximum pressure drop in the oxygenator. For design purposes a value of 50 mm Hg, although arbitrary, is realistic for an oxygenator with a good hemodynamic design.

In conclusion, blood trauma can be minimized if the following considerations are taken into account in designing a blood oxygenator:

1) Good hemodynamic design, avoiding areas of flow stagnation, low blood flow rates and either abnormally high or unduly low local shear rates.
2) Mass transfer area kept as small as possible.
3) Keeping shear stresses in the conduit well below 1000 dynes/cm^2.
4) A surface/volume ratio as small as possible.
5) Use of biocompatible materials.
6) Maximum allowable ΔP across the oxygenator, 50 mm Hg.

1.3.4. Priming Volume and Overall Dimensions

Oxygenator priming volumes in existing designs vary from 200-1000 cc/litre-min blood flow throughput. As a design parameter the lower figure is preferable, as large priming volumes place a great strain on blood banks, and result in excessive hemodilution of blood. On the other hand, there is little point in reducing the priming volume below the lower figure, as an extra supply of blood is desirable in case blood leaks develop in the circuit. Overall dimensions should be kept minimal to facilitate handling and incorporation into complete heart-lung machines.

1.3.5. Setting-up and Operation

Ideally, an oxygenator should be fully disposable and easily connected to an extracorporeal circuit. It should also be supplied sterile to avoid lengthy sterilizing and rinsing procedures.

Oxygenators built up from modules should avoid too many blood lines and connections. The individual modules should be of a convenient size to provide flexibility without having too great a

multiplicity of units. In practice, there is little clinical use for an artificial lung with an oxygenation capacity under 1 litre blood/minute, a duty commonly required in pediatric applications and partial bypass during circulatory assist.

If a motor or external drive is incorporated; it should produce as little vibration, noise and dust as possible. Moving parts should be covered to prevent hazards to operating staff.

1.3.6. Cost

The market for oxygenators is divided between two technically different types of device; blood-gas interface oxygenators and membrane oxygenators. The first lack the additional complication of separating the blood and gas phases; because of this, they allow a cheap and simple construction. Furthermore, these oxygenators have been in use for some time and there is considerable clinical experience in their use; these factors outweight the damaging effects of the blood-gas interface in short term perfusions.

The market for membrane oxygenators is therefore, at present limited to applications in the small but growing field of long term bypass and cardiopulmonary support. Although there are practical, totally disposable membrane oxygenators available on a commercial basis, there is considerable room for improvement in their gas transfer rates and blood handling characteristics. The problem of producing a technically improved oxygenator then becomes one of offering the design in an attractive, fully disposable package at a cost comparable with that of existing designs.

Table 1.1

Oxygenator Design Parameters

1)	O_2 Duty	-Introduce into blood 50 c.c. O_2/min.-Litre blood. Maximum blood flow rate - 5 litres/min.
2)	CO_2 Duty	-Allow the elimination of the CO_2 molar equivalent of the oxygenation duty.
3)	Pressure drop	-Maximum allowable pressure drop across the oxygenator - 50 mm Hg.
4)	Shear stress	-Bulk shear stress not greater than 1000 dynes/cm^2. Wall shear rate greater than 300 sec^{-1}.
5)	Hemodynamics	-No areas of flow stagnation and low shear rates.
6)	Mass Transfer Area	-Less than 0.5 m^2/litre blood flow-min.
7)	Surface/volume ratio	-As small as possible.
8)	Priming Volume	-Less than 700 cc/litre blood flow-min.
9)	Overall dimensions minimal.	
10)	Easy to assemble.	
11)	All parts in contact with blood fully disposable.	
12)	Reliable and highly permeable membrane.	
13)	Free from vibration, noise and complicated mechanical arrangements.	

1.4. Historical Survey of Oxygenator Design

The use of extracorporeal oxygenation as an aid to cardiac surgery was pioneered by Gibbon (27,28) in 1937; nevertheless, the concept of artificial circulation dates back to the perfusion of isolated organs in the early nineteenth century (14). The need to oxygenate the perfusing blood was demonstrated by Brown-Sequard during the decade 1848-1858 (14). An apparatus to infuse arterial blood from a reservoir was built by Ludwig and Schmidt in 1868 (29), and continuous perfusion of organs in a circuit was possible in the apparatus of Von Frey and Gruber (30) presented in 1885. In this, blood was spread in a thin film over the inner surface of a rotating steel drum into which O_2 gas was introduced; water baths for heating and cooling blood, and provision for blood-gas analysis were included. An excised animal lung (31) was used to interpose a barrier between blood-gas for the first time towards the end of the last century.

The main problem encountered by early researchers was blood itself. Knowledge of hematology was limited, and as a result the incompatibility of the blood of different species, or of different blood groups, was not appreciated. The often occuring toxic effects were attributed to the practice of defibrinating blood to prevent clotting. The perfusion of animals with their own blood (32) resulted in a great step forward and the use of heterologous blood was abandoned (14).

The identification of blood groups and the discovery of heparin - making defibrination unnecessary - made possible the application of perfusion techniques on humans. Gibbon (27,28) first appreciated the potential that a dry, bloodless field offered to cardiac surgery;

his pioneering work was concerned with the maintenance of circulation during the temporary occlusion of the pulmonary artery.

After the second world war, new materials, anticoagulants and improved post-operative care encouraged the great development of extracorporeal circulation and cardiac surgery of the last 25 years. Oxygenator development initially concentrated on the development of heart-lung machines with direct blood-gas contact. These oxygenators were characterized according to their two different operating principles; oxygen was bubbled, usually concurrently with blood or alternatively, blood was exposed as a thin film to an O_2 atmosphere. A comprehensive review of direct blood-gas contact oxygenators is presented in (14); the two designs still widely used are the disposable bag bubble oxygenator (33,34)(Fig. 1.4), and the rotating disk oxygenator (35,36)(Fig.1.5).

Early interest in membrane oxygenators arose from the main drawbacks of blood-gas interfaces evident at the time. These were: the difficulty in eliminating air emboli, which are potentially fatal (37), and the difficulty in maintaining a nearly constant blood volume in the oxygenating chamber. The preferability of separating the blood and gas phases with a semipermeable membrane, was demonstrated by Lee et.al.(2,3) and subsequent work discussed in section 1.1.

The feasibility of a membrane oxygenator was demonstrated by Marx et al.(38), who proved theoretically and experimentally, that if a sufficiently permeable membrane is used, and the blood film is thick compared to the erythrocyte diameter, then the main resistance to oxygen transfer would lie in the blood film. Therefore, increased

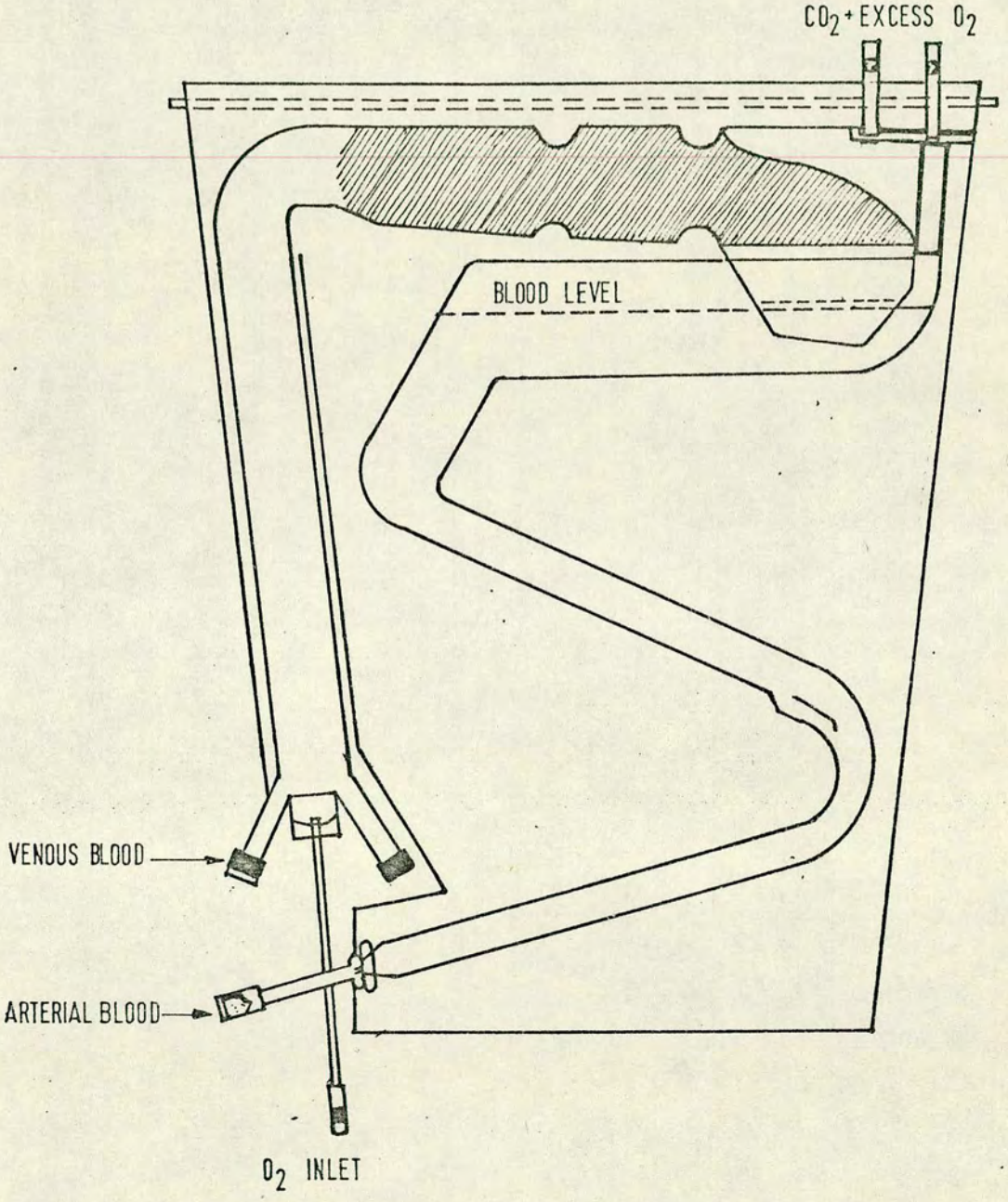

Fig.(1.4): Disposable Bag Bubble Oxygenator. Oxygen is Bubbled into the Rising Column of Blood.

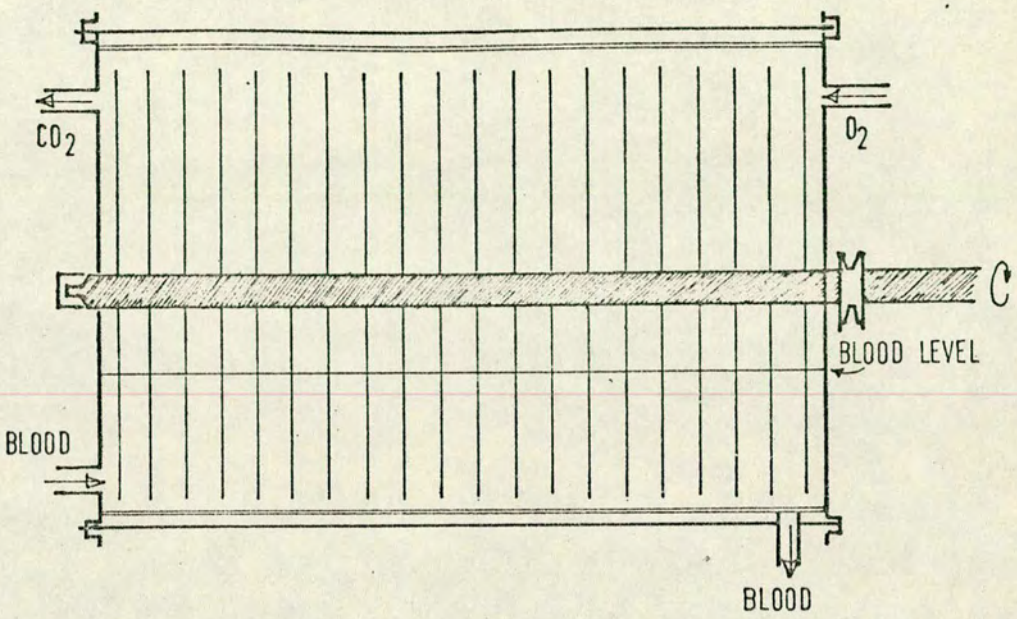

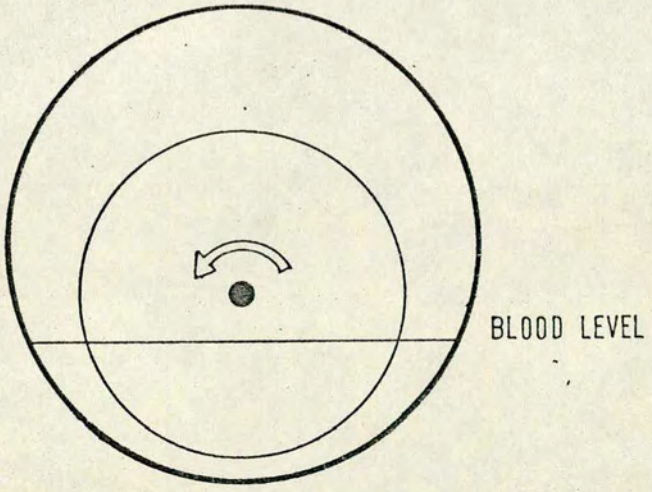

Fig. (1.9): Rotating Disk Film Oxygenator.
A Thin Film of Blood is Formed on the Surface of the Rotating Disks Mounted on an Externally Driven Shaft.

blood mixing, thin blood films and other approaches could be used to make a practical, compact oxygenator, if a highly permeable membrane were available.

1.5. Significant Membrane Oxygenator Designs

A comparative review of existing membrane oxygenators is hindered by the lack of an adequate basis for comparisons.

The only data widely reported refers to oxygen uptake. Comparisons on this basis alone are difficult, since there may be considerable variation in conditions having a direct influence on oxygenation, e.g. inlet venous saturation, blood pH, hematocrit, and arterio-venous saturation differences. In addition, data on CO_2 transfer, pressure drop, assembly, cleaning and rinsing procedures are only occasionally reported. Moreover, blood related factors, i.e. hemolysis, clotting, thrombus formation, protein absorption, are difficult to quantify for comparison, and are in any case, strongly dependent on the conditions of experimental blood. A further point rarely discussed, concerns the problems of scaling-up to practical clinical sizes the small prototypes often used to obtain oxygenation data.

Only recently (39) has an attempt been made to establish rules for the evaluation of mass transfer data and blood and gas fluid resistances in membrane oxygenators. Even these provide no basis for determining the relative importance of factors like cost, appearance, ease of assembly and connection to extracorporeal circuits; obviously these factors are also quite important in the evaluation of a design for clinical use.

Clowes et al. (40) first reported on a membrane oxygenator in 1956, which was a precursor of the modern commercial "sandwich" oxygenators. Essentially, blood flowed in laminar fashion inside membrane envelopes supported on metal screens or plates. Several of these envelope units could be stacked to meet the required oxygenation duty. The oxygen transfer figures reported by Clowes (3-8 cc/min-m^2), are very low and were most likely limited by the relatively impervious ethylcellulose and teflon membranes used. A rather voluminous version of this oxygenator was successfully used in human perfusions (41), and further modifications by Peirce (42) improved performance and made the oxygenator partially disposable. Gentsch et al. (43) reported on the complicated and lengthy assembly procedure.

Contemporary to Clowes, Kolff (44) described a coiled membrane oxygenator; although of a practical design, it is likely that in this case also, the polyethylene membranes represented the limiting O_2 transfer resistance since O_2 transfer rates were rather low.

The idea of membrane envelopes, made by sealing two flat membranes at the edges, was further developed by stretching the envelopes over a frame to create taut corrugations (45); as blood flowed over the corrugations, it was hoped that some degree of mixing would be achieved. A multiple unit prototype (46) using $\frac{1}{8}$ mil teflon membranes on this principle was also tested.

An alternative approach was to adapt a successfully used dialyzer design by incorporating teflon and silicone oxygenation membranes (47). At the same time research was undertaken in the building and operation of a combined oxygenator-dialyzer (48,49). The idea was based on using separate paths for blood, a dialyzing solution, and oxygen. Blood flowed in envelopes made of two membranes; on one side a dialyzing membrane (cellulose), and on the other side an oxygenation membrane. Several envelopes could be stacked together with like-membranes facing each other, forming in this manner, paths for the dialyzing solution and oxygen flows.

The purpose of the dialyzing solution was to maintain the mineral balance in the body by supplying the required minerals, and eliminating excess CO_2. The former factor has nevertheless, not proven to be critical, and does not justify the additional bulk of the oxygenator due to the use of only $\frac{1}{2}$ of the potential area for oxygenation.

To overcome this, Firme et al. (50), used water as both a dialyzing and oxygenating fluid. The results were nevertheless, unsatisfactory due to the absence of a membrane capable of efficiently combining both duties. The material used, regenerated cellulose, has a low oxygen permeability.

Crystal et al. (51) installed screen supported membrane envelopes in a cabinet, which was rocked through a 45°-60° lateral arc at a rate of 30-80 c.p.m. Despite this mixing, O_2 uptake by blood remained low probably due to the formation of rather thick blood films, and blood channeling in the envelopes. Another innovation was the stainless steel tubing incorporated into the screen; by passing hot or cold water through the tubing an inbuilt heat exchanger was provided.

In the early 1960's, highly permeable silicone and silicone copolymer membranes became available, whose high gas permeability allowed a significant improvement of the rate of oxygen uptake by blood before the membrane became once again the limiting resistance. Unfortunately, flat membranes made from these materials are extremely delicate and prone to tearing and pinholes, apart from being difficult to handle. In practice, use of silicone membranes was at the time restricted to two options; the use of thicker membranes, thereby annuling part of the advantage of their high permeability, or using the membranes in the shape of a thin capillary, where the tubular geometry overcomes the inherent weakness of the material. Consequently, the emphasis in membrane oxygenator research shifted towards the shell and tube principle.

The shell and tube design consists of bundles of capillaries inside a shell or jacket, with blood flow either in the shell side (52,53,54), or through the capillaries (55,56,57,58,59). Pulsatile flow oxygenators were also built on this principle (60,61); in this case, blood flow was tube side with oxygen pulsed intermittently into the shell. Marx (61) used a dimethylsiloxane oil as the oxygen carrying medium in the shell side, instead of a pure gas phase; the high heat capacity of these oils allowed the combination of the oxygenation, pumping and heat exchange duties within the same unit.

Another attempt at disturbing the blood boundary layer was provided by rotating multiple capillaries (62) mounted on headers carried by an externally driven shaft. As the capillaries rotated, they stirred the blood inside the casing. Unfortunately, no details

are given concerning the joints between the headers and the housing, but ideally these should be leakproof and atraumatic to blood.

The shell and tube design has been troubled by hematologic problems. When blood flows in the shellside, areas of hemostasis are difficult to avoid, and local regions of turbulence can easily develop between the capillaries. As a consequence, the pressure drop also tends to be high. Flow patterns can be more easily controlled when blood flows inside the capillaries, but in this case, the problem becomes one of header design, and how to distribute blood into hundreds or thousands of capillaries with diameters between 100-300 μ. Experience (55,63,64) has demonstrated that these oxygenators are particularly prone to header thrombus and white plug formation. Furthermore, if the design criteria of section 1.3 are followed; the practical combinations of diameter, length, and tube number are limited, and none can be expected to have an exceptionally good oxygenation efficiency (Section 2.3).

Multiple double capillaries have also been proposed, with blood flow in the annular space (65). Good mass transfer rates are reported, although paying the penalty of an extremely high pressure drop. These results were obtained with a small prototype, and the problems of scaling a multiple double capillary oxygenator to clinical size would be formidable. Also, the problems of header design and flow distribution would presumably be as great as with multiple capillary tubes.

Kolobow (66) proposed an extremely compact design, offering a blood film of nearly constant thickness. The oxygenator consisted of a long silicone membrane envelope, containing a polymer screen and wrapped under tension on to a moulded polycarbonate spool (Fig.1.6).

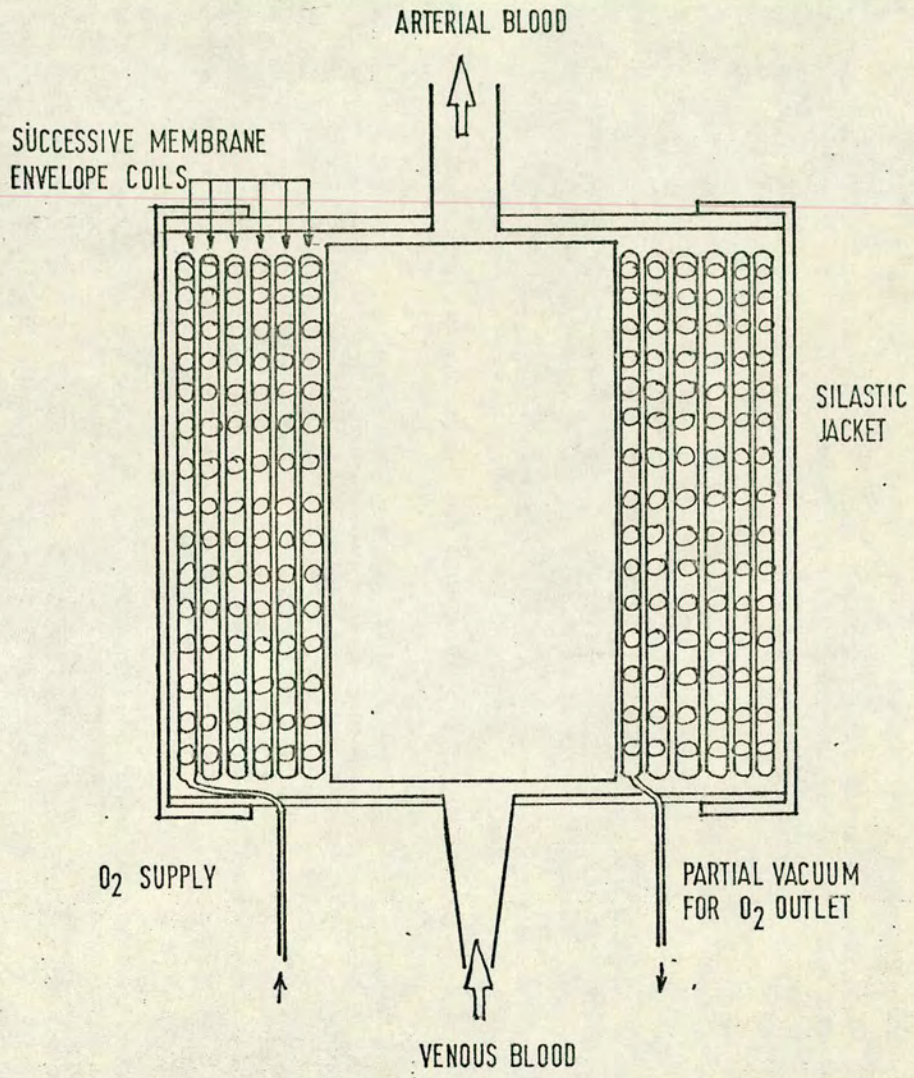

Fig.(1.6): Oxygenator of Kolobow et al.(66)

A tight silicone jacket was then fitted. Blood flowed in and out of ports provided at either end of the spool, while inside the oxygenator it flowed through the narrow spaces between successive coils of the membrane envelope. Oxygen was sucked into the membrane envelope by applying negative pressure, and in this manner, preventing the distension of the membrane envelopes, and the leakage of air emboli into blood as a result of membrane failure. Oxygenator sizes ranging from 0.2 to 9.1 m^2 membrane were built; in this last case, the 18 m long membrane envelope was assembled into an oxygenator 17 cm in diameter x 25 cm long.

With the advent of reliable, thin silicone membranes, offering a large spare capacity for oxygen transfer, it became advantageous to investigate ways to augment the oxygen transfer into blood by diminishing the resistance of the liquid phase. It soon became apparent that some regular disturbance was necessary to overcome the mass transfer boundary layer resistance. Frantz et al. (67), Rush et al. (60), and Marx (61) applied external pulsation to blood flow in the oxygenator, attempting in this manner to combine blood mixing with pulsatile blood pumping. Bellhouse (68) combined pulsatile pumping with secondary flows created in blood as it flowed across a grooved surface.

A main limitation to pulsed flow membrane oxygenators has been the fragility of the membranes, which often fail under the positive and negative pressures of the pulse. A more promising method of improving O_2 transfer is to induce secondary flows on the main blood flowstream. This approach has the additional advantage of offering a controllable, laminar flow pattern, which would be expected to be relatively atraumatic. Such secondary flows are formed in a liquid flowing at sufficiently high axial velocity through a coil having an appropriate coil diameter to

tube diameter ratio. The principle of these "Dean vortices" has been applied by Dorson et al. (57) to a multiple coiled capillary oxygenator used in pediatrics.

Such secondary flows can also be obtained when a suitable geometry is combined with an external drive, which provides the energy for the formation of these vortices; therefore, they do not require additional pressure energy to be supplied to the stream. An added advantage is the possibility of instantaneous variation of the oxygenation rate by controlling the intensity of the secondary flows.

One such design is the toroidal flow oxygenator, consisting of blood filled channels oscillated about their axis of curvature, thereby creating regular vortices inside the channel (69,70,71)(Fig.1.7). The oxygen transfer is strongly dependent on the oscillation rate, and on the basis of reported O_2 transfer values, an oxygenation area slightly greater than 1 m^2 would be required for an adult perfusion, if the criterion of section 1.3.1. is applied. This represents a four-fold improvement over commercial "sandwich" type oxygenators, pointing to the effectiveness of the vortices in augmenting gas transfer. The main disadvantage of the toroidal flow oxygenator is the added complexity of its drive mechanism, which must be vibration free and involves some intermediate step to convert rotary motion to reciprocating motion.

The added complexity of generating secondary flows, or pulsatile action, has so far not been justified by the increased oxygen transfer rates obtainable in these oxygenators. The basic reason for this is that at present, long term bypass is still an experimental rather than routine procedure; therefore, there is little demand for complex

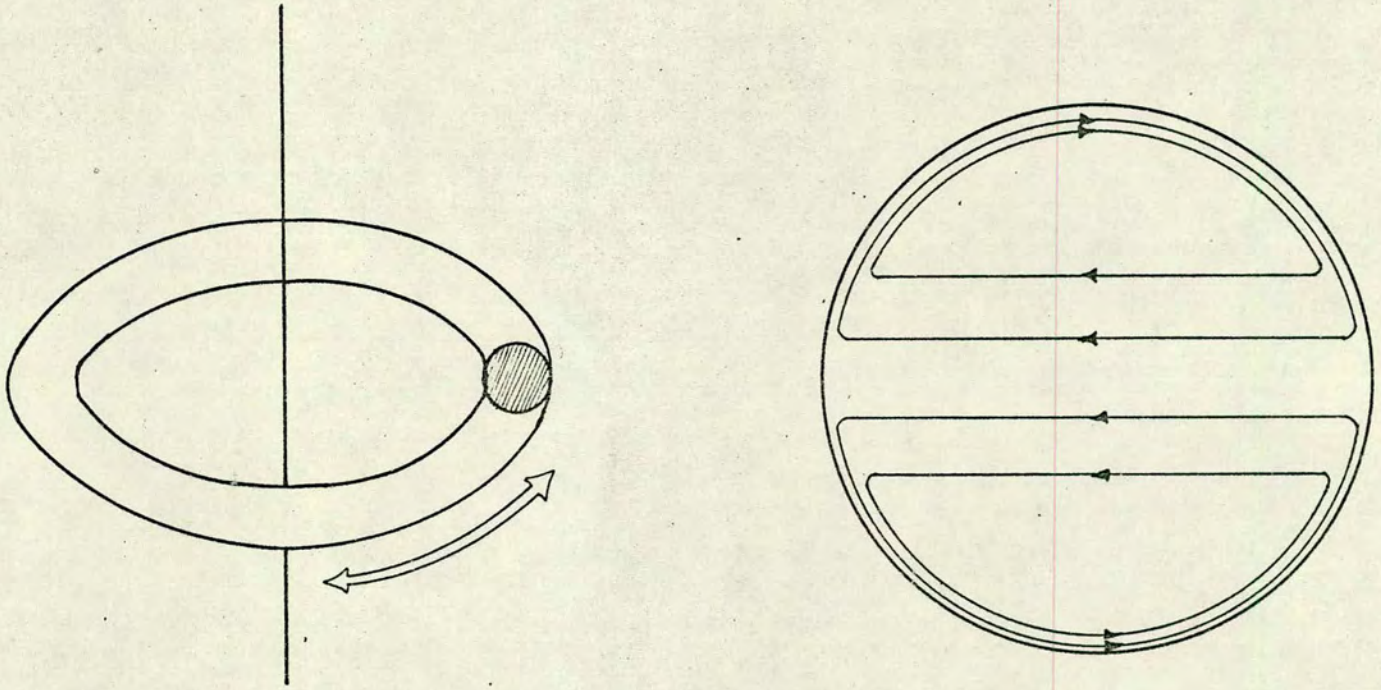

Fig. (1.7): Principle of the Toroidal Oxygenator. As the Torus Oscillates about its Axis of Curvature, Regular Secondary Flows are Created Inside the Channel.

membrane oxygenators, but rather for simple, fully disposable membrane devices, which have improved blood handling characteristics over bag oxygenators. In short and medium term perfusions, the cumulative blood trauma, due to large mass transfer areas, and poor hemodynamic design of the available, laminar flow-based membrane oxygenators, is acceptable.

The commercially available membrane oxygenators are mostly based on the "sandwich" principle (72,73,74,75,76,77). The design of these oxygenators is strikingly similar, and has been perfected to the point where the units are fully disposable. Unit sizes range from 1 m^2 - 3 m^2, with the total area needed for a full adult perfusion being 4-6 m^2. An interesting concept is provided by the Travenol integrated console (34), comprising heat exchangers, blood pump, oxygenator height regulation, necessary instrumentation, and optionally, a stretcher, all integrated into a trolley. The disposable bag oxygenator, or a membrane oxygenator can be fitted to this trolley. The advantages of such a system are obvious, since bypass must not be limited to the operating room; also, considerable time can be saved if a patient is placed on bypass before reaching the operating theatre.

An alternative method of blood oxygenation has been proposed (78,79), relying on the mixing of blood and an oxygen-carrying inert liquid. There is still considerable doubt about the safety of these liquid-liquid contactors, mainly in relation to the complete removal of the O_2-carrying fluorocarbons before blood is recirculated into the body. Substantial equipment must be provided to centrifuge and filter out the blood and fluorocarbon phases. Furthermore, there is still not enough knowledge about the toxicity of the fluorocarbons to allow them to be used with confidence.

1.6. Membranes

Originally, polyethylene and ethylcellulose membranes (40,44) were used as oxygenation membranes; but it was soon apparent that their oxygen permeability was very low, and that membrane resistance, was the limiting factor in blood oxygenation. Membrane oxygenators therefore, require more permeable materials; of the various membranes considered (Table 1.2), only teflon and silicone, or silicone copolymer membranes have proved suitable. Teflon has a relatively low oxygen permeability but is mechanically strong, and can be produced in thicknesses of $\frac{1}{8}$ mil. These ultrathin membranes have good O_2 transfer capacity.

Silicone and silicone copolymer membranes are currently the most widely used. Nevertheless, it is only recently that production techniques have overcome the weakness of the material, giving reliable, and sufficiently thin (< 1 mil) membranes, thereby allowing exploitation of the good gas permeability of the material.

In the ideal case when there is no membrane resistance, all the resistance to mass transfer lies in the blood film. The concentration of oxygen at the membrane-blood interface is then equal to the saturation concentration. On the other hand, for the extreme case when there is no resistance to oxygen transfer in the blood film, and all the resistance lies in the membrane, the concentration of oxygen at the membrane wall will be equal to the concentration C_b in the blood bulk. In oxygenators, there is resistance to oxygen flux both in the membrane and the blood film, and the concentration of oxygen at the interface will be some concentration C_w, where $C_b<C_w<C_s$. As the relative resistance of the membrane increases, C_w will approach C_b, resulting in a decrease in the concentration driving force, and a larger mass transfer area will be required to meet a specified O_2 duty.

Table 1.2.

OXYGENATION MEMBRANES

Membrane	O_2 Permeability cc-cm/min-m^2-cm Hg	CO_2/O_2	
Polyvinilidine chloride	$.30 \times 10^{-6}$	.08	(14)
Monochlorotrifluoro Ethylene	$.54 \times 10^{-6}$	10.7	(14)
Mylar Polyester	$1.35\text{-}4.02 \times 10^{-6}$	1.8	(14)
Nylon 6	2.3×10^{-6}	-	(14)
Cellulose Acetate	$36\text{-}47 \times 10^{-6}$	5.1	(14)
Polypropilene	67.2×10^{-6}	3.4	(14)
Butyl Rubber	78×10^{-6}	-	(14)
Polyethylene	$23\text{-}330 \times 10^{-6}$	2.6-4.6	(14)
Teflon	1002×10^{-6}	2.6	(81)
	968×10^{-6}	-	(82)
Ethylcellulose	$576\text{-}1590 \times 10^{-6}$	4.1-4.3	(14)
Natural rubber	$1380\text{-}1962 \times 10^{-6}$	5-5.6	(14)
Silicone rubber	$15{,}600\text{-}39{,}000 \times 10^{-6}$	4-5	(14)
	$40{,}414 \times 10^{-6}$	5.2	(82)
Silastic	$38{,}410 \times 10^{-6}$	-	(81)
Methyl Silicone	$36{,}473 \times 10^{-6}$	-	(81)
X-D Lexan Silicone Polycarbonate	$10{,}955 \times 10^{-6}$	-	(82)
Permax-Porous Polyethylene	$780{,}000\text{-}2{,}400000 \times 10^{-6}$	-	(83)
Porous Silicone-Coated Paper	-	-	(84)

In the first case, where there is no membrane resistance, the rate of oxygen uptake by blood is limited to say, 50 cc/min-m^2, for a very thin film (.01 cm) in laminar flow in a duct (Section 2.3). The flux of oxygen for the best diffusional membranes, 1 mil silicone, is 1260 cc/min-m^2-atm, which is obtained when transport of oxygen is across the membrane into an oxygen-free gaseous phase; it follows that in an oxygenator where there is an oxygen concentration C_w at blood membrane interface, the flux of oxygen across the membrane will be less. Therefore, for the laminar blood film described above, the rate of oxygen uptake will be less than 48 cc/min-m^2, and a proportionally larger mass transfer area will have to be provided.

The use of membranes poses two problems:

1) Oxygen uptake by blood can be augmented only up to a certain point before membrane resistance becomes the limiting factor in oxygen transfer. Even the best semipermeable membranes available, the fragile 1 mil silicone membranes, would not be convenient if O_2 transfer rates higher than say, 300 cc/min-m^2 are desired.

2) As the oxygen uptake by blood approaches the membrane capacity, CO_2 elimination becomes a serious problem. This arises from the different pressure driving force available for transfer of O_2 and CO_2 in an oxygenator; in the case of oxygen, perfusing gas is generally pure O_2, ($\simeq$ 700 mm Hg, after allowance for water vapour pressure), while venous O_2 tension is approximately 40 mm Hg. By comparison, CO_2 tension is approximately 50 mm Hg in the venous side and 40 mm Hg in the arterial side; since there is no CO_2 in the gas side of the membrane, the venous CO_2 partial pressure also represents the CO_2 pressure driving force. Although the blood film itself poses little resistance to CO_2 diffusion, most membranes have a permeability ratio

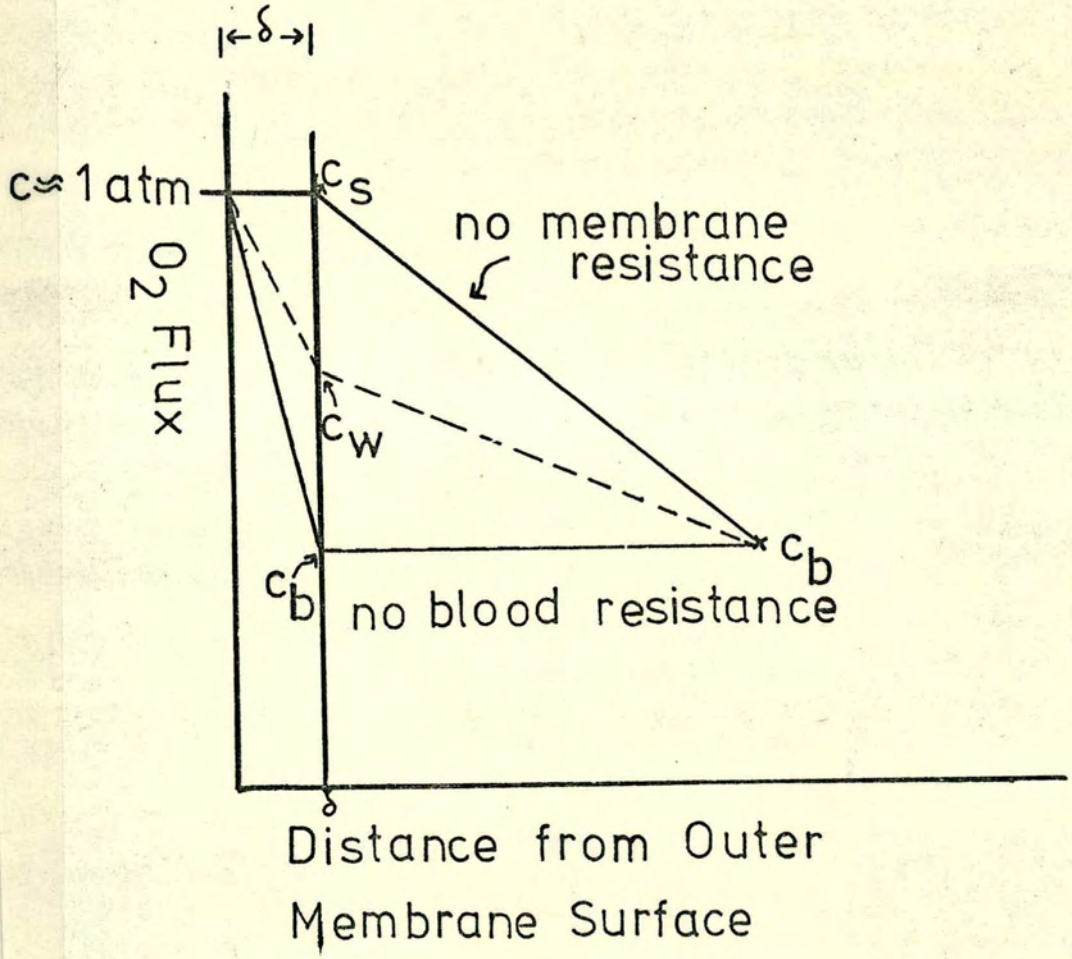

Fig. (1.8) The relative resistances of the blood film and the membrane to the transfer of oxygen in membrane oxygenators.

CO_2/O_2 (silicone ≈ 5) which does not compensate for the unfavourable pressure driving force ratio $\Delta P_{CO_2}/\Delta P_{O_2} \simeq 1/13$. The CO_2 transfer is therefore, in the case of silicone, practically limited to ½ to 1/3 of O_2 transfer when the latter approaches the membrane limit. Therefore, if present membranes are to be used, any improvement in the oxygen transfer rate is limited by the necessity to maintain an acceptable rate of CO_2 elimination in the oxygenator. The work of Melrose (80) illustrates this; carbon dioxide transfer rates were reported to be about ¼ of O_2 transfer for a permeability ratio of $CO_2/O_2 = 4$ at the limit of the O_2 transfer capacity of the polyethylene membranes used.

1.7. Materials

Extracorporeal circuits and blood oxygenators are in contact with blood for a relatively short time; therefore, they do not provide such an extreme test of the blood compatibility of materials as heart valves or vascular prosthesis. Nevertheless, it is desirable that the following requirements are met for the materials of construction:

The materials must be inert, not interacting with blood in any way; they must not induce clot formation i.e. be non-thrombogenic, and they must be free from chemicals capable of being leached from the surface; be inactive in causing surface-induced hemolysis and should not alter blood proteins.

These stringent requirements make it unlikely that any man-made surface can compare with the endothelial lining of the blood vessels in blood handling characteristics. The problem of formulating a biocompatible surface, is that no single physical property or

characteristic completely correlates with biocompatibility. Attempts to correlate blood compatibility with wettability (14), zeta potential (14), surface tension (14), and surface free energy (85) have had limited success as there are always important materials that do not confirm the findings. The discovery that the lining of the blood vessels and the blood cells are negatively charged, has stimulated research into materials that have negative surface charges (86).

Three classes of negatively charged surfaces are classified by Gott et al. (87) for their good biocompatibility; the only other requirement that is generally accepted for good biocompatibility is smoothness; highly polished stainless steels, for example, present a very smooth surface, which is known for its gentle handling of blood.

1.7.1. Inert Materials

These types of surfaces comprise the traditional materials used in extracorporeal circulation. Foremost among this is glass, which has been used since the beginning of medicine. Its clotting resistance is not good, but siliconizing techniques have helped to overcome this; hard glass and Pyrex have reduced the problem of fragility. There are now however, transparent plastics like epoxy, plexiglass and Lucite that have replaced glass in many applications, being more resilient and easy to machine. Another traditional material is stainless steel, especially the Cr-Ni alloys which have great mechanical strength, are easy to machine, and can be polished to a high degree of smoothness. Copper and brass are toxic to blood, and there is evidence that Al and Ni are likewise toxic; gold and silver are expensive, although they find applications where materials

with good thermal and electrical conductivities are needed.

On the whole it is polymers that have become the most important materials in medicine, as they are generally inert to blood, cheap and easy to manufacture; nevertheless, some polymers like nylon, epoxy, Lucite, PVC, PE, generally contain fillers, plasticizers, monomer residues, and catalyst residues, more or less soluble in blood with possible toxic effects. Materials like PVC and PE are heat-sensitive and therefore, not autoclavable.

Teflon and silicone polymers are the two most widely accepted plastics for blood-handling applications. Teflon has high chemical inertness, is heat resistant, unaffected by humidity, it is also strong and has good dielectric properties and a very low coefficient of friction. Silicones compete with teflon in some of these characteristics; furthermore, they can be formulated to meet a wide range of requirements. Variations of chain length and degree of crosslinking give a wide range of properties. Medical grade silicones (with no additives) are of several types; methyl, dimethyl, phenyl, vinyl, and fluorinated aliphatic groups can be added to the basic silicone-oxygen backbone (88). Copolymers with polycarbonates are also widely used, recently as membranes.

Natural rubber containing no additives and crosslinked by radiation (89) has also been used. Most polyurethanes (90) have proved unsatisfactory when tested in vivo for long periods, but many have short term blood compatibility.

A number of inert materials, as well as negatively charged surfaces, listed by Gott et al. (87), have been developed and show good

biocompatibility, although cost would not at present justify their use in extracorporeal circuits; these find applications mainly for valves and vascular prosthesis, areas where materials are of paramount importance.

Chapter 2

2.1. Blood Modelling

When oxygenating blood in a membrane oxygenator, there are a number of resistances in series in the path of oxygen before its final chemical reaction with hemoglobin. Oxygen must first diffuse across the oxygenation membrane, and subsequently, the mass transfer boundary layer in the plasma adjacent to the membrane; the diffusion path then proceeds through the mass transfer boundary layer surrounding the red cell, followed by a substantial resistance at the red cell membrane (14). Once inside the red cell oxygen diffuses through hemoglobin to the active sites where the extremely fast oxyhemoglobin reaction takes place.

Taking into account the actual physical events in the uptake of oxygen by blood, three approaches to blood modelling are possible (91).

2.1.1. Macroscopic Modelling

Blood is in this case, assumed to be a homogeneous incompressible fluid with uniformly distributed oxygen sinks. The local effect of diffusion in the vicinity of the red cell, the red cell membrane, and the rate of chemical reaction, are lumped together into a macroscopic diffusion coefficient for whole blood; similarly, the oxygen capacity of whole blood is used in lieu of the solubility coefficient. It is furthermore necessary to know the macroscopic velocity field, and the chemical equilibrium relationship if the mass transfer driving force is expressed in pressure units.

2.1.2. Microscopic-Macroscopic Model

In this approach, RBC's are included in the analysis. They act as before, as uniformly distributed oxygen sinks whose behaviour is described by a set of microscopic equations for diffusion in the red cell membrane, and red cell interior. The microscopic model is then coupled with the macroscopic model using the boundary conditions at the red-cell plasma interface. In addition to the data required for the macroscopic model, the following must also be known; the diffusion coefficient and solubility of oxygen in the red cell membrane and interior, the oxyhemoglobin reaction rate, the number of cells per unit volume, and a partition coefficient for oxygen between plasma and the red cell membrane.

2.1.3. Statistical Model

More comprehensive and complicated, the statistical model considers blood at a microscopic level, with erythrocytes randomly located and following irregular paths; furthermore, the relationship to local plasma oxygen concentration is constantly changing. The problem then becomes one of defining a distribution function of the probability of finding the erythrocytes within an element of plasma. The distribution function can then be incorporated into a microscopic mass balance describing O_2 exchange between plasma and the red blood cell. Therefore, it is necessary to collect enough data to generate a distribution function, in addition to the data required for the microscopic model.

Analyzing these three approaches to blood modelling, Spaeth (91) concluded that the macroscopic model was adequate for the purpose of oxygenator design, since the controlling resistance to O_2 uptake is in the plasma, while the combined effect of diffusion and chemical reaction inside the red blood cell is negligible, due to the very fast O_2-Hb reaction rate. Experimental results, furthermore, agree closely with published macroscopic models (92,93,94). On the other hand the microscopic-macroscopic, and statistical models are limited by the lack of adequate data, especially concerning the red cell membrane and surroundings.

Summarizing, the following assumptions must be made for macroscopic modelling of blood;

1) Blood is a homogeneous, incompressible fluid.
2) The reaction rate of O_2 with Hb is infinitely fast, and the main resistance to oxygen transfer is in the plasma.

The following have to be defined:

3) The fluid is either Newtonian (93,95) or non-Newtonian; in the latter case the velocity profile is given by the Casson equation (92,94). In either case the flow must be assumed to be fully developed.
4) The effective diffusion coefficient for whole blood, obtainable experimentally from oxygenation data (93), or calculated from heterogeneous media theory (91,92). The diffusion coefficient is normally assumed constant, although Villaroel (94) assumed it dependent on the rotation of the erythrocytes. In any case, this did not significantly alter the diffusion coefficient.

5) The chemical equilibrium relationship is defined by the oxyhemoglobin dissociation curve (Fig. 1.1 .).

To simplify the solution, further assumptions can be made;

6) Constant pH,

7) Isothermal system,

8) Axial diffusion in the membrane is negligible,

9) Axial diffusion in the fluid is negligible compared to convective axial transport,

10) Metabolic consumption of O_2 in blood is negligible,

11) The resistance of the oxygenation membrane is negligible (93,94).

This assumption is valid only if highly permeable membranes are used (section 1.7).

2.2 Application to Oxygenator Design

Using the macroscopic blood oxygenation model, we now examine the essential characteristics and inherent limitations of membrane oxygenators of various kinds, according to physical mass transfer coefficients associated with the flow conditions prevailing in them.

2.2.1 Mass Balance for a Parallel Plate Oxygenator

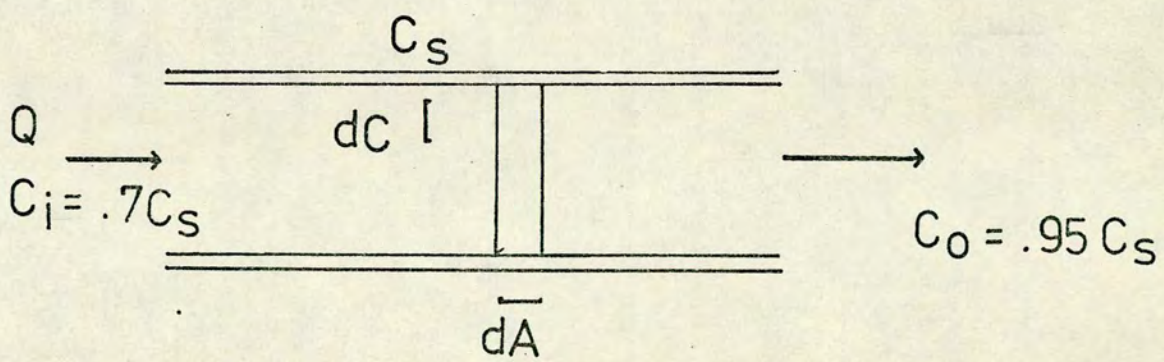

Let the axial concentration of oxygen in the element of fluid between two parallel plates be represented as follows:

2.1 $$Q \frac{dc}{dA} = h_D (Cs-C)$$

integrating, 2.1) becomes

2.2) $$Q \ln \frac{C_s - C_i}{C_s - C_o} = h_D A$$

where $C_i = .7\ C_s$ and $C_o = .95\ C_s$;

then assuming that the effective diffusion coefficient in blood is constant in this range of 70% - 95% veno-arterial saturation

2.3) $$Q \ln 6 = h_D A$$

Since $Q = 83.33\ cm^3/sec$

2.4) $$Ah_D \equiv 150\ cm^3/sec$$

Values for the overall mass transfer coefficient can be obtained by analogy with heat transfer from

2.5) $$\frac{h_D d}{D_{AB}} = Sh = .667\ Re^{\frac{1}{2}}\ Sc^{\frac{1}{3}} \quad (96)$$

which is the correlation for mass transfer to a fluid in laminar flow past parallel plates.

Realistic values of the mass transfer coefficient applicable to blood oxygenators, can be obtained when eq. 2.5 is solved together with the respective eq. for the pressure drop in a fluid flowing between parallel plates.

$$-\Delta P = \frac{12\,\mu\,L\,\blacksquare\,b\,V_z}{b^3\,g_c} \qquad 2.6)$$

Where the maximum allowable pressure drop is 50 mm Hg (Section 1.3.3.).

The simultaneous solution of eqns. 2.5 and 2.6 for the mass transfer coefficient and the length of the blood passages, given the gap width b, supports the following conclusions; even for the smallest blood film thickness used in blood oxygenators (100 μ), oxygen transfer into blood flowing in a laminar regime is limited to a value of 40-60 cc/min-m^2 if the blood velocity in the tubes is kept within levels that allow a low pressure drop. This implies an oxygenation area of 4-6 m^2, which can be provided in the longitudinal dimension or in width. When such thin blood films are used the length of the plates must be kept small because of the pressure drop restriction of section 1.3.3. It follows that the plates must be very wide, or multiple parallel flow paths must be provided to accommodate the required mass transfer area. This creates a substantial problem of blood distribution, and due to the large conduit crossectional area, the velocity in the channel becomes very low, a factor which may be undesirable from the hematologic point of view (99). Increasing the effective thickness of the blood film allows the use of larger blood passages, but there is also a large increase in the

required mass transfer area, and the problem becomes once again one of blood distribution, apart from the resulting large priming volume.

Similar results are obtained for laminar blood flow in ducts of different geometry. Solving the solution to the models presented in literature for round tubes (93,94,98) and annular conduits, (97) together with the appropriate pressure drop expression, it can be seen that the oxygen transfer rate is likewise limited to 40-60 cc/min m^2 for the thinnest practical blood films (Fig. 2.1); the problem then again becomes one of blood manifolding if a large number of parallel passages are used, or longer blood passages with the resulting large pressure drop.

2.3 Alternative Flow Patterns

A turbulent flow oxygenator, is impractical due to the high pressure drop that can be expected, in relation to the mass transfer augmentation. Turbulence, furthermore, may have a hemolytic effect on blood (100,101), due to the high shear stresses encountered.

Pulsating blood as a means of disturbing the mass transfer boundary layer is an attractive possibility, and has as such been investigated by several workers (60,61,68). An oxygenator with an external pulse source, can combine its duties with those of a pulsatile blood pump, thereby reducing circuit priming volume; it also handles blood in a more physiologically desirable manner than a separate continuous blood pump (102). A major limitation remains membrane failure due to the long term pulsatile action. Furthermore, theoretical studies on pulsatile flow in rigid tubes (103,104) and distensible conduits (105), show that no substantial mass transfer

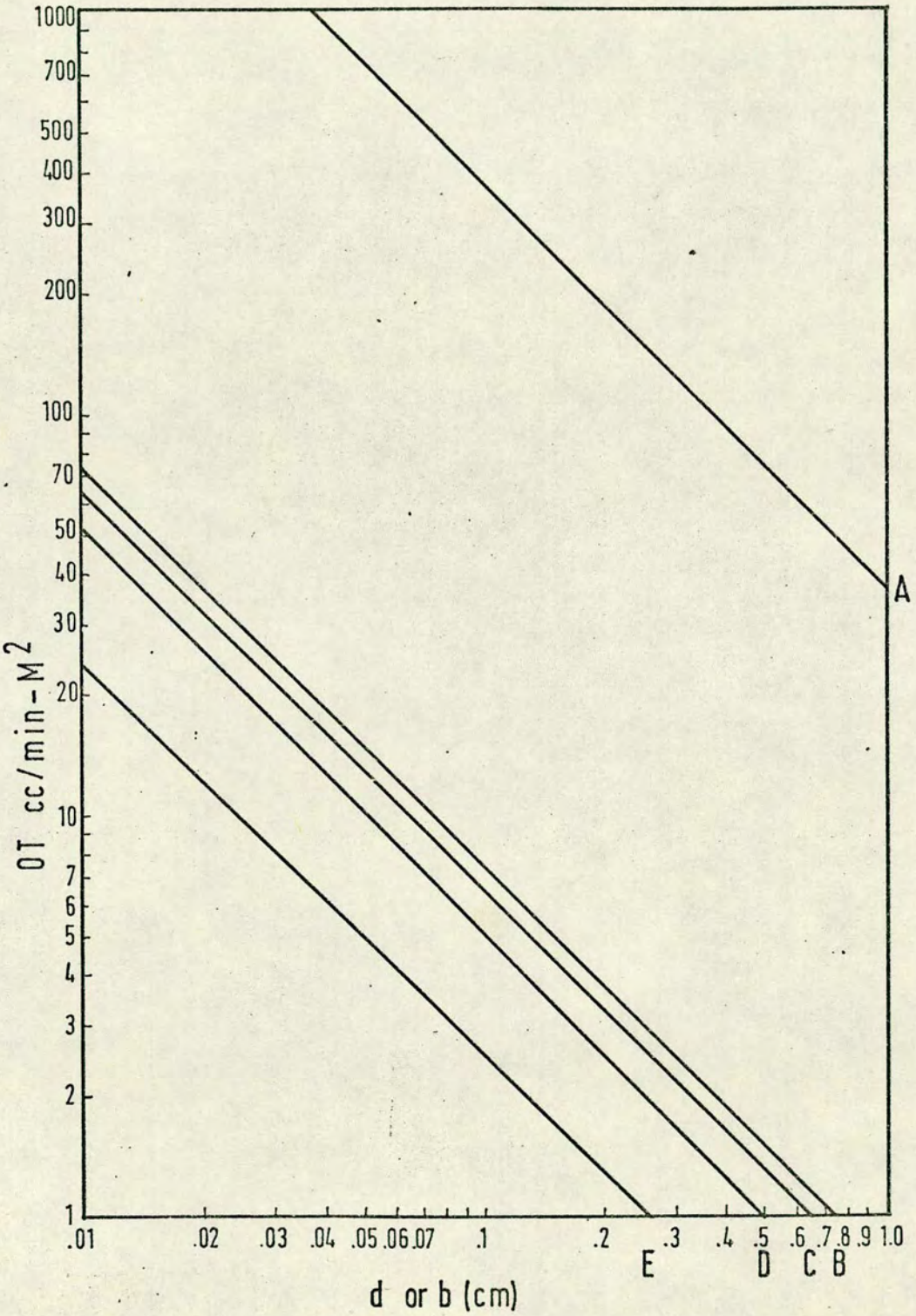

Fig.(2.1): Rate of Oxygen Uptake by Blood Films of Different Thicknesses for: A) Coiled Tubes; B) Tubular Oxygenator(93); C) Tubular Oxygenator(96); D) Annular Exchanger(97); E) Flat Plates(98).

augmentation may be expected by using pulsatile flow, as opposed to purely laminar flow. Indeed, at low frequencies there may be a reduction in the mass transfer rates.

More substantial improvement can be obtained by inducing secondary convective flows on the main blood stream. In order to induce such secondary flows, ducts of suitable geometry must be provided; one such geometry is the coiled tube, where secondary flows are created when the Reynolds number of the axial flow exceeds a certain critical value. Oxygen transport by these "Dean vortices" has been studied by Weissman and Mockros (106) and Dorson (57). Although substantial reduction in the mass transfer area can be obtained, compared with laminar flow, for blood films of the same effective thickness, the problem remains that of blood distribution to large numbers of capillaries. Furthermore, for a given coil, the oxygenation rate varies as the intensity of the vortices, and therefore, cannot be regulated independently of the blood throughput.

The toroidal flow oxygenator, where secondary flows are created inside oscillating toroidal passages, overcomes this problem (69,70,71), since the intensity of the vortices, and therefore oxygenation rate, is largely dependent on the regulation of an external power source. Unfortunately, the toroidal flow oxygenator involves the additional complications of reciprocating motion, difficult to achieve without vibration. On the other hand, the mass transfer data obtained with toroidal flow oxygenation (69,70,71) does point to the effectiveness of secondary flows in improving oxygen transfer rates.

2.4 Proposed Oxygenator Design

Convective secondary flows superimposed on an axial stream of fluid are also formed when the inner cylinder of a coaxial cylinder arrangement rotates above a certain critical speed (107) (Fig.2.2). The state of the fluid in the annulus is described in this case by the Taylor number

2.7) $$Ta = \frac{V \phi b \rho}{\mu} \left({}^{b}/_{R_o} \right)^{\frac{1}{2}}$$

relating the viscous and inertial forces with the geometry of the conduit. This definition of the Taylor number describes the state of the fluid in the annulus, if there is no axial flow, when the ratio of the annular gap to outer annular radius is less then .4 (108). If there is an axial stream, four modes of flow are possible which can be mapped as a function of the Ta and Re_z numbers (109)(Fig.2.3):
1) purely laminar, 2) laminar axial flow with superimposed vortices, 3) turbulent flow, and 4) turbulent plus vortex region.

The onset of the second of these regions, as well as the fluid dynamics of the flow have been widely studied (108) since it provides a classical example of hydrodynamic instability. It was proposed therefore, to design a membrane blood oxygenator operating in the laminar plus vortex region, using the vortices as the convective agent to increase oxygen transfer rates into blood. Such a system can be built with a very good hemodynamic design, and would provide oxygenation flexibility, as the mass transfer rate would be dependent on the angular velocity of the rotor. From past investigations, (108)

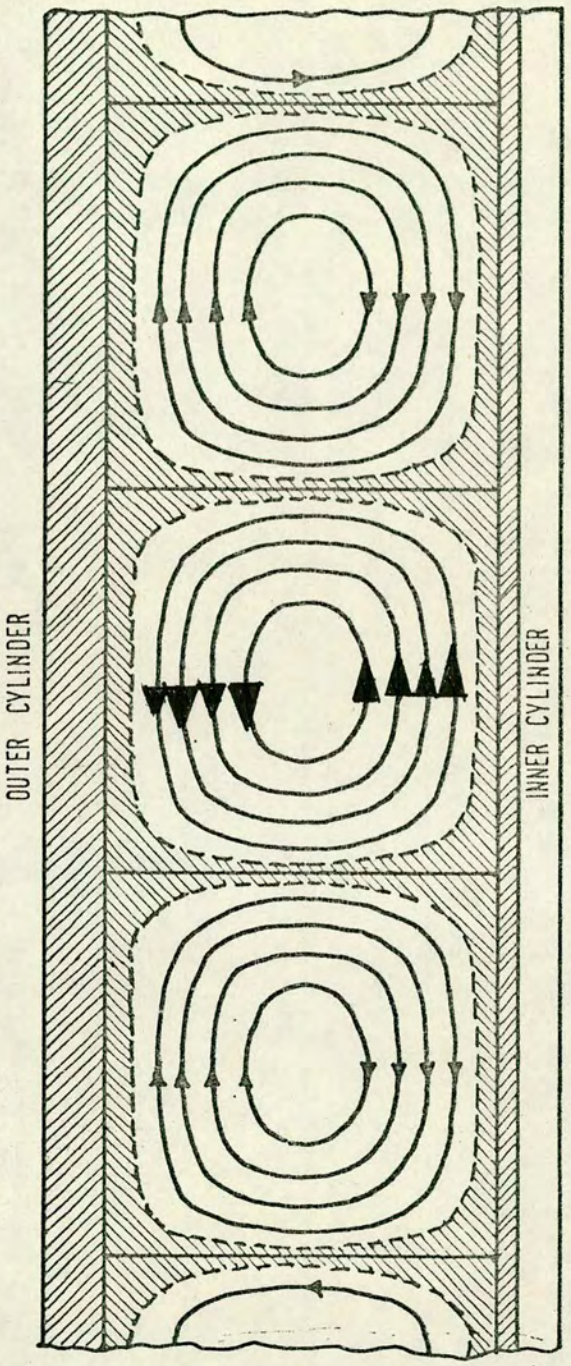

Fig. (2.2): Taylor Vortices.

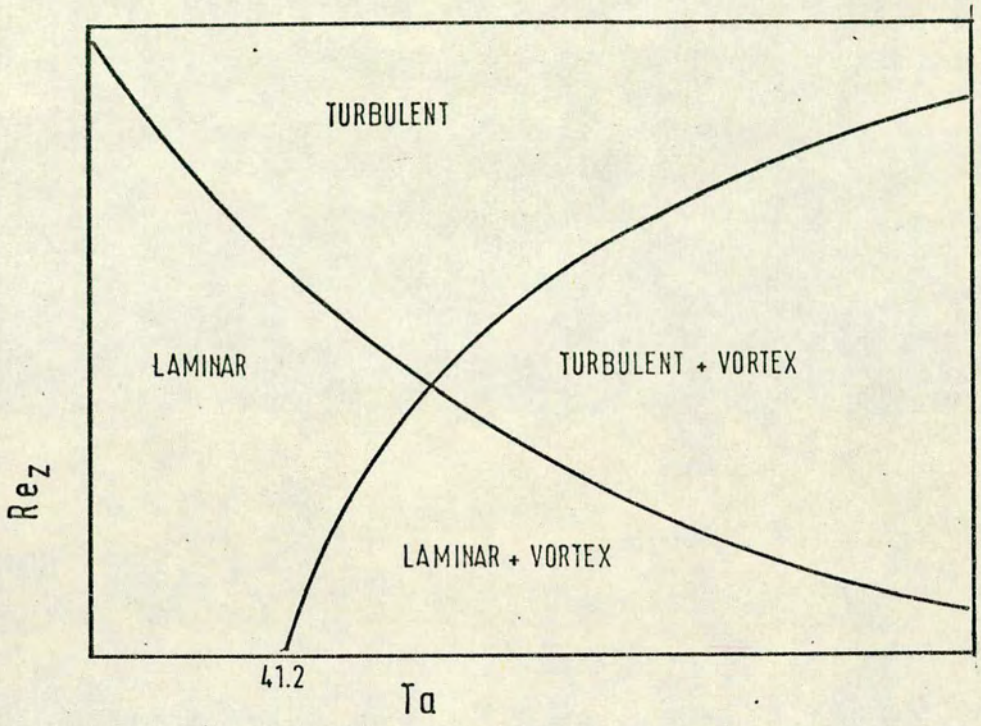

Fig.(2.3): Regions of Flow Created When the Inner Cylinder of a Coaxial Cylinder Assembly Rotates, while the Outer Cylinder Remains Stationary.

it also appears possible to operate this system to obtain increased oxygen transfer rate without paying a large penalty in the axial pressure drop through the annulus.

In order to design an oxygenator based on the coaxial rotating cylinder principle, it is necessary to know the mass transfer correlation for such a system; once this is known, the mass transfer area, as well as the other dimensions of the apparatus, can be calculated for the required oxygenation duty.

Chapter 3

3.1 Transfer Processes in the Laminar and Vortex Region

The literature on transfer processes in the annulus between rotating coaxial cylinders has been extensively reviewed by Flower (110). From this review it is of interest to point out that most theoretical models and experimental investigations show a dependence of heat and momentum transfer with $\simeq Ta^{\frac{1}{2}}$, both for purely rotational flow above a critical T_a number (111, 112, 113, 114, 115, 116), and for axial and rotational flows in the laminar and vortex region (117, 118).

Similarly, two of the most extensive investigations of mass transfer in a coaxial cylinder system (119, 108) agree with this dependence of transfer coefficients with $Ta^{\frac{1}{2}}$. Flower, Macleod and Shahbenderian (108) combined the results obtained in two different experimental systems to obtain the following correlation

$$Sh = Ta^{.52} Re_z^{-.1} Sc^{\frac{1}{3}} \qquad 3.1)$$

In their experiments, the T_a number range covered (100-3000) was fairly large, and despite considerable data scatter the relationship of Sh with $\simeq Ta^{.5}$ was substantiated. On the other hand the Sh and $Re_z^{-.1}$ dependence was approximative, as pointed out by the authors, since the experimental scatter was greater than the effect of such small negative power of Re_z on Sh.

One common feature of these mass transfer experiments was the use of systems involving the transfer of mass to an air stream; in (108) the systems used were: water-air, mercury-air and

n-heptane-air giving an Sc number range of .6 to 1.9. These are Sc numbers three orders of magnitude smaller than the Sc characterizing oxygen-blood systems. Similarly, reported heat transfer investigations (113, 117) were generally carried out in systems with low Pr numbers, and it does not seem justifiable to extrapolate these finding with low Sc and Pr number systems to describe the mass transfer behaviour in systems with Sc numbers many times greater.

This doubt arises from the fact that at low Sc and Pr, the momentum, heat, and mass transfer boundary layers are of nearly the same thickness, and the mechanism of transport can therefore be assumed similar for all three properties, hence their common dependence on $\simeq Ta^{\frac{1}{2}}$. On the other hand, at Sc numbers over 1000, typical for blood-gas systems, the mass transfer boundary layer is much thinner than the momentum boundary layer, and will fill only a small section of the annular passage. Accordingly, while the momentum boundary layer increases in thickness very quickly, and due to this is disturbed by the Taylor vortices almost as soon as the fluid enters the channel, it is possible that a much thinner mass transfer boundary layer is not appreciably disturbed by the vortices that fill the greater part of the annulus. Mass transfer in such a system would be a boundary layer process, independent of the far boundary, rather than the convective process in low Sc systems; therefore, it is reasonable to expect a different dependence of Sh with Ta.

Eisenberg, Tobias and Wilke (120) studied the dissolution

of cast rotors of benzoic and cinnamic acids, and the rate of ion transfer in a ferro-ferricyanide redox system, which between them gave a Sc range of 835-10,000. Their results correlate $^{h_D}/_{v_\phi}$ with $Re_\phi^{-.3}$ for mass transfer from the inner cylinder; nevertheless, this was a system of no axial flow, and more important, only a few experimental data points were obtained in systems with $^{b}/_{R_o} < .4$ where the state of the fluid can be characterized by the Ta as defined in (108). Furthermore, the lengths of the annuli used were not very long compared with the gap widths and the results may therefore have been complicated by end effects.

The results of Eisenberg et al. (120), though inconclusive due to the uncertainty about the state of the fluid in the annulus, justify further investigation of the mass transfer correlation for high Sc systems, particularly since experiments conducted in this laboratory with small $^{b}/_{R_o}$ (121) were in agreement with the findings of Eisenberg et al. For the present purpose of oxygenation design based on a rotating coaxial cylinder system, it is therefore desirable to investigate the mass transfer correlation for a high Sc system with small $^{b}/_{R_o}$ and a relatively large $^{L}/b$.

3.2 Experimental Method

To study the mass transfer behaviour of a high Sc system like O_2-blood, it was decided to use an adaptation of the shrinking plasticized polymer film technique developed at the University of Edinburgh (122), and previously used mainly for the determination of mass transfer to air. The mass transferring surface was coated with a permanent layer of insoluble elastomer and swollen before each experiment with a swelling agent slightly soluble in water. During the experiment,

as water flows in the annulus, the swelling agent is eluted into the water stream from the rubber phase, and if the swelling agent is correctly chosen, its concentration in the effluent water can be determined by a convenient method, such as ultraviolet spectroscopy. The mass transfer coefficient can then be calculated if the water flow rate, the concentration of the outlet stream of water, the interfacial area between the rubber phase and water, and the concentration of the swelling agent in the layer of liquid immediately adjacent to the swollen coating is known.

Extending the theory presented in (122) for transfer to a stream of air, to a system where transfer occurs to a stream of water, it can be initially assumed that the swelling agent is in equilibrium with the rubber phase, and that the concentration in the liquid layer immediately adjacent to the coating, is the saturation concentration of the swelling agent in water. It is desirable that the activity of the swelling agent in the liquid adjacent to the coating and in equilibrium with it, should remain within 5% of the initial value for a sufficiently long period to conduct an experiment. Within this "constant rate" period, the rate of elution of the swelling agent remains sensibly constant if the water flow is fixed, and the experimental uncertainty is small compared with other sources of error. The concentration driving force initially, and effectively throughout this "constant rate" period, is equal to the solubility of the swelling agent at the experimental temperature, when the initial concentration of swelling agent in the water is zero, and the coating is swollen to equilibrium.

At the end of the "constant rate" period, the surface

composition of the rubber coating corresponds to equilibrium with an adjacent layer of aqueous solution having 95% of the concentration at saturation. If the aqueous solution behaves ideally, in the sense that the concentration of the solute is proportional to its partial pressure, the terminal composition of the initially saturated rubber coating surface would be such that the vapour pressure of solute above it is 95% of the vapour pressure of the swelling agent, which corresponds to the condition of the coating at the end of the "constant rate" period when transfer is to a gaseous stream. If the aqueous system obeys Raoult's Law, the length of this "constant rate" period can be determined from the charts given in (122) when the mass flux from the coating, the composition of the coating, and the diffusivity of the swelling agent in the rubber phase are known. The implementation of this method to determine mass transfer coefficients therefore requires knowledge of a) the relationship between concentration of swelling agent in water and u.v. absorption, b) the solubility of the swelling agent at experimental temperatures, and c) the diffusivity of the swelling agent in water, in order to generalize the results on a dimensionless basis. To estimate the duration of this "constant rate" period under the given experimental conditions, it is also necessary to know d) the degree of equilibrium swelling of the polymer, and e) the diffusivity of the swelling agent in the swollen rubber coating. Finally, in case the liquid mass transfer system does not obey Raoult's Law, and there is no reliable vapour-liquid equilibrium data for the system, a check by direct measurement of the "constant rate" period should be made.

3.3 Apparatus

The experimental apparatus used for the mass transfer experiments is shown in figures 3.1 and 3.2. The outer cylinder was a vertical glass tube 57cm. long with an ID of 5 cm. with a water inlet at the lower end and a water outlet at the top. The rotor was an aluminium alloy tube of 3.81cm. OD, fitted with steel end plugs, of which that at the base was sealed with an internal O-ring to avoid seepage of fluid into the rotor due to the considerable hydrostatic head. The driving shaft, integral with the top plug, was journalled in the ball race (A), and driven through a flexible coupling (B) from a coaxial pulley (C), journalled in independent bearings, which was driven from a constant speed motor and variable speed gear.

The lower plug turned on a 9mm stainless steel ball which engaged a conical recess in the fixed brass pedestal (D) which supported, centralized and closed the lower end of the glass tube. At the upper end, the glass tube was supported and centralized by means such that the rotor could be taken out for reactivation without disturbing the glass tube.

The apparatus was mounted on a 15cm. wide steel column of channel section, set vertically and anchored to the roof structure and floor of the building to ensure rigidity and minimize vibration. Distilled water used in the experiments was supplied from a head tank and reservoir; its flow rate was measured by a rotameter. The experimental temperatures were constantly monitored with thermometers at the inlet and outlet of the experimental annulus. The rotor speed was found by stopwatch timing of revolutions counted visually or mechanically.

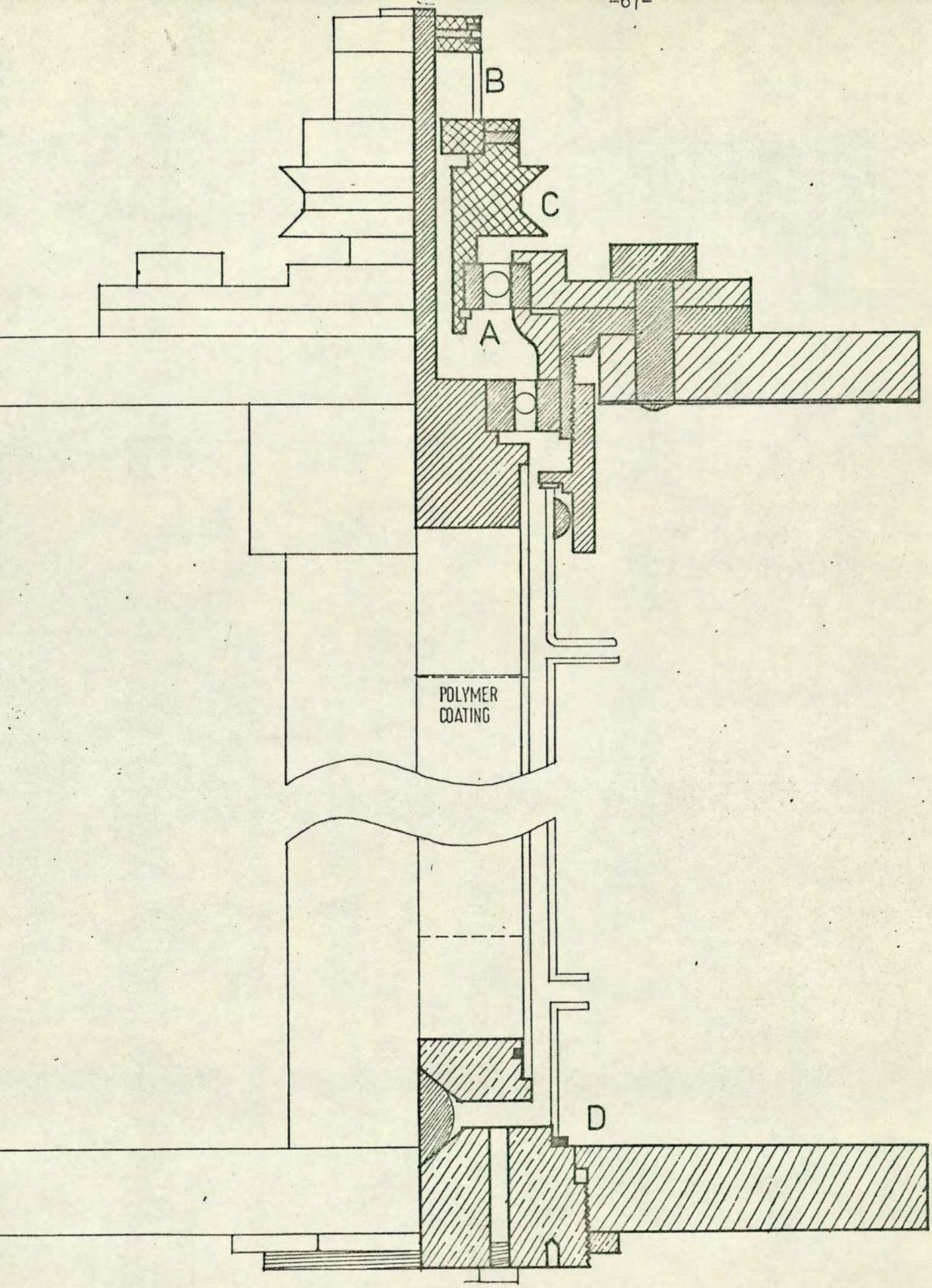

EXPERIMENTAL APPARATUS

Fig.(3.1):

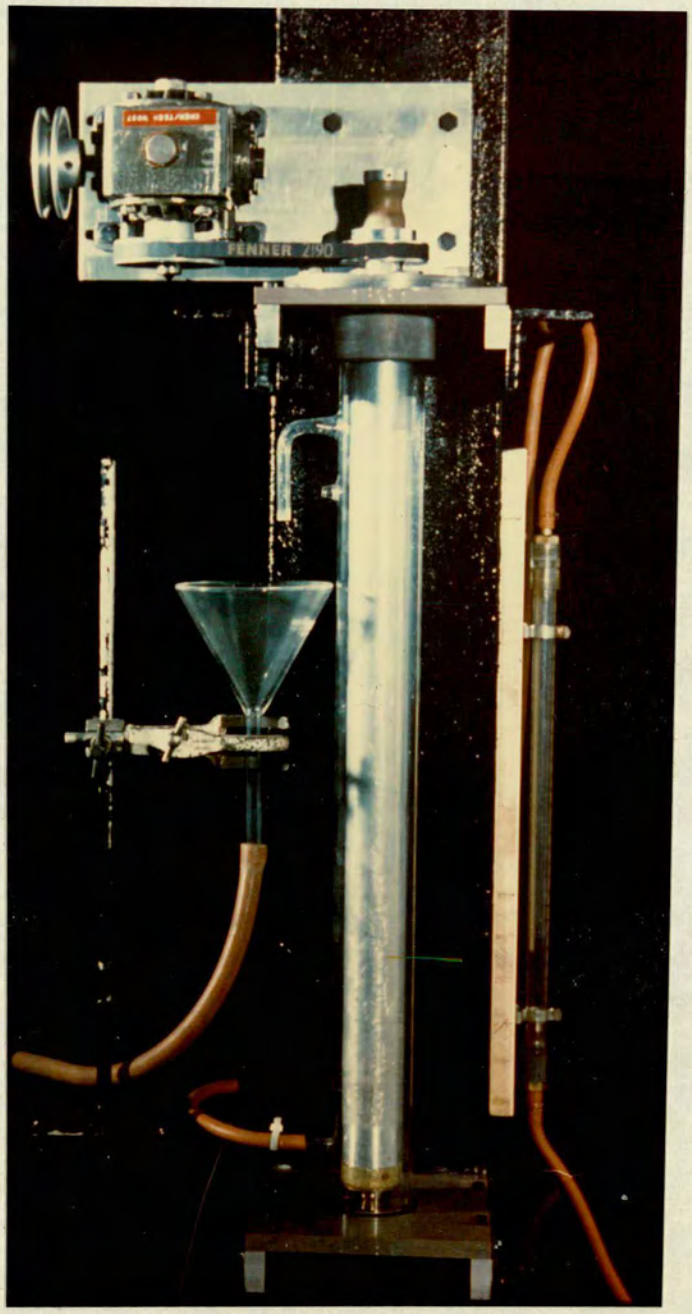

Fig.(3.2): Experimental Apparatus, Ester Experiments.

3.4 Materials

The mass transferring surface was coated with Silcoloid 201 silicone rubber (ICI Ltd. Stevenston, Ayrshire). The surface was treated with the recommended primer and in the case of the rotor, sprayed with a solution of rubber and curing agent in toluene, as it slowly turned on the lathe. The inner surface of the glass tube was coated by rinsing it with a small amount of solution. The coatings thus obtained were .04 $\pm$ .01 cm. thick. After curing, the cylinders were immersed in a bath of ethyl salicylate for approximately 1 hour, in which time equilibrium swelling was attained.

The choice of swelling agent was narrowed to methyl and ethyl salicylate, both of which met the following requirements: swell the rubber to a small extent to avoid excessive deformation of the polymer coating, and a low solubility in water, which is at the same time readily measured by ultraviolet spectrophotometry. Ethyl salicylate was chosen as it appeared that its stability in aqueous solution is better than methyl salicylate.

3.5 Calibration of the Ultraviolet Spectrophotometer

Aqueous solutions of ethyl salicylate were prepared by dissolving weighed amounts of ethyl salicylate in known volumes of water. Solutions of 5-25% saturation were prepared this way, and the ultraviolet absorption of these solutions was measured at the absorption minimum of 262 nm. Over the concentration range of the solutions the absorption was found to vary linearly with concentration within the limits of experimental error. Fifty samples were analyzed and the resulting readings clustered within $\pm$ 7% of the Absorption vs.

Concentration line of best fit, with the majority of the points clustered within ± 2% of the line having a slope of 3.1 x 10^3cc/gm. The errors in preparing the samples with the small quantities of ethyl salicylate involved, and "noise" in the spectrophotometer account for this scatter.

3.6 Determination of the Solubility of Ethyl Salicylate in Water

Since no solubility data for ethyl salicylate in water was found in the literature, the following method was used to determine the saturation concentration. Disks of Silcoloid 201 rubber, swollen to equilibrium in an ethyl salicylate bath, were weighed and placed in a sealed stirred glass flask containing a measured amount of water and immersed in a constant temperature water bath controlled by a thermostat. After a suitable length of time the disks were removed, dried and weighed, the total weight loss corresponding to the ethyl salicylate dissolved in the water.

Both the time required to approximate equilibrium, and the minimum number of disks required so that the total weight loss was independent of the number of disks, were determined by trial and error. These limits were then exceeded to ensure that the water effectively obtained a concentration corresponding to the saturation concentration of ester in water.

Most values fall within ± 7% of the equilibrium concentration vs. temperature curve best fitting the data (Fig 3.3), the principal source of error being temperature control; the water bath temperature was found to vary by ± .5°C sufficient to account for the data scatter.

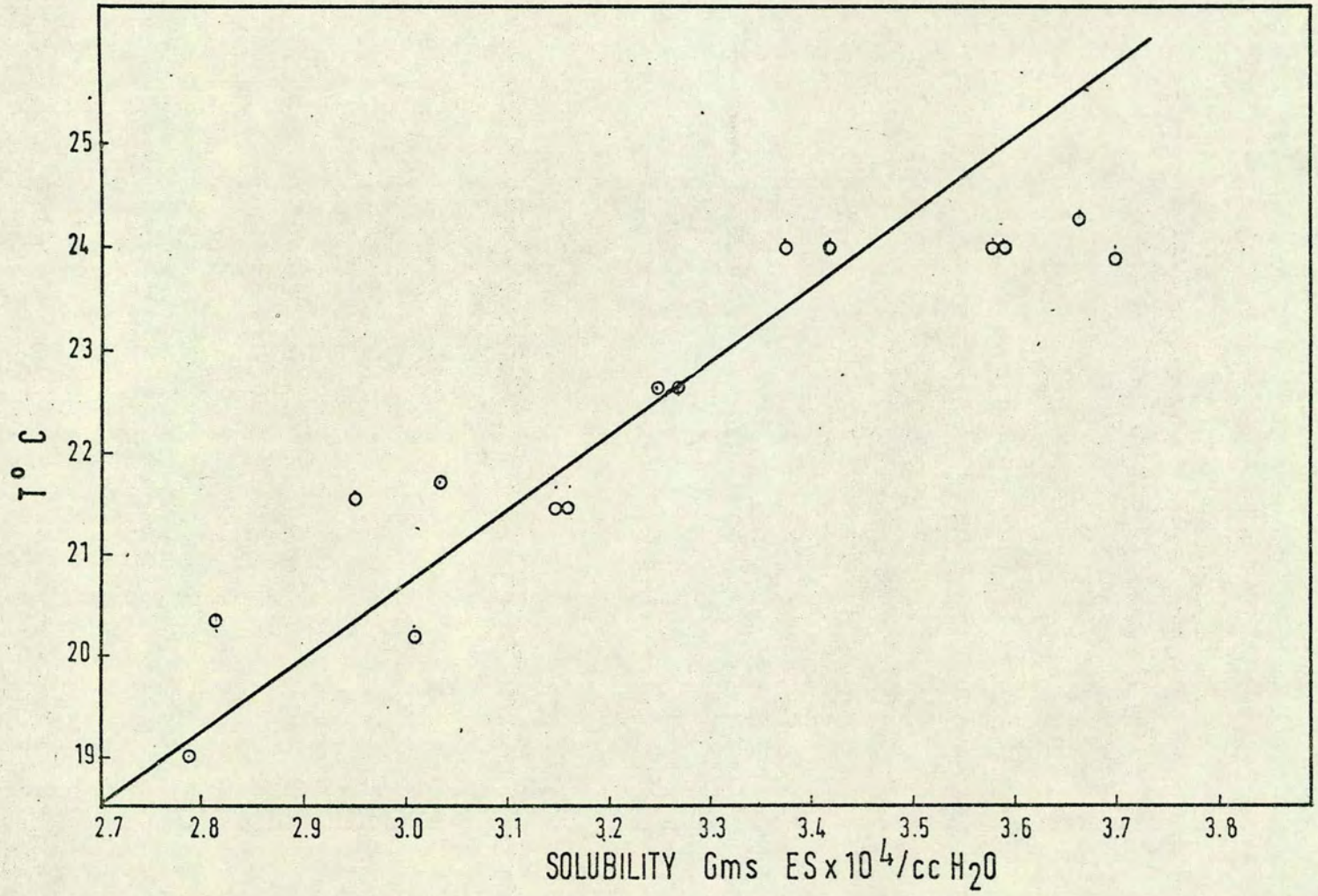

Fig.(3.3): Solubility of Ethyl Salicylate in Water as a Function of Temperature.

A probable source of error was the difficulty in drying the disk surfaces thoroughly before weighing.

These experiments were repeated using methyl salicylate to test the reliability of the method; the results were very satisfactory agreeing closely with the value of 7.74×10^{-4} gm/cc at 30^{o}C reported in the literature (123).

3.7 Determination of the Diffusivity of Ethyl Salicylate in Water

The diffusion coefficient of ethyl salicylate in water was determined using the experimental apparatus as an annular channel with the rotor stationary and with the inner wall transferring. Measured values of the effluent concentration at known flow rates and temperatures, together with the values of the solubility obtained above, were substituted into an expression analogous to the corresponding heat transfer problem ((124) case II).

The experimental diffusivities thus obtained were plotted as a function of temperature in figure 3.4 in which values estimated from the Wilke-Chang equation are also presented for comparison. The difference between the experimental values and the theoretical estimates is considerable (20-50%), but not unusual, since for aqueous solutions at infinite dilution experimental and theoretical values differ by as much as $\pm$ 30%, and by +153, -50% for other solvent-solute systems (125).

Errors in the determination of the solubility are reflected in the determination of the diffusion coefficient, as are errors in the measurement of the ester concentration in the outlet stream.

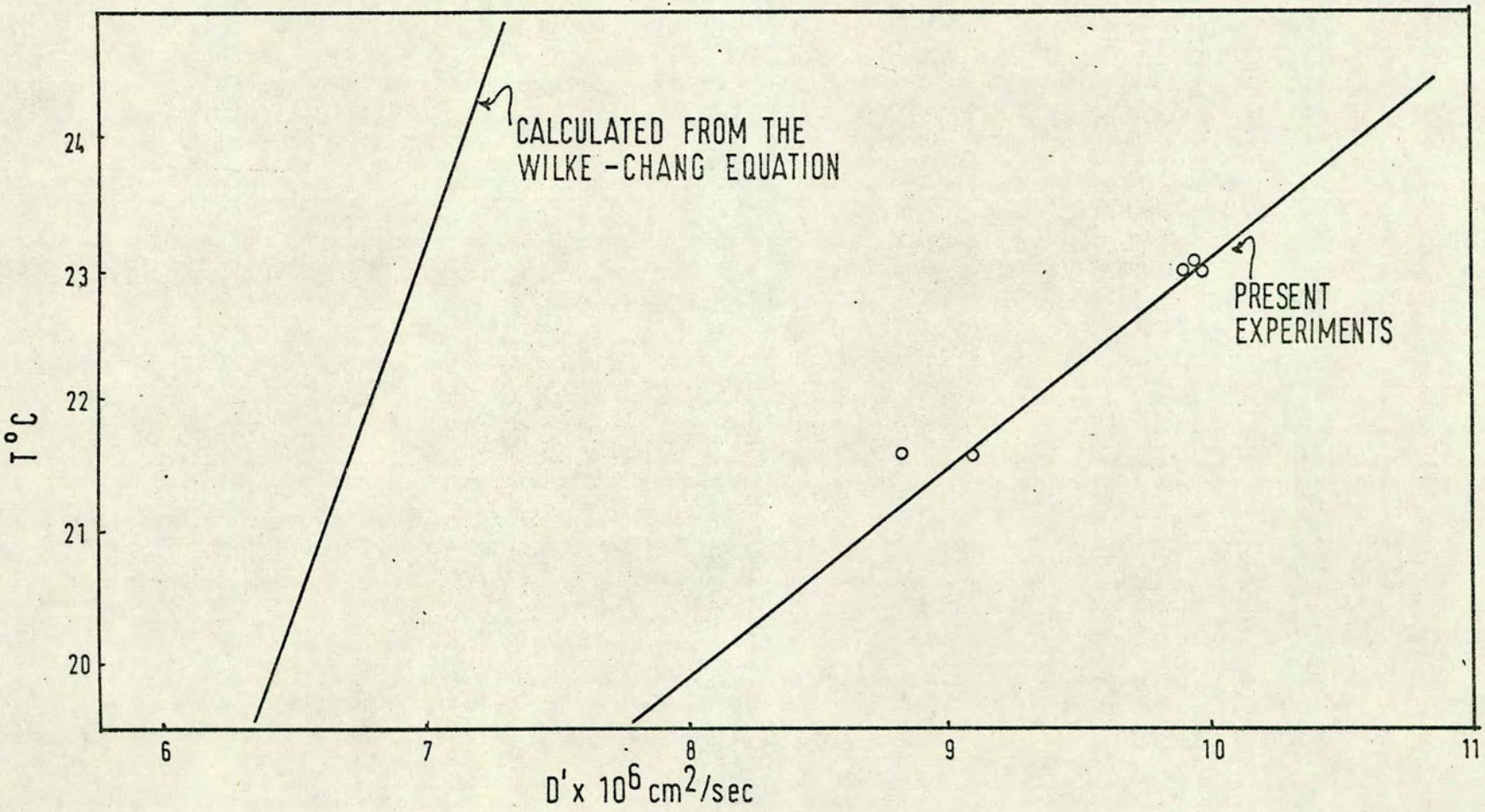

Fig.(3.4): Experimental and Wilke-Chang Diffusivity Values for Ethyl Salicylate in Water as a Function of Temperature.

If an uncertainty of ± 7% is assumed in each of these factors, and assuming negligible temperature and flow rate variations, the maximum error in the dimensionless cup-mean concentration will be approximately ± 8% at these low ester concentrations, giving a maximum ±12% error in the diffusivity coefficient estimation. The data, nevertheless is quite consistent suggesting that the random errors incurred are much smaller.

3.8 Determination of the Diffusivity of Ethyl Salicylate in the Polymer.

The solid phase diffusivity was found on the provisional assumption that it is not concentration dependent, by measuring the rate of uptake of pure swelling agent by weighed polymer disks of known thickness as a function of time (Fig 3.5). The diffusion coefficient of ethyl salicylate in the rubber phase was thus calculated as 1.76×10^{-6} cm^2/sec ± 5%; the diffusion coefficient adjusted to account for the increase in volume of the disks as swelling progresses is

$$D = D_{AB}(1-\phi)^{-3} \qquad 3.2)$$

where $\phi = V_S/1-V_S$, the volume fraction of solvent penetrating the polymer. At equilibrium, ϕ was found to be .140 for the present polymer-swelling agent system. The value of D is then 2.29×10^{-6} cm^2/sec.

3.9 Estimated "Constant Rate" Period

In order to calculate the "constant rate" period, it is necessary

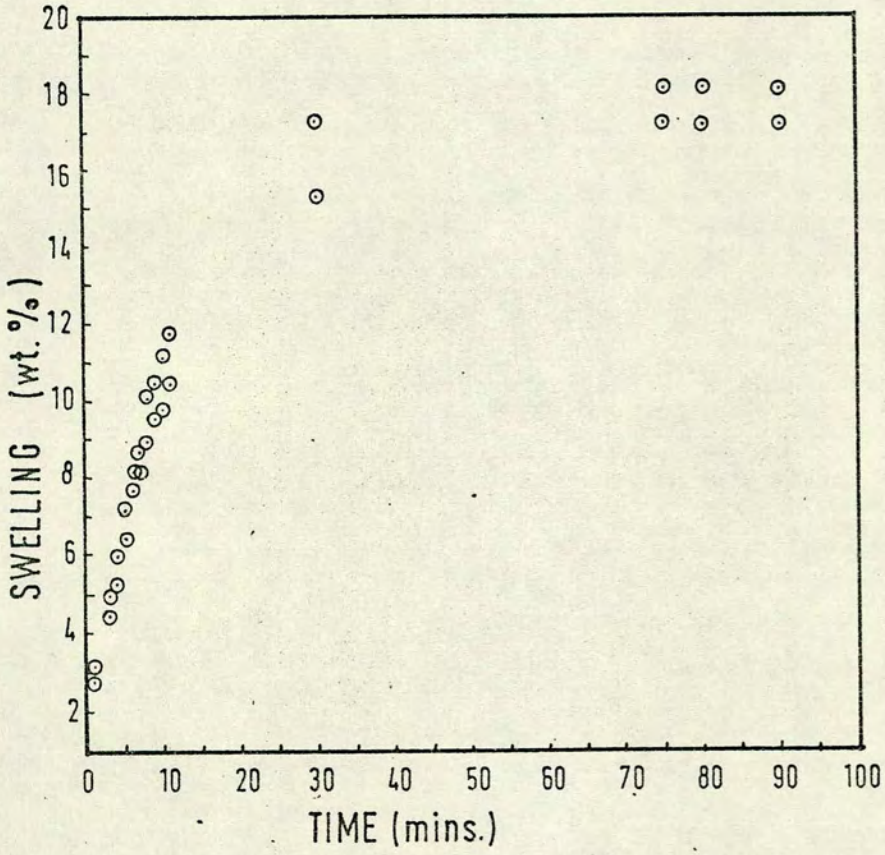

Fig.([3.5]): Percent Swelling of Silcoloid 201 Disks by Ethyl Salicylate as a Function of Time.

to find χ for the present polymer-swelling agent. This can be obtained using the Flory-Huggins equation and the equilibrium value of ϕ; χ accordingly has the value of 1.50. Using figures 3 and 4a of Macleod and Todd (122) extended by Kapur (126) to include the low values of f_1 and ϕ_E in this system, the maximum permissible fractional recession of the film $\delta'/\delta_1 = .016$ for the highest mass flux obtained in the mass transfer experiments, which was

$$F_S = h_D C_S = 3.87 \times 10^{-7} \text{gm/cm}^2\text{sec.}$$

The allowable recession of the film δ' is

$$\delta'/\delta_1 \; \delta_1 = 6 \times 10^{-4} \text{cm.}$$

and the "constant rate" period T' is

$$T' = \frac{\rho_R \delta'}{F_S} \simeq 25 \text{ min.}$$

3.10 Experimental Procedure

Before each experiment the polymer coating was reswollen to equilibrium in an ethyl salicylate bath and the apparatus was assembled. The rotational velocity was set initially and maintained constant throughout each run, it was then rechecked at the end of the experiment to verify that it had remained constant, this was done by stopwatch timing of revolutions counted visually or mechanically. Distilled water from the head tank was then allowed to flow through a rotameter and the experimental annulus, its flow rate being varied during each run to give an Re_z range of 30-100 for each rotational velocity studied. The temperature was controlled continuously with thermometers both at the inlet and outlet of the annulus. The samples to be analyzed in a Pye Unicam SP-1800

ultraviolet spectrophotometer were collected in glass-stoppered weighing bottles at the exit of the experimental apparatus.

3.11 Experimental Results

3.11.1 "Constant Rate" Period

The estimated "constant rate" period was checked experimentally for the maximum obtainable mass transfer rate from the inner cylinder of the apparatus. Samples of outlet water were collected at intervals and analyzed for the concentration of ester by ultraviolet spectrophotometry. The experimental results are shown in figure 3.6, T' is given by the point where the outlet concentration is 95% of the initial value, and was found to be approximately 9 min, or approximately $^1/_3$ of the calculated duration of the "constant rate" period.

This large discrepancy between the calculated and experimental values is probably due to the non-ideality of the ethyl salicylate-water system; this solution may be expected to show a positive deviation from Raoult's Law due to the difference of polarity and degree of association of the components. If this solution behaved ideally, the coating at the end of the "constant rate" period will be in equilibrium with an ethyl salicylate solution having a solute vapour pressure equal to 95% of the vapour pressure of pure ethyl salicylate. If there is a positive deviation from Raoult's Law, the concentration of ester in the layer of fluid adjacent to the polymer surface will be less than 95% of saturation, and the actual "constant rate" period will be shorter than the calculated value obtained by the methods of (122) for transfer into the gas phase.

Another source of error in the estimation of the "constant

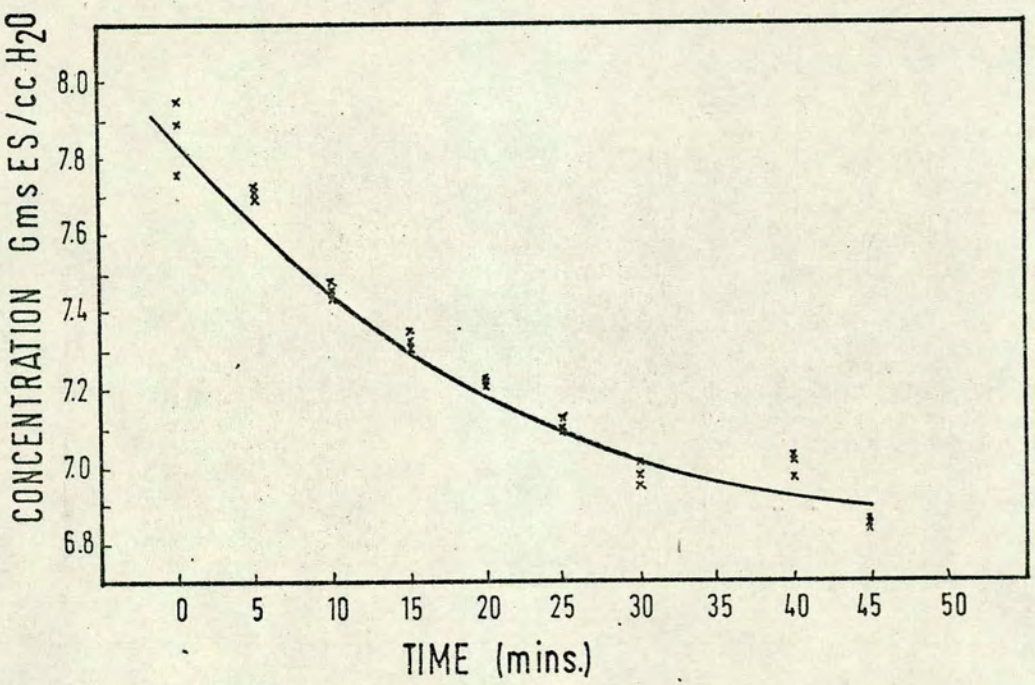

Fig.(3.6): Effluent Concentration of Ethyl Salicylate as a Function of Time in an Experimental "Constant Rate" Period Determination.

rate" period is the uncertainty in the value of the diffusivity of the swelling agent in the rubber phase, arising from the assumption of concentration independence in the calculation of diffusivity by the methods used here (Section 3.8). Since the diffusivity of the ester in the polymer probably increases with concentration, the concentration averaged value obtained here would then lead to an underestimate of the length of the "constant rate" period, while in this case the opposite is true.

3.11.2 Effect of Axial Flow on Mass Transfer

The range of Re_z studied (33-100) corresponded to fluid axial velocities of 18-57 $cm/_{sec}$. The experimental data, obtained by mass transfer measurements at fixed rotor speeds, covering a Ta range from 209-680 is scattered irregularly about their mean, and show no significant trend with Re_z. These results are in agreement with a similarly weak influence of axial Re_z on wall mass transfer rate reported in (108) for rotating coaxial cylinders operating with system having Sc numbers three orders of magnitude smaller. In the present experiments this weak defendence of mass transfer coefficient with Re_z holds whether mass transfer is from the inner wall (rotor), outer wall (stationary) or both walls.

3.11.3 Variation of Mass Transfer Rate with Rotor Speed

The results of the present experiments are presented in figure 3.7 plotted as Sh vs Ta for transfer rates from a) inner wall, b) outer wall, and c) both walls of the channel simultaneously. Since there was no observable influence of the axial Re on the mass transfer coefficient, the mass transfer results were taken irrespective of the Re_z for each

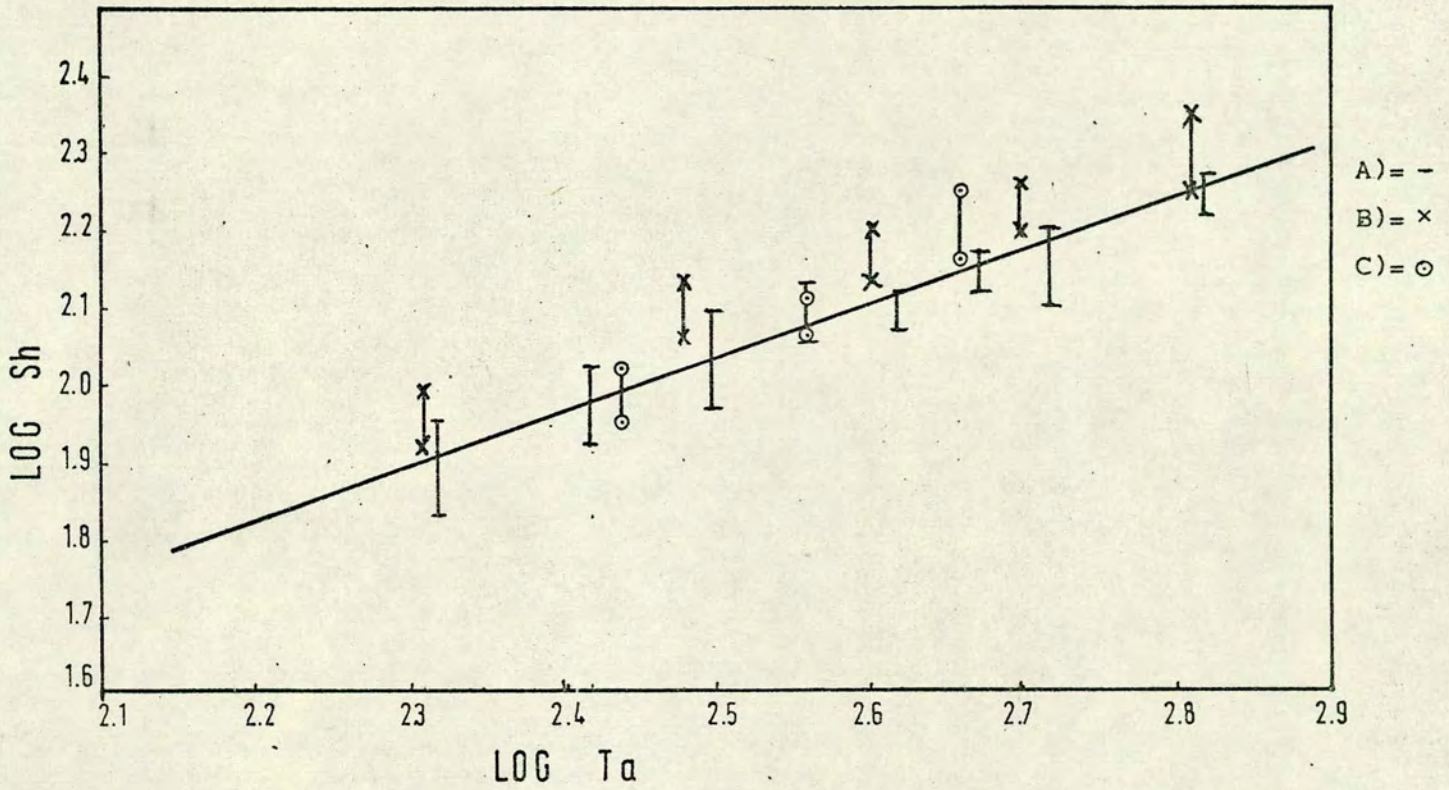

Fig.(3.7): Sh vs. Ta for Transfer from: A)Inner Cylinder; B) Outer and C) Both Annular Walls. Re=33-43.

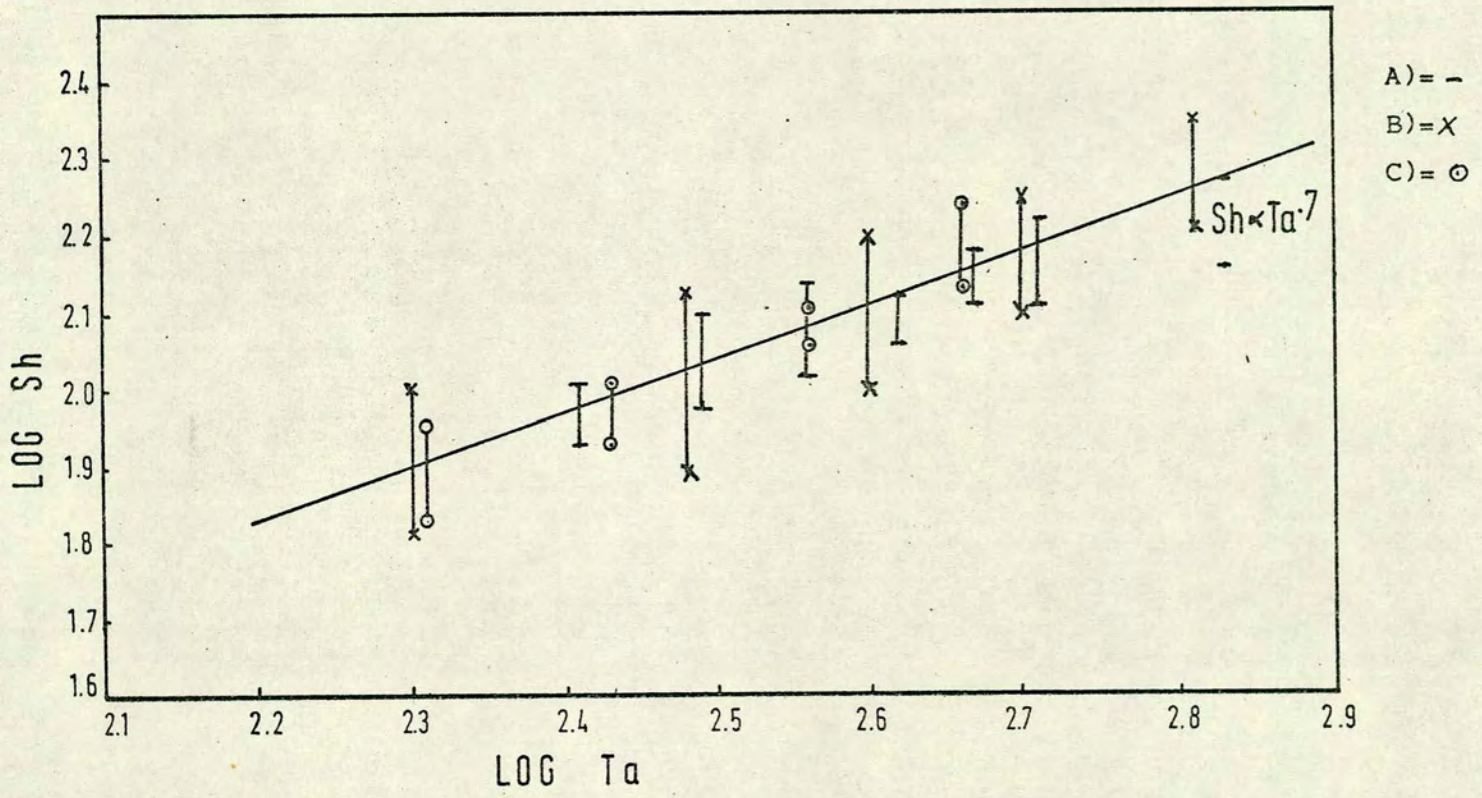

Fig. (3.8): Sh vs. Ta for Transfer from: A) Inner, B) Outer, and C) Both Annular Walls. Re= 33-100.

speed of rotation investigated, and averaged to find the effect of rotor speed on mass transfer rate. The dependence of mass transfer rate on rotor speed is significantly greater ($Sh \propto Ta^{.7}$) in this case than in the low Sc number systems of(108) which showed a dependence of Sh with $Ta^{\frac{1}{2}}$, also proposed by earlier studies on other low Sc or Pr number systems.

The second notable feature of the present experiments is the consistently higher mass transfer coefficients for mass transfer from the outer wall, compared with mass transfer from the inner wall; further, the average mass transfer coefficients for transfer from both walls, have intermediate values, thus there is no evidence of interaction between transfer processes at different walls of the annulus, such as was suggested in (108) for low Sc number systems.

3.12 Discussion of Results

Within the laminar and vortex region of flow the state of fluid motion in a narrow annulus ($0 < {}^{b}/R_{o} < .4$) is characterized by the dimensionless groups Ta and Re_z (108) and it follows that the mass transfer behaviour in the flow system can be characterized as follows:

$$Sh = f(Ta, Re_z, Sc, \text{mass fluxes at boundaries})$$

The results obtained from experiments in which only the axial flow rate and the rotor speed are varied, can therefore, be presented on plots of Sh vs Re_z and Sh vs Ta for constant specified Sc and wall fluxes, and it appears from comparison between present results and those reported in (108), that a large change of Sc, of three orders of magnitude, alters the dependence of Sh on Ta, but not the small dependence of Sh on Re_z. From figure 3.7, the relation between Sh and Ta for the present results with systems having an

Sc = 1260 can be expressed as follows:

3.3) $$Sh \propto Ta^{.7}$$

$$\text{or} \quad \frac{h_D 2b}{D_{AB}} \propto \left[\frac{\Omega_i R_i b}{\nu} \sqrt{\left({}^{b}/_{R_o} \right)} \right]^{.7}$$

$$\frac{h_D \nu}{\Omega_i R_i D_{AB}} \propto \left(\frac{\Omega_i R_i b}{\nu} \right)^{-.3} \left({}^{b}/_{R_o} \right)^{.35}$$

3.4) $$\frac{h_D}{\Omega_i R_i} \cdot 2Sc \propto \left(\frac{\Omega_i R_i b}{\nu} \right)^{-.3} \left({}^{b}/_{R_o} \right)^{.35}$$

3.5) $$\frac{h_D}{\Omega_i R_i} \cdot 2Sc \propto \left(\frac{\Omega_i R_i^2}{\nu} \right)^{-.3} \left(\frac{b}{R_o} \right)^{.05} \left(\frac{R_i}{R_o} \right)^{.3}$$

Equation (3.5) yields the same dependence of mass transfer coefficient on rotor speed as the equation proposed by Eisenberg, Tobias and Wilke (120) to correlate their results for systems of no axial flow and Sc numbers similar to those used here.

3.6) $$\frac{h_D}{V_\phi} Sc^{.644} = .0791 \left[\frac{2\Omega_i R_i^2}{\nu} \right]^{-.3}$$

Unfortunately, only a few of the results of Eisenberg et al., were obtained with sufficiently small ${}^{b}/R_o$ values to justify the use of Ta to characterize the state of fluid motion.

Equations 3.5 and 3.6 show the same dependence of mass transfer coefficient with rotor speed; furthermore, the present experimental results obtained with an asymmetric system, ie. when mass transfer was from the rotor alone, or symmetric, when there was simultaneous mass transfer from both annular walls, supports the hypothesis that the

mass transfer rate in this high Sc number system is affected only by the situation in the immediate neighbourhood of the mass transferring surface and the far boundary effects are insignificant. This is further supported by the agreement between the results obtained by Eisenberg et al.'s electrochemical mass transfer measurements at rotating cylindrical electrodes (where the wall flux conditions were anti-symmetric, ie. mass transferred into the fluid at one surface is removed at the other) which are also in agreement with their experiments involving the rate of elution of benzoic acid from rotating cylinders (asymetric system).

These findings that the mass flux situation in one boundary is practically independent of the mass transfer rate at the other, contrasts with the interdependence of the corresponding momentum fluxes, or wall shear stresses which are essential, by Newton's Third Law to maintain steady motion; this implies, in the absence of axial flow, that the torques on the inner and outer cylinder have to be the same. In a system with axial flow, the fluid enters the annulus with virtually zero angular momentum, and the same principle ensures that the torque at the outer cylinder can not exceed the torque on the inner cylinder, it follows that the momentum flux at the outer cylinder can not exceed that at the rotor surface.

The above reasoning is in disagreement with the current findings which reveal a mass flux at the outer wall greater than the mass flux at the rotor surface, and there seems to be no uniform relation between mass and momentum transfer rates at the two walls of the annulus in the present case. It is therefore possible that momentum and mass are transported in this case by different mechanisms, a conclusion

consistent with the different influence of rotor speed on torque and on mass transfer coefficient. There is little doubt that the angular momentum is transported in these systems by a mechanism involving the secondary vortices in the fluid, at least at high Ta numbers, and this leads to a variation of the friction factor with $Ta^{\frac{1}{2}}$ reported in literature. A similar variation of Sc with $Ta^{\frac{1}{2}}$ reported in (108) would imply that at low Sc numbers (≈1), where the momentum and mass transfer boundary layers are of similar thickness, both mass and momentum are transported by similar mechanisms. Accordingly, it seems reasonable to assume that in the present high Sc number system the concentration boundary layer is too thin to be significantly entered by the closed streamlines of the vortices which span the greater part of the annulus and serve as agents of momentum transport.

The dependence of mass transfer coefficient with $^{b}/R_{o}$ over the range $0 < {}^{b}/R_{o} < .4$ is small as can be seen from equation 3.5, and is in general agreement with the findings of (120). The smallest annular gap used by Eisenberg et al. was .173; over the range of $^{b}/R_{o}$ from 0-.4, eq. 3.5 predicts a change of about 6% whereas eq. 3.6 predicts no change of mass transfer coefficient with $^{b}/R_{o}$. In any case, a small dependence like that in eq. 3.5 would not have shown in the experiments of Eisenberg et al in view of the data scatter, and the small number of measurements made by them in this range of $^{b}/R_{o}$.

Equation 3.5 is therefore consistent with the experimental observations of Eisenberg et al. concerning the influence of the variables on h_D, but has the advantage over eq. 3.6 (for small gap widths) of consistency with the known dependence of the state of the fluid in the annulus on the group Ta, rather than the angular Re alone. Finally, the feeble

dependence of mass transfer coefficient on axial flow rate observed here and in (108) suggests that the strong influence of rotor speed on mass transfer would remain essentially unchanged at the limit where Re_z approaches zero; therefore, it is justified to compare the Sh-T_a relation in the present experiments with the results of (120) where there is no axial flow.

3.13 Conclusions

The assumption that the concentration boundary layer is so thin in the present high Sc system, as to be effectively outside the vortical core of the annular stream, is consistent with published measurements (127) of velocity and temperature profiles in rotating coaxial cylinder systems, and is consistent with the three main features of fig. 3.7 1) Channel wall layers are generally more disturbed at concave than convex surfaces (128), so that higher mass transfer rates can be expected at the outer wall of the annulus if it is a boundary layer process; 2) the independence of the transfer processes at the opposite walls is consistent with the hypothesis that the vortices do not enter the thin boundary layer, and are not the primary agents of mass transfer, therefore, the effect of rotor speed on transfer rate can be expected to reflect the influence on boundary layer resistance, rather than increased vortex convection, which supposedly control the transfer of momentum and mass at low Sc numbers.

3.14 Design Equation

The correlation proposed by Eisenberg et al. (eq. 3.6) can be rearranged into a more convenient form for design purposes:

3.6) $$\frac{h_D}{V_\phi} Sc^{.644} = .079\ Re_\phi^{-.30}$$

where $Re_\phi = \frac{V_\phi d\rho}{\mu}$ as defined in (120),

hence

3.7) $$\frac{h_D \cdot 2b}{D_{AB}} \cdot \frac{D_{AB}}{2b}\left(\frac{1}{V_\phi}\right) Sc^{.644} = .079\left[\left(\frac{V_\phi b\rho}{\mu}\right)\left(\frac{b}{R_o}\right)\cdot\left(\frac{d}{b}\right)\left(\frac{R_o}{b}\right)\right]^{-.3}$$

3.8) $$Sh = .079 \times \left(\frac{V_\phi b^2}{D_{AB} Sc^{.644}}\right) Ta^{-.3} \times 2^{-.3} \left(\frac{R_o}{b}\right)^{-.45}$$

and

3.9) $$Sh = .079 \times 2^{.7}\left[\left(\frac{V_\phi b\rho}{\mu}\right)\sqrt{\left(\frac{b}{R_o}\right)}\right]^{.7} \left(\frac{\mu}{\rho D_{AB}}\right)^{.356} \left(\frac{R_o}{b}\right)^{.05}$$

or

3.10) $$Sh = .128\ Ta^{.7}\ Sc^{.356}\ \left(b/R_o\right)^{-.05}$$

The line calculated from eq. 3.10 closely fits the present experimental data (Fig 3.7), and for design purposes is a more convenient form of equation 3.6, since the mass transfer coefficient is a function of the Ta number as defined in (108). Equation 3.10 will therefore be used as the main design equation for a membrane blood oxygenator.

Chapter 4

4.1 Design Equations

To investigate the mass transfer performance of a coaxial cylinder blood oxygenator, it was decided in the first instance, to build a prototype able to oxygenate 1 liter of blood/minute following the design guidelines of section 1.3. An oxygenator of this size allows fundamental blood-oxygenation studies and in-vitro testing without requiring large blood volumes; furthermore, it is of a useful size for meaningful tests in-vivo with experimental animals and for eventual clinical trials.

The principal design equation is the mass transfer correlation obtained by rearranging the correlation proposed in (120), the validity of which was supported by the experimental results of Chapter 3. In the modified form,the expression of Eisenberg, Tobias and Wilke for systems of high Sc numbers and perfect rotating coaxial cylinders becomes (Section 3.14)

$$4.1) \qquad Sh = \frac{h_D 2b}{D_{AB}} = .128\ Ta^{.7} Sc^{.356} (b/R_o)^{-.05}$$

Defining the logarithmic mean driving force for a veno-arterial percent blood saturation increase of 70-95%, with the corresponding inlet and outlet saturation concentrations Ci =.7 Cs and Co = .95 Cs, the required mass transfer area becomes

$$4.2) \qquad A = \frac{Q}{h_D} \left[\frac{.95Cs - .7Cs}{\text{Ln} \dfrac{(Cs-.7Cs) - (Cs-.95Cs)}{Cs - .95Cs}} \right]$$

4.3) $$A = \frac{Q}{h_D}\left(\ln 6\right)$$

The shear stress in the annulus can be calculated from the expression relating shear stress to the torque transmitted to the outer annular wall by the rotation of the inner cylinder

4.4) $$T = G \,/\, 2\pi R_i^2 L$$

Where G is obtained from the expression derived by Batchelor (130) from theoretical considerations

4.5) $$G \propto L\rho V\phi^2 Ri^2 (Re\phi)^{-\frac{1}{2}} (b/Ri)^{\frac{1}{4}}$$

The value of the constant of proportionality was obtained by substituting into eq. 4.5, the experimental values of Donnelly & Simon (129); accordingly, the value of the proportionality constant was found to be approximately 1.5.

The pressure drop across the annulus was calculated using the expression by Asamuna, quoted by Yamada (118) as best fitting the latter's experimental results in the laminar and vortex region.

4.6) $$\lambda = .27 Re_z^{-.25}(1.0 + (.5(\frac{Re\phi}{Re_z})^2))^{3/8}$$

and $$\Delta P = \lambda\rho L V_Z^2 / 4b(981).$$

The oxygenator length, priming volume, and surface to volume ratio are easily calculated; assuming both walls of the annulus are used for mass transfer

4.7) $$L = A/(2\pi(Ri + Ro))$$

4.8) $$PV = L.(\pi(Ro^2 - Ri^2))$$

4.9) $$S/V = A/PV$$

It is also of interest to know the rate of rotation of the inner cylinder as there is an upper mechanical limit which should not be exceeded.

4.10) $$RPM = 60\ Ta\ \mu/2\pi Rib\rho\sqrt{b/Ro}$$

Finally, the following values were assigned to the physical properties:

μ = .0291 gm/cm sec

ρ =1.05 gm/cc

D_{AB} =1.03 x 10^{-5} cm^2/sec.

4.2 Oxygenator Design

Three parameters can be varied independently when optimizing the size and operating conditions of a rotary coaxial cylinder membrane oxygenator. These parameters are the Ta number, the annular gap width b, and the outer annular radius Ro.

The Ta number range of interest covers the laminar and vortex region of flow up to the Ta numbers where transition to turbulence may be expected to occur (127,131), that is, a Ta number range from

100 to approximately 4000.

Similarly, upper and lower limits can be placed to the annular gap and outer cylinder radius. In the former case the range of interest of b is between .1 and 1 cm. Below .1 cm, the shear stress, surface to volume ratio and pressure drop are excessive, quite apart from the practical difficulties of rotating relatively large cylinders at high speeds with such small clearances between them. Finally, an upper limit has been placed on the outer cylinder radius corresponding to 20 cm. for an oxygenator handling 1 liter blood/minute. Again, in this case, mechanical and handling difficulties are the primary reasons for this specification; furthermore, it is difficult to obtain readily available cylinders of greater dimensions.

From the design equations of section 4.1) it becomes apparent that for a given oxygenation duty, the specifications of an oxygenator based on true coaxial cylinders will depend on the design parameters Ta, b, Ro as follows:

$$A \propto \frac{b^{1.05}}{Ta^{.7}\, Ro^{.05}}$$

$$T \propto \frac{Ta^{1.5}\, Ro^{.5}}{b^{2.5}} \qquad \text{assuming } Ri \simeq Ro$$

$$RPM \propto \frac{Ta^{1.0}\left(Ro^{.5}\right)^{-1}}{b^{1.5}}$$

The mass transfer area can be estimated using figure 4.1. The pressure drop and shear stress data obtained using the three

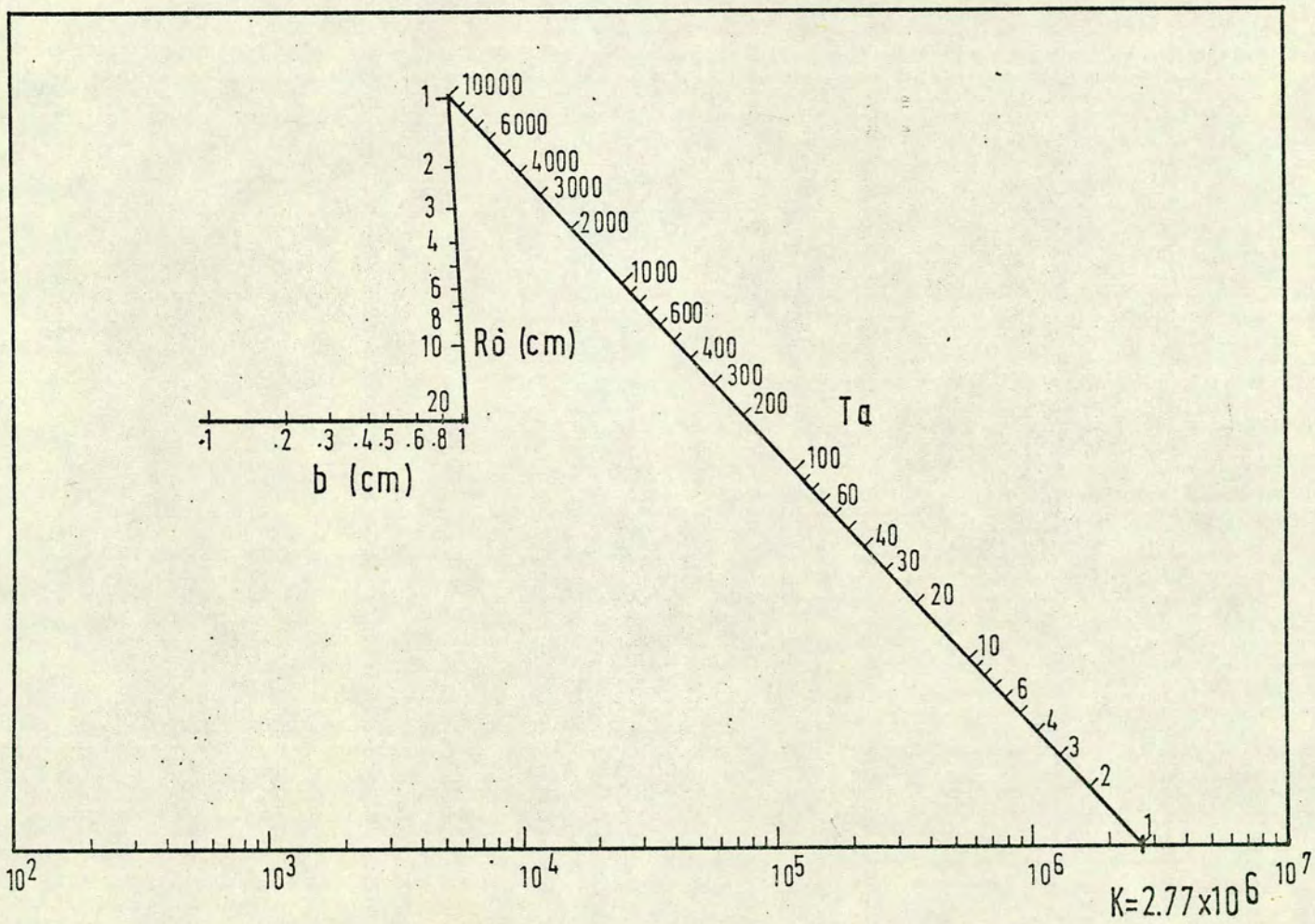

Fig.(4.1): Chart to Estimate the Oxygenation Area Required for a Coaxial Cylinder Oxygenator When the Parameters Ta,b,and Ro are Specified.

(APPENDIX 3)

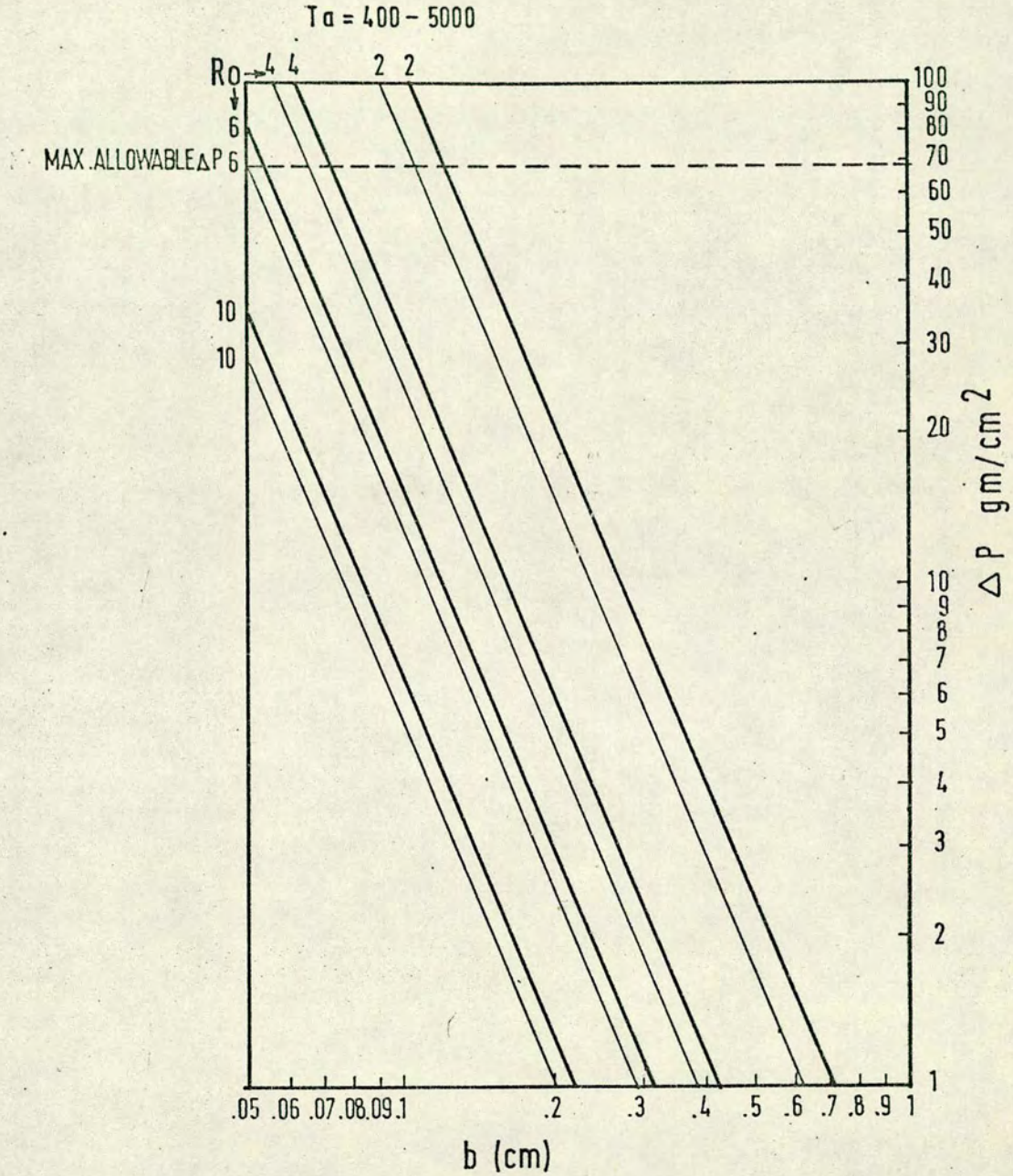

Fig. (4.2): Chart to Estimate the Pressure Drop Through the Annulus in the Oxygenator.

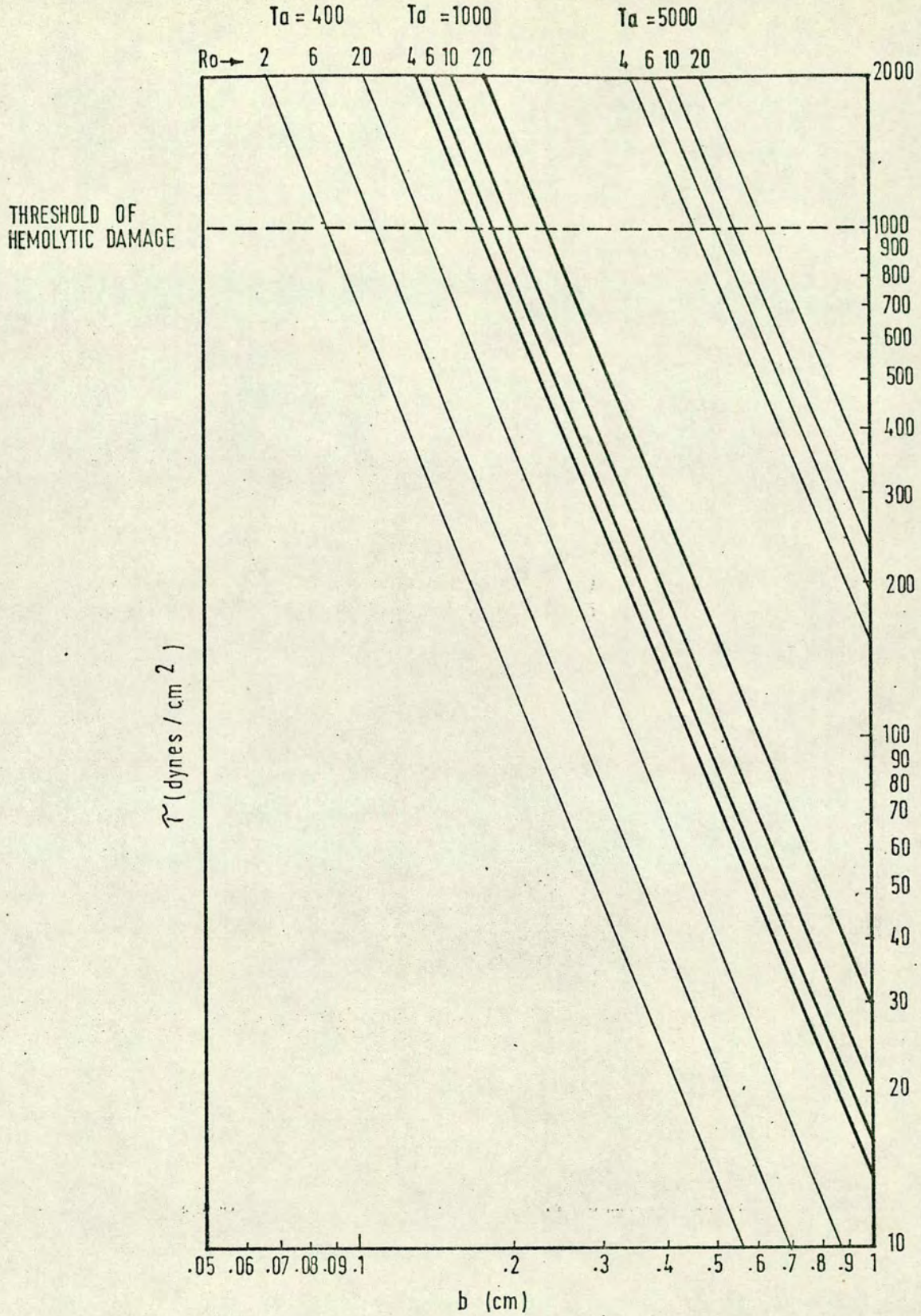

Fig.(4.3): Chart to Estimate the Shear Stresses at the Rotor Surface.

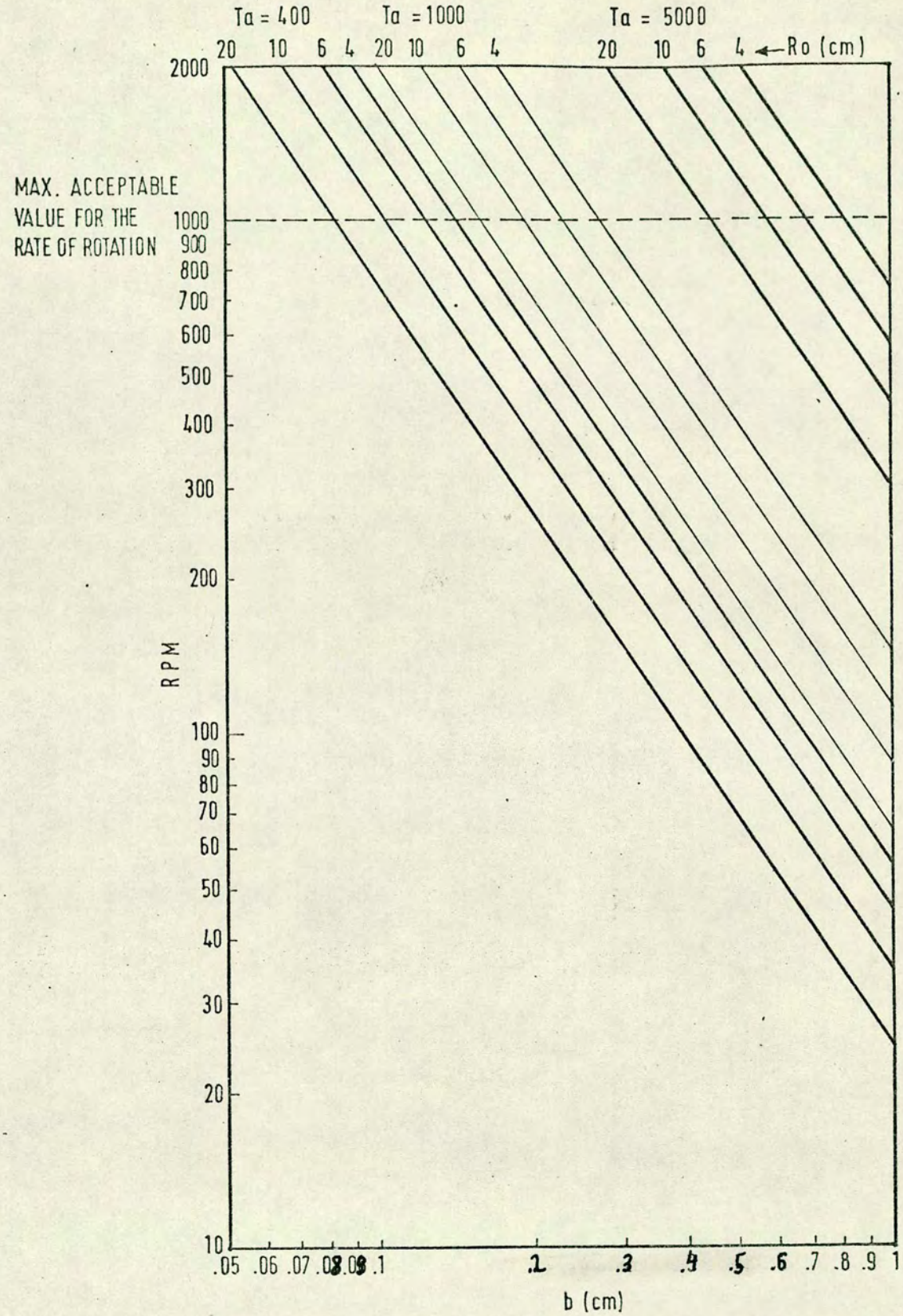

Fig. (4.4): Chart to Estimate the Rate of Revolutions of the Rotor Required to Meet the Oxygenation Duty When the Parameters Ta, b, and Ro are Specified.

parameters Ta, b and Ro, is presented in figures 4.2 and 4.3.

Within the specified ranges for the design parameters it can be seen from figures 4.1 and 4.2, that very few configurations satisfy the requirements laid out in section 1.3.3. At low Ta numbers and small annular gaps, the mass transfer area is left relatively small, but the shear stress in the annulus, and the required speed of revolution is prohibitively high, as in the pressure drop if Ro is also small. Therefore, in balance the best configurations have intermediate annular gaps of .4-.6 cm. In order to maintain the mass transfer area less than 0.5 m^2/liter of blood throughput, Ta numbers at the upper region of thelaminar and vortex regime (3000-5000) are required. If larger annular gaps are used, turbulent annular flow may be required to maintain the mass transfer area within the specified limits. Similarly, an optimal design requires intermediate outer annular radii of 6-10 cm. While the cylinder radius has little influence on the mass transfer area, it has a substantial direct bearing of the shear stress and the rate of revolution. On the other hand, cylinder radii smaller than 6 cm mean a longer apparatus, since the required mass transfer area must be accommodated in the longitudinal dimension; this in turn poses problems as the pressure drop quickly increases beyond permissible levels.

Summarizing, the optimal design will have annular gaps between .4 and .6 cm with an outer annular radius of 6-10 cm, and operating at Ta numbers of 3000-4000. The actual dimensions of the oxygenator, dictated by the availability of materials, are given in table 4.1.

Table 4.1 Dimensions of the Rotating Coaxial Cylinder Oxygenator

Diameter of inner cylinder (without membrane)	11.5 cm
Diameter of inner cylinder (with membrane in place)	11.7 cm
Diameter of outer cylinder (ID)	12.9 cm
Annular gap	.6 cm
Length of fluid path	40.4 cm
Length of transferring section	32.9 $\pm$ .5 cm
Lengths of transferring section used for mass transfer experiments	19.7 cm 20.4 cm
Mass transfer areas used in mass transfer experiments	636.4 cm^2 748.1 cm^2

4.3 Description of the Apparatus

The principle of the stationary shaft construction (132) was adopted as the basis for the membrane oxygenator design. This arrangement has no moving seals or bearings directly in contact with the annular fluid (Figs. 4.5-4.8), and is based on a stationary shaft fixed rigidly to a carrying plate, upon which the hollow closed rotor turns in journal bearings. The rotor was belt driven around the bearings, while the outer, stationary cylinder was supported on guiding rods, independently of the rotor.

The shaft itself was made from a 3.81 cm OD aluminium alloy tube fitted with hollow steel end plugs. The plug at the top end was machined integral with a flange 5 cm in diameter, and above it was a threaded extension and gas inlet nozzle. The shaft assembly was secured in place by a washer and nut screwed onto the plug thread from the opposite side of the carrying plate. Oxygen was supplied to the interior of the rotor through the gas nozzle (A) and the hollow shaft.

At the lower end, the shaft plug accommodated the lower bearing, a ball-race supported from underneath by a nut (B) screwed onto the threaded plug extension. In this manner, substantial weight was added to the base of the shaft, thereby reducing the period of vibration of the assembly. The rotor itself was made from a 4" nominal bore PVC tube with a substantial wall thickness to ensure dimensional stability. The rotor tube (48.9 cm long) was machined to an OD of 11.5 cm, and fitted with a conical PVC plug at the lower end. Inside the tube, a steel insert engaged the lower bearing,

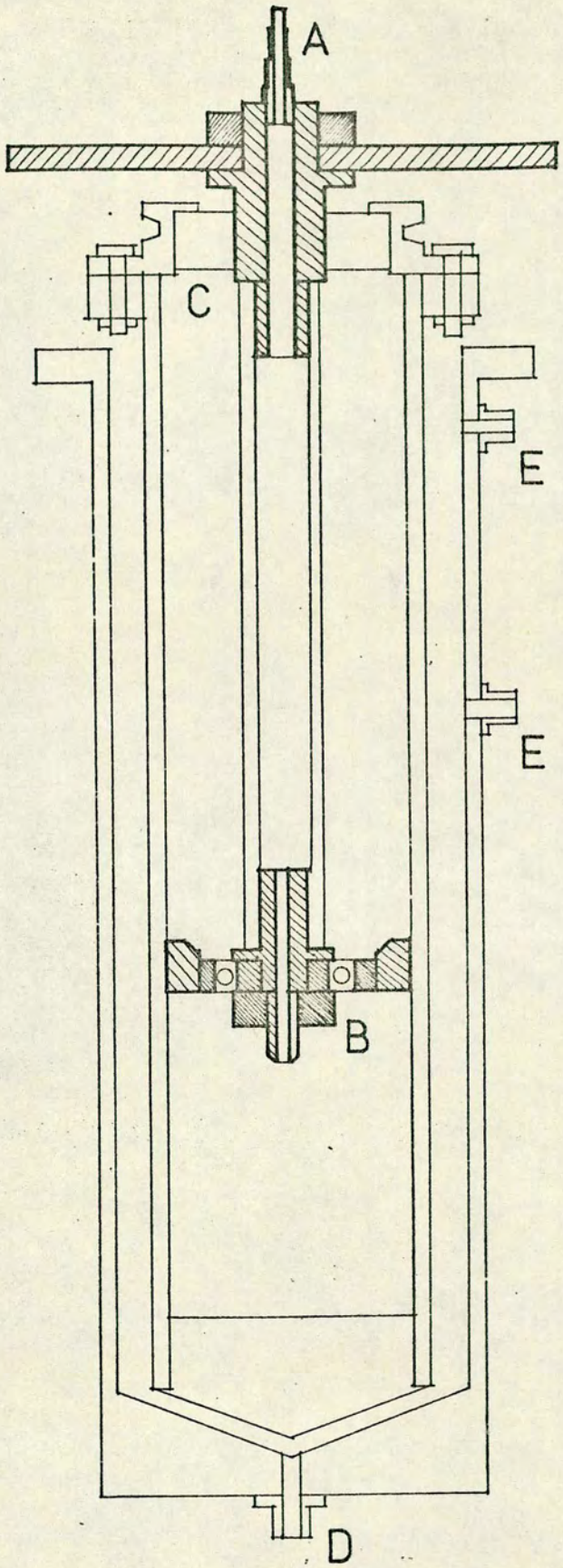

Fig.(4.5): Coaxial Cylinder Oxygenator.
Shaft Assembly.

while at the top end, the rotor tube was fitted with a PVC flange by means of which the rotor could be bolted to a similar aluminium flange integral with the drive pulley. This pulley, and therefore the weight of the rotor, was carried by a duplex bearing (C), designed to accept both axial and journal loads, fitted to the shaft. Holes (1.27 cm diameter) were drilled at regular intervals in the wall of the rotor allowing the perfusing gas to leave the interior of the tube; therefore, a porous underlayer to the oxygenation membrane was necessary to ensure proper gas distribution to the entire oxygenation area. Excess O_2, as well as waste CO_2 left at the top through the bearings.

Although it would have been desirable to use glass, which allows flow visualization, for the outer cylinder, the weight and cost of precision bore glass of such large diameters would have been prohibitive and plastic materials were chosen. Thick walled PVC tubing was chosen rather than perspex, due to its better dimensional stability.

The outer cylinder was a tube 43.2 cm long of 5" nominal bore, machined to an ID of 12.9 cm. At the base it was fitted with a PVC plug with a conical recess matching the rotor plug. An axial blood inlet at the center of the plug (D), ensured a good hemodynamic entry section with no regionsof flow stagnation; furthermore by accelerating the incoming blood outwards, it was expected that a centrifugal pumping action would be obtained. Blood outlets were provided 35 and 46 cm from the base (E), although only the former was used in the mass transfer experiments. At the top of the outer cylinder, a PVC flange was provided for external support, while inside the tube a removable PVC

while at the top end, the rotor tube was fitted with a PVC flange by means of which the rotor could be bolted to a similar aluminium flange integral with the drive pulley. This pulley, and therefore the weight of the rotor, was carried by a duplex bearing (C), designed to accept both axial and journal loads, fitted to the shaft. Holes (1.27 cm diameter) were drilled at regular intervals in the wall of the rotor allowing the perfusing gas to leave the interior of the tube; therefore, a porous underlayer to the oxygenation membrane was necessary to ensure proper gas distribution to the entire oxygenation area. Excess O_2, as well as waste CO_2 left at the top through the bearings.

Although it would have been desirable to use glass, which allows flow visualization, for the outer cylinder, the weight and cost of precision bore glass of such large diameters would have been prohibitive and plastic materials were chosen. Thick walled PVC tubing was chosen rather than perspex, due to its better dimensional stability.

The outer cylinder was a tube 43.2 cm long of 5" nominal bore, machined to an ID of 12.9 cm. At the base it was fitted with a PVC plug with a conical recess matching the rotor plug. An axial blood inlet at the center of the plug (D), ensured a good hemodynamic entry section with no regionsof flow stagnation; furthermore by accelerating the incoming blood outwards, it was expected that a centrifugal pumping action would be obtained. Blood outlets were provided 35 and 46 cm from the base (E), although only the former was used in the mass transfer experiments. At the top of the outer cylinder, a PVC flange was provided for external support, while inside the tube a removable PVC

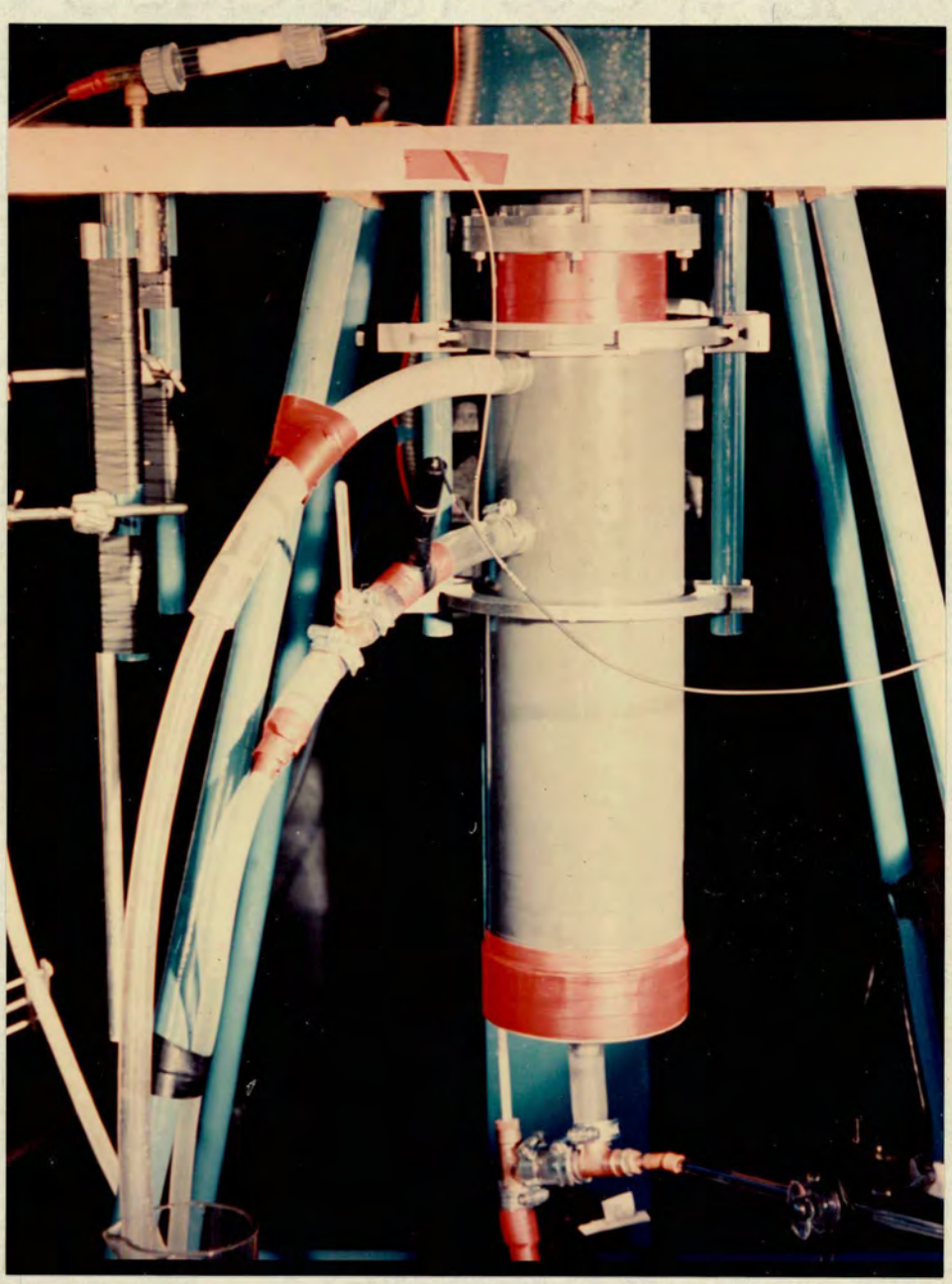

Fig.(4.6): Assembled Coaxial Cylinder Oxygenator.

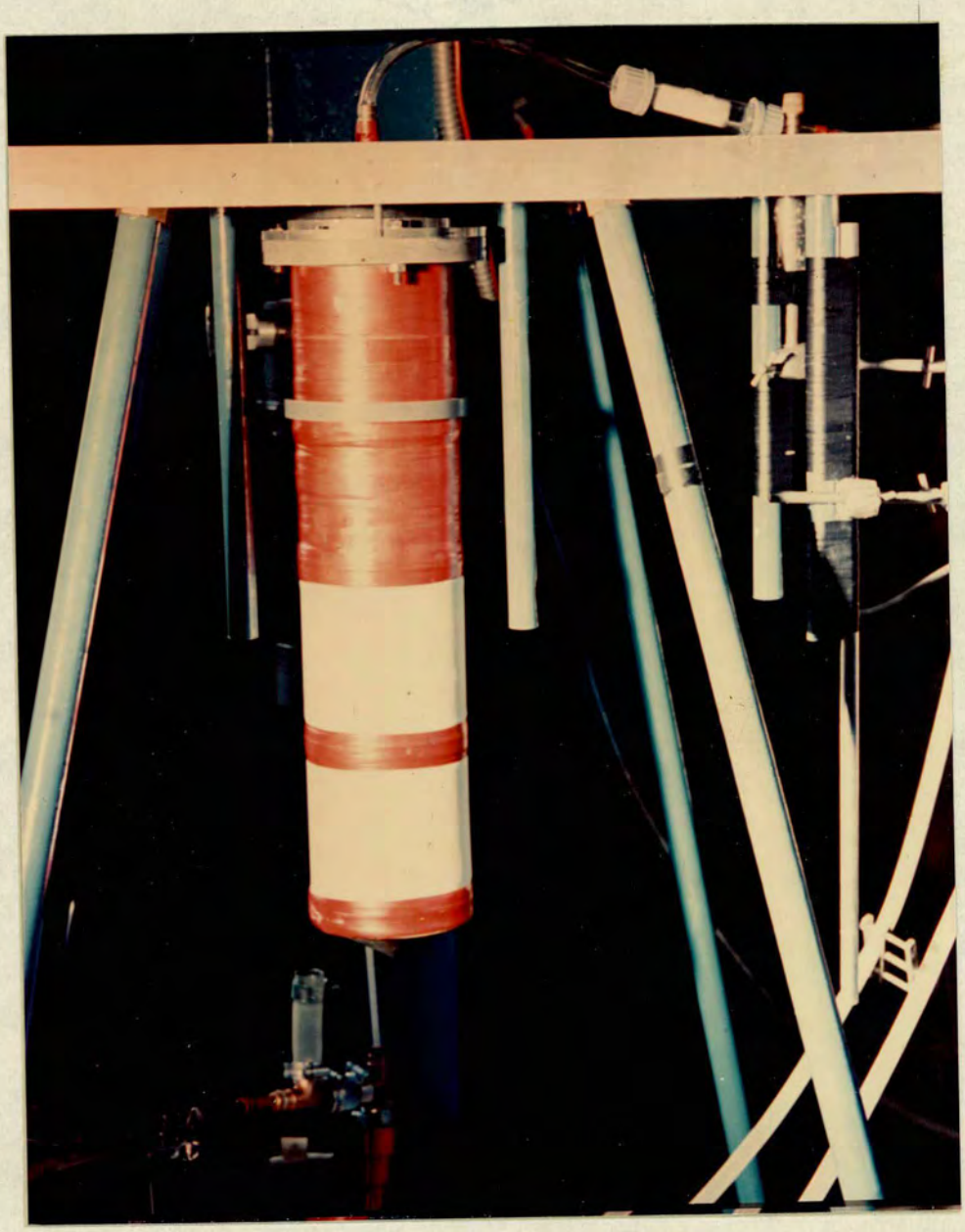

Fig.(4.7): Rotor with Membrane in Place.

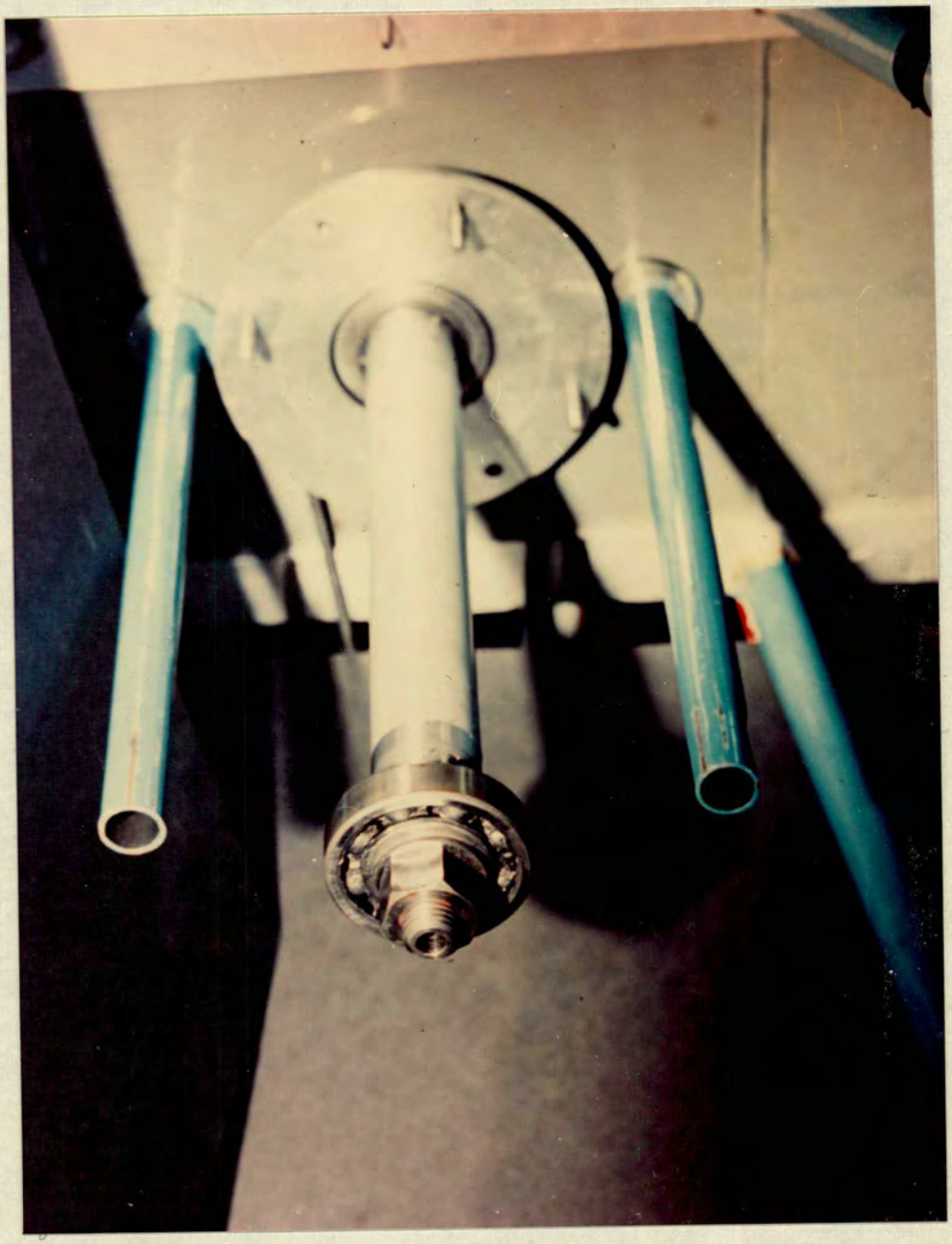

Fig.(4.8): Stationary Shaft Assembly.

ring barely cleared the rotor and served to prevent fluid overflow.

The support and positioning of the outer cylinder was accomplished with two clamps (fig.4.9) which were in turn secured by clamping screws to the guiding rods. The weight of the cylinder was borne by the recessed portion of the upper clamp, while the precise centering of the tube with respect to the rotor was accomplished by adjusting the radial nylon screws passing through the walls of the clamp at 120^{o} to each other and engaging the cylinder walls.

The guiding rods, made from steel tubes 3.17 cm OD fixed rigidly to the oxygenator carrying plate, also served as guides when assembling or dismantling the apparatus, thereby avoiding damage to the membrane as a result of accidental contact of the inner and outer cylinders.

No sliding seals, traumatic to blood, were provided between the rotor and the outer cylinder, and therefore a small free liquid surface (3.8 cm^2) was exposed to air. Blood trauma due to this small interface was assumed to be of no importance, since the interfacial area is some orders of magnitude smaller than that present in bubble or film oxygenators.

Three oxygenator cylinder assemblies like that described could be installed on the oxygenator stand, which was designed to provide rigidity and stability, while at the same time having a light construction (Fig. 4.10). Four legs made from 3.17 cm steel tubes were joined by tie bars 10 cm from the base, and fitted with brass plugs at either end. These legs were tilted inwards at an angle of 60^{o} to the horizontal. In this manner a square 1 meter per side was delineated at the base, and a 30 cm per side square at the top.

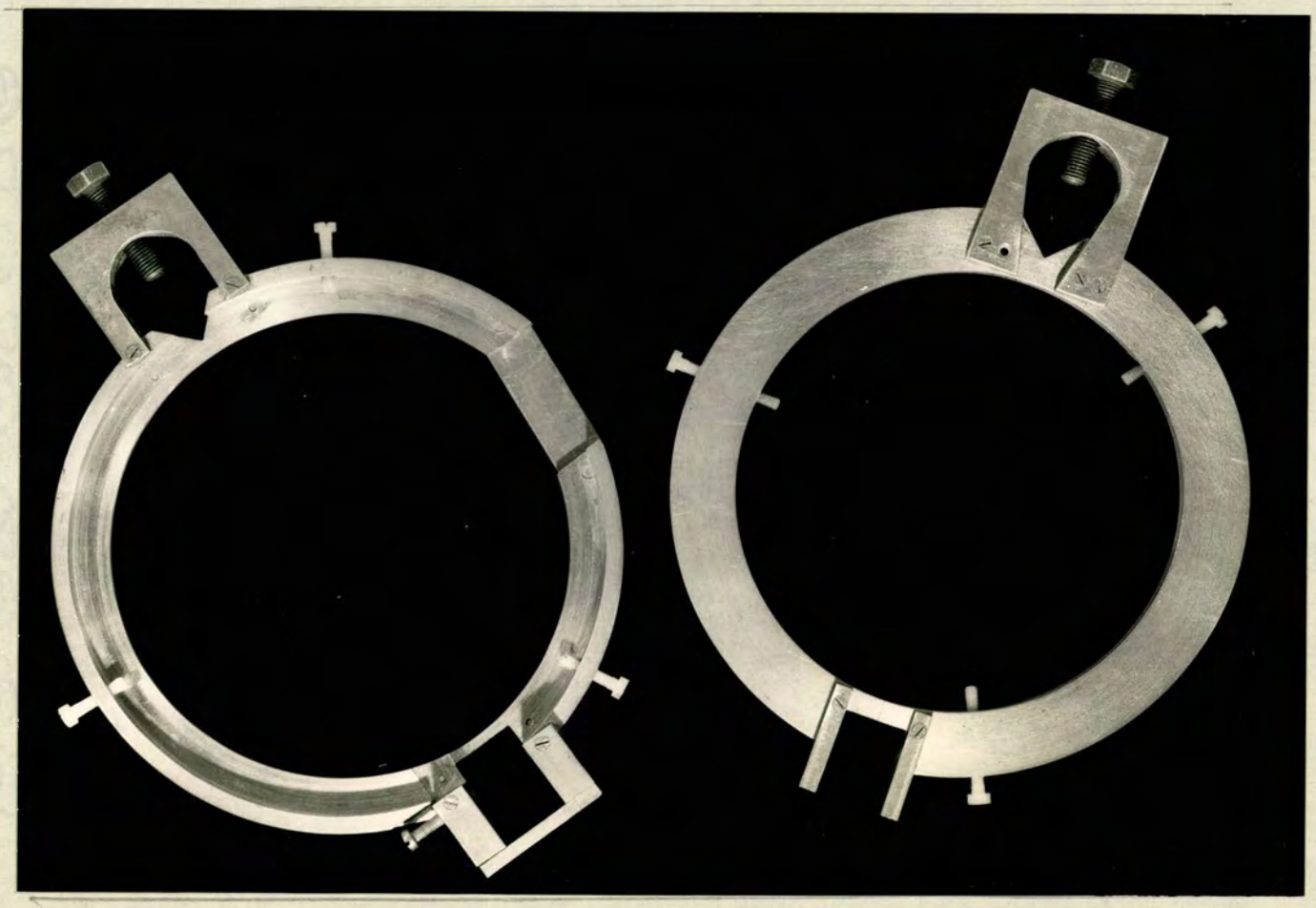

Fig.(4.9): Outer Cylinder Support Rings.

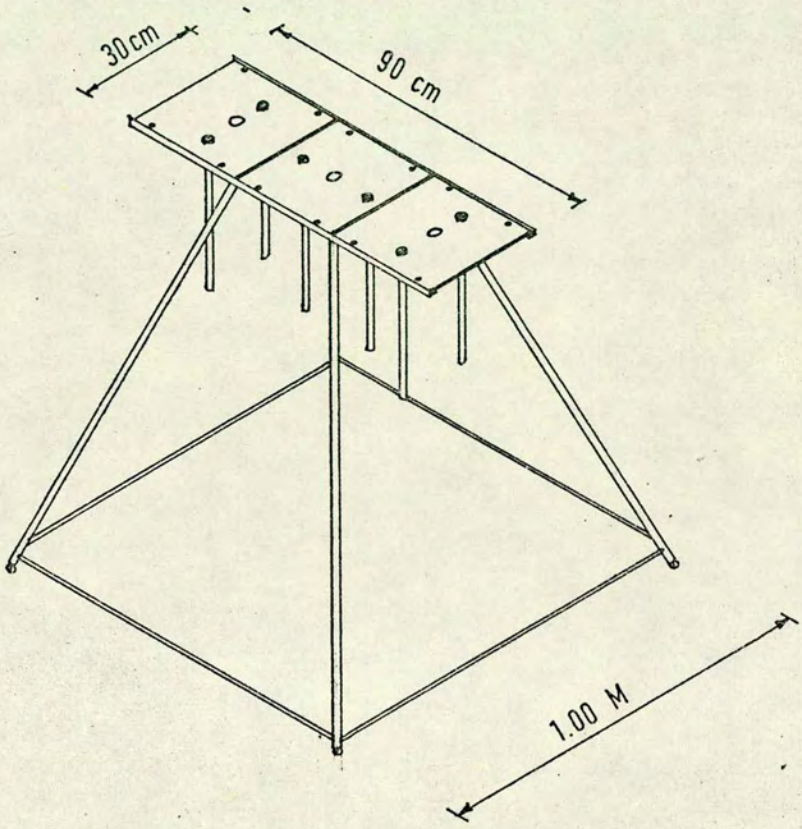

Fig. (4.10): Oxygenator Stand.

At the lower end the brass plugs accepted threaded brass spheres. By means of these, the height could be regulated to overcome irregularities in the floor; alternatively, castors could be fitted if mobility of the stand is desired. At the top, two 90 cm long - 2.54 cm aluminium angle lengths were fixed to the brass plugs, and three oxygenator carrying plates fixed between them. The oxygenator carrying plates were 30 cm a side steel squares 1.27 cm thick, with a large circular hole in the center to accommodate the shaft assembly, and two round holes equidistant from the center to accommodate the guiding rods.

The drive was provided by a three phase $\frac{3}{4}$ HP motor with variable speed gear, giving an output between 320 and 2880 RPM; lower speeds were then obtained by using additional pulleys. The motor was mounted independently of the stand, on a 6" channel beam anchored to the floor and roof of the laboratory, to minimize the transmission of vibration to the apparatus.

4.4. Membrane Selection

The ultrathin and fragile silicone membranes available proved extremely difficult to handle and assemble in place. While these difficulties can be overcome by producing membrane "socks" which would stretch over the rotor, the problems of lining the concave surface of the outer wall of the annulus are obvious, and might preclude the use of both annular walls for oxygenation. Furthermore, it is at least in principle, possible to improve the oxygen transfer rates in this apparatus indefinitely, but it would be pointless to do so if present membranes are used, since membrane resistance would soon become the

limiting factor to O_2 transfer, and before the O_2 transfer capacity of the membrane is reached, the mass transfer area required would be dictated by insufficient CO_2 transfer.

Accordingly, new materials were sought, and a microporous membrane was chosen. Goretex (W.L. Gore Associates, Newark, Delaware, USA) an expanded, cold drawn PTFE membrane, free of additives, can be manufactured to a required pore size and void space fraction. Its permeability to gases is orders of magnitude greater than the best diffusional membranes (133)(Fig.4.11), and due to its hydrophobic nature, liquids can not penetrate the pores, except at hydrostatic pressures much greater than those encountered in an oxygenator (133). Similarly, if a small pore size is specified, it is unlikely that gas bubbles will be formed in the blood phase due to the gas pressure in the oxygen phase at the opposite side of the membrane.

The high gas permeability of this material allows relatively thick and strong sheets to be used. The advantages in handling and reliability are therefore substantial, and as it can be obtained with a porous backing, there is no need to assemble a separate porous underlayer onto the cylinder surface.

Goretex appears to have good biocompatibility (134,135) and it, as well as other porous materials have been used in oxygenators before (136,83,84), although not in a situation where the blood-side mass transfer coefficient was high enough to take advantage of their high gas permeability.

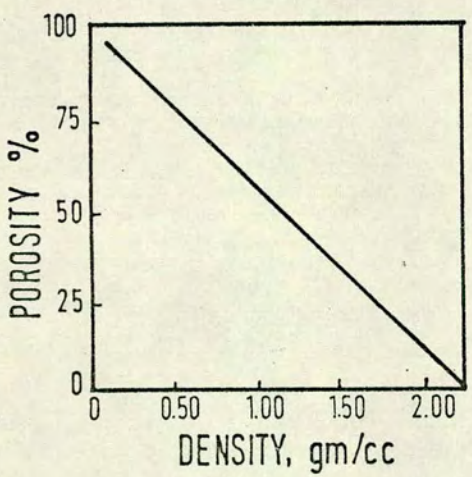

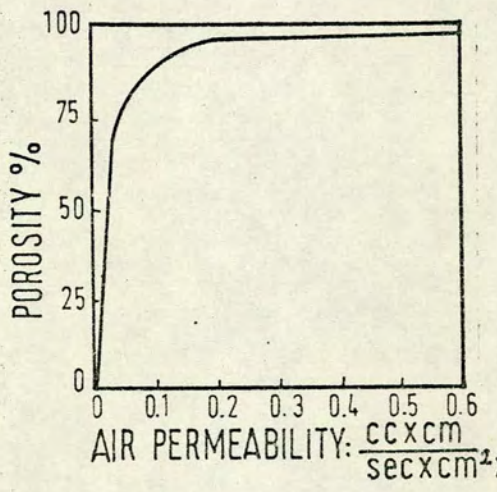

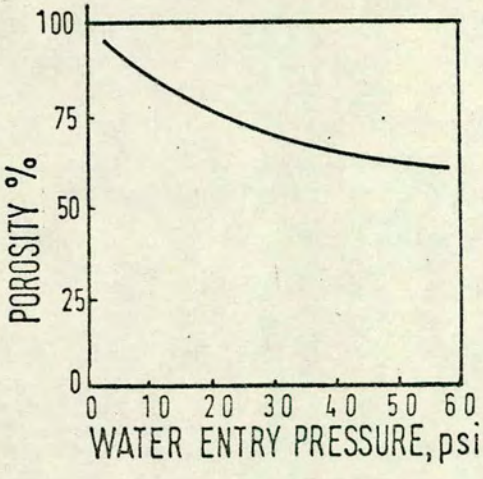

Fig. (411): Membrane Data Graphs.

When using microporous materials as oxygenation membranes, it must be kept in mind that these are not diffusional membranes, and a gas-blood interface is present. Therefore, long term atraumatic use of these membranes is dependent on the traumatic effects of the blood-gas interface. If these effects are mainly due, as is currently suggested, to the unstable nature of this interface, resulting in the continuous renewal of protein at the interface where it is denatured and remixed into the bulk of the blood (section 1.1); then use of porous materials for long term perfusion would depend on the solid surface being able to immobilize the denatured protein present at the interface, and acquire a protective coating in the same manner as other solid surfaces (section 1.1).

On the other hand, if there are more complex physical-chemical reasons for the traumatic nature of the blood-gas interface to the plasma proteins, porous materials may well prove unsuitable, as oxygen transported by diffusion across the membrane will have different interfacial properties as compared with oxygen transported by convection through the pores of Goretex; hence, some blood oxygenation and blood damage experiments, particularly the investigation of protein denaturation, would be required once the mass transfer performance of the oxygenator is established.

Chapter 5

5.1 Mass Transfer Experiments

5.1.1 Experimental Method

When investigating the mass transfer performance of the oxygenator, the non-circular crossection of the rotor had to be considered, including what effect, if any, such geometry would have on mass transfer. The non-circular, but smooth and cylindrical form of the rotor was due to the addition of a 2.5 cm wide longitudinal adhesive tape required to assemble in place the foam-backed Goretex membrane. At the centre of the tape the maximum protrusion was 2 mm. into the .6 cm annular gap.

For a systematic investigation of the oxygenation performance of the apparatus, a system involving the oxygenation of blood was deemed impractical, both because of the large blood volumes required, and because of the uncertainty about the physical properties and the state of blood. Therefore, it was decided in the first instance, to oxygenate water in the apparatus under test. The Sc numbers for oxygen-water systems at mains temperatures vary between 400-500, and are thus much lower than those common in blood oxygenation, or in the ester experiments described in Chapter 3. Hence, additional experiments oxygenating .4M and .568M sucrose solutions were also proposed. These systems have Sc numbers of 969 and 1962 respectively.

The experimental method involved the deoxygenation of the experimental fluid, and its subsequent oxygenation as it flowed through a coaxial cylinder assembly. To implement this method the following measurements are necessary: a) the inlet and outlet O_2 concentrations in the experimental fluid, b) the inlet and outlet fluid temperatures,

c) the flow rate of the experimental fluid, and the required O_2 flow rate, d) the angular velocity of the rotor, and e) the atmospheric pressure. Furthermore, if the physical properties of the oxygen-fluid systems are known, it is possible to present the data in dimensionless form.

5.1.2 Oxygenator Testing Circuit

The oxygenator testing circuit (Fig. 5.1, 5.2) consisted of rotameters for measuring the experimental flow rates of liquid and O_2, and a Travenol disposable bag bubble oxygenator used for deoxygenating the experimental liquid by bubbling nitrogen gas through the rising column of liquid. The circuit also included thermometers inserted at the inlet and outlet of the annulus, and the inlet and outlet O_2 concentrations were monitored with an EIL Oxygen meter, and a Beckman Oxygen Field Analyzer respectively. To ascertain whether both meters gave mutually consistent readings for the oxygen content, they were tested at the beginning and at the end of the experimental work, by immersing the oxygen probes in the same solution through which air was bubbled, and ensuring that there was agreement between the two readings.

For the experiments involving the lower Sc number system, water from the mains was used in an open circuit, and discarded at the sink after flowing through the rotameter, deoxygenator and coaxial cylinders. The test circuit was then converted to a closed circuit for the experiments using sucrose solutions as the experimental liquid. In this case, the solutions were collected in a reservoir replacing the mains-sink connections. A roller pump was incorporated to drive the fluid through the circuit.

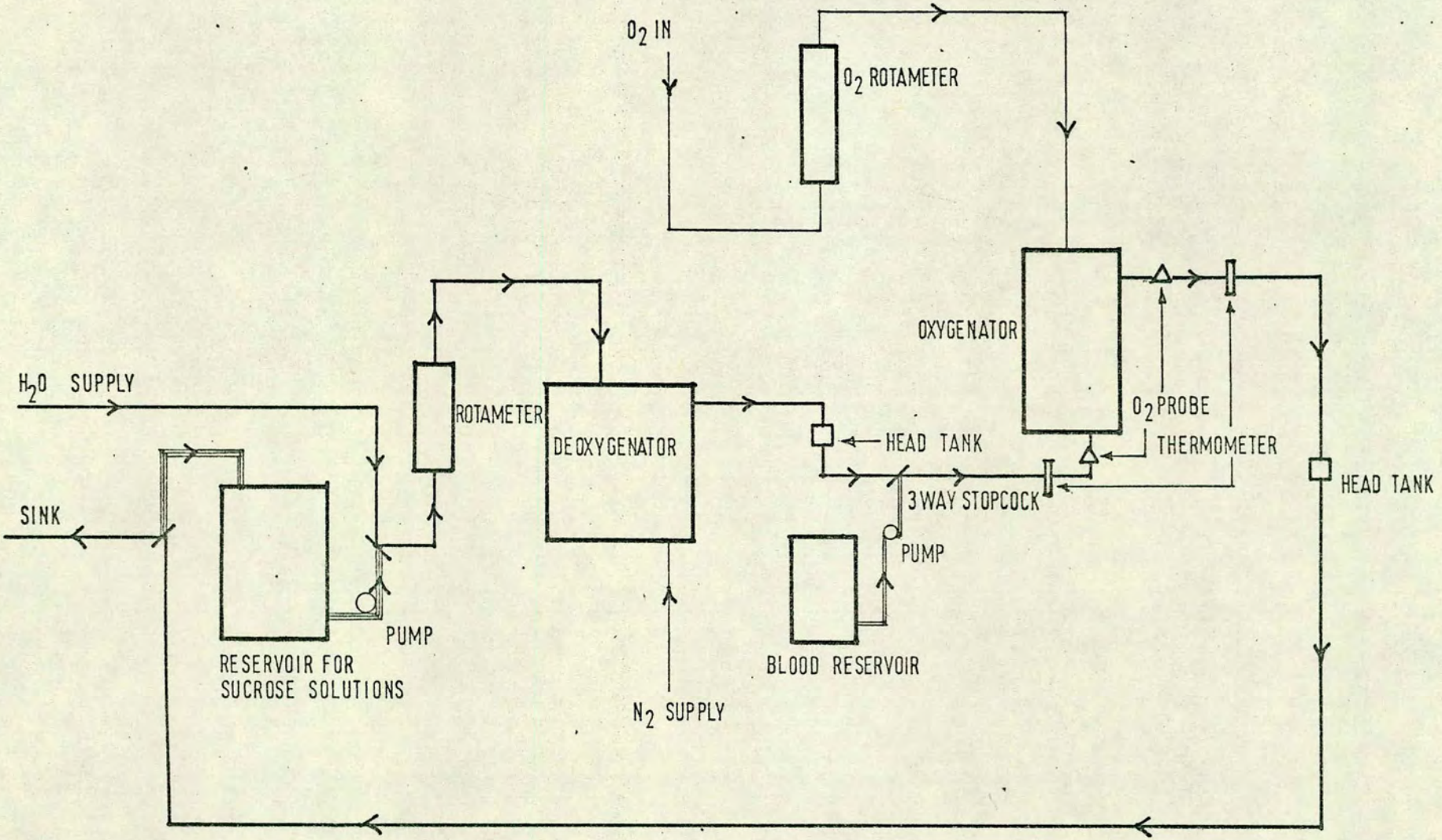

Fig. (5.1): Oxygenator Testing Circuit.

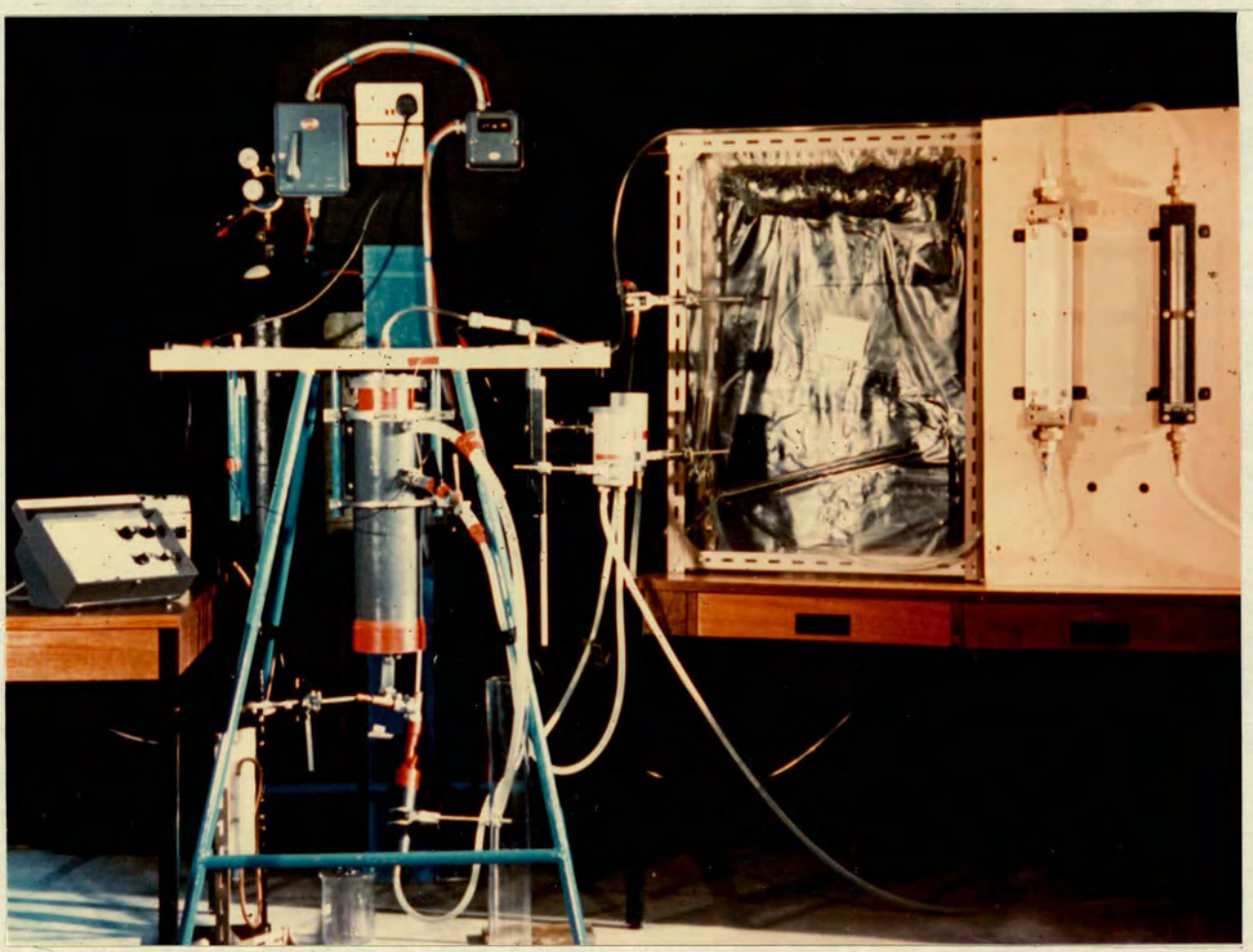

Fig.(5.2): Oxygenator Testing Circuit.

- 114 -

5.1.3 Experimental Procedure

After the fluid flow was started either from the mains, or by operating the roller pump, the following measurements were taken after all the readings and conditions had stabilized: The water flow rate as measured by a previously calibrated rotameter; the inlet and outlet temperatures; the inlet and outlet O_2 concentrations; and the angular velocity of the rotor as measured by a mechanical revolution counter. When the required readings were complete, the angular velocity of the rotor was varied while the fluid flow rate was maintained nearly constant, although it was continuously monitored. The atmospheric pressure was measured from time to time to ensure that substantial changes would not be undetected.

The minimum oxygen flow rate required to ensure independence of the mass transfer coefficient from oxygen flow was determined by trial and error; subsequently, oxygen flow rates were monitored with a rotameter to ensure adequate gas flows and an oxygen tension inside the rotor nearly equal to atmospheric pressure.

The viscosity of the sucrose solutions and the solubility of oxygen in the experimental solutions were also measured. The viscosity was determined by comparative measurement using an Ostwald viscometer, and the solubility by measuring the oxygen content near equilibrium as air was bubbled through the solutions. The two oxygen meters used in the mass transfer experiments were also used in this case.

5.1.4 Presentation of Results

In these experiments with a rotor of non-circular crossection, for Taylor numbers up to 4000, the Sh number varies approximately as the square root of Ta (Fig. 5.3-5.7) at the three Sc numbers studied. This dependance is in disagreement with the experimental data reported in Chapter 3 for a rotor of circular crossection and for a similar high Sc number system.

A second feature of these results with the non-circular rotor is that for Ta < 4000 the absolute level of mass transfer is higher, in the present experiments, than the values predicted from equation 3.10, which closely agrees with the data from the ester experiments.

Above Ta ≃ 4000, the experimental data for the non-circular cylinder show considerable scatter (Fig.5.5), due to the vibration present at the rotor speeds corresponding to the Ta range 4000-10,000. Nevertheless, the experimental points fall uniformly below the line calculated from eq. 3.10. Above Ta = 10,000 the vibration subsided and further experimental data was obtained. Although there is considerable scatter in these data, the general position of the points is significant and may well indicate a regime change, due to the discontinuity compared with the data up to Ta = 4000.

The dependence of Sh on Re_z, though weak, in a direct relation, contrary to previous studies in the laminar + vortex region that show a similarly weak although inverse dependence of Sh on Re_z.

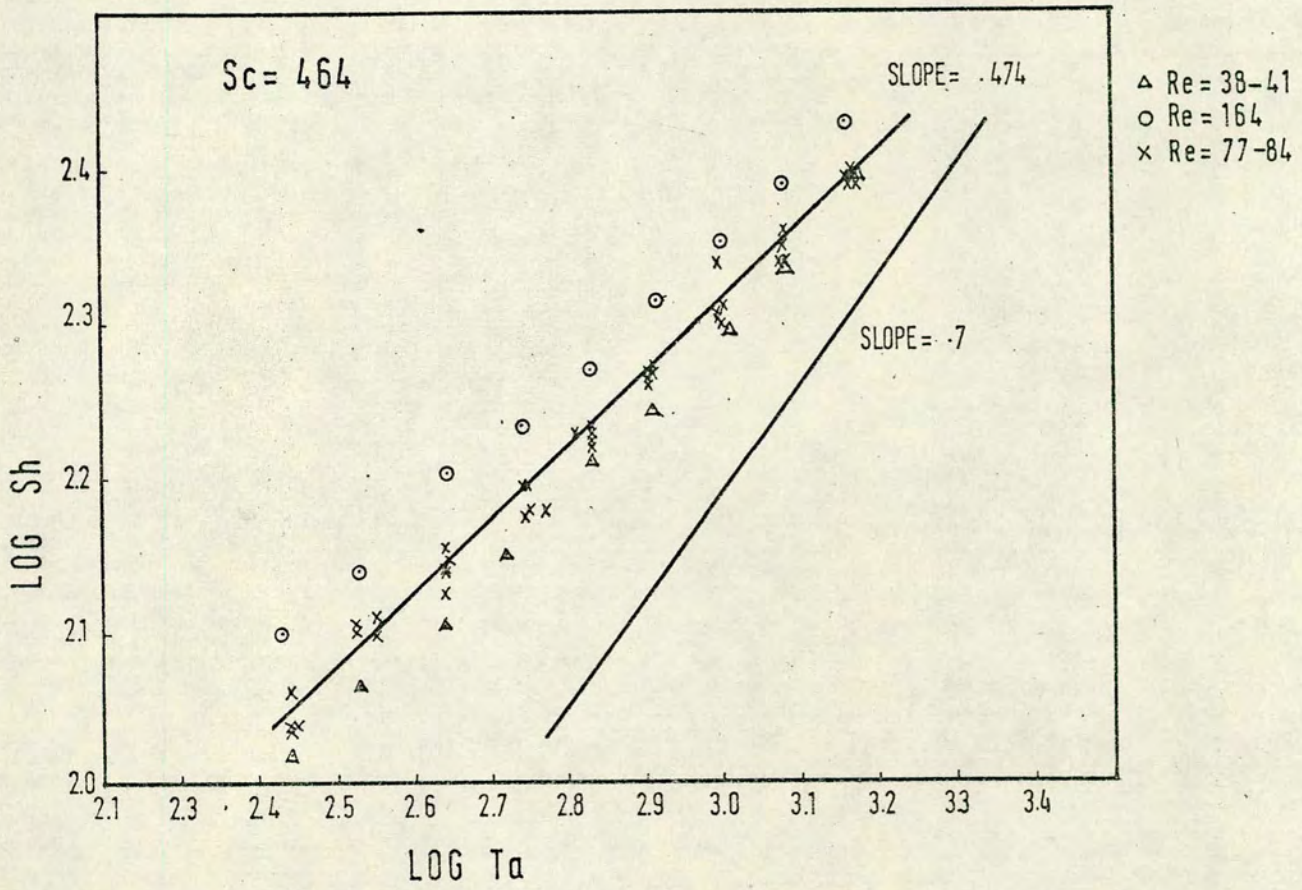

Fig. (5.3): Log Sh vs. Log Ta. Ta= 250-1600.

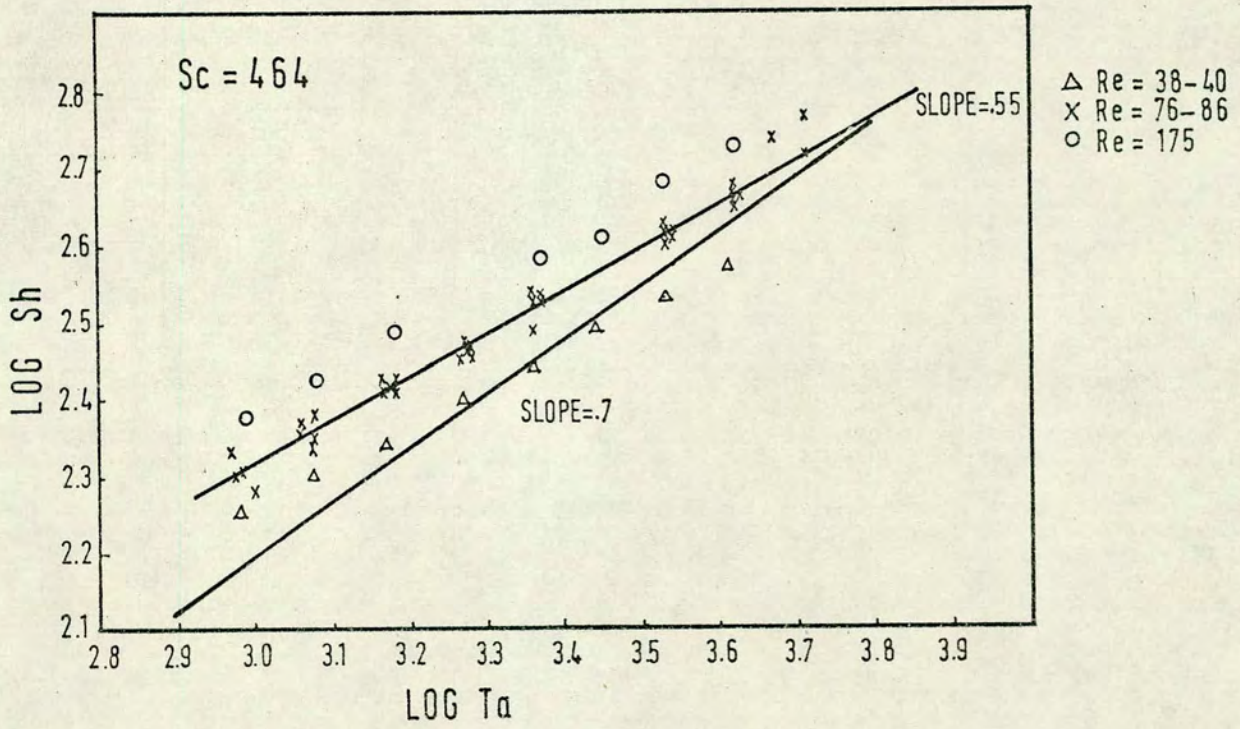

Fig.(5.4): Log Sh vs. Log Ta. Ta =800-5200.

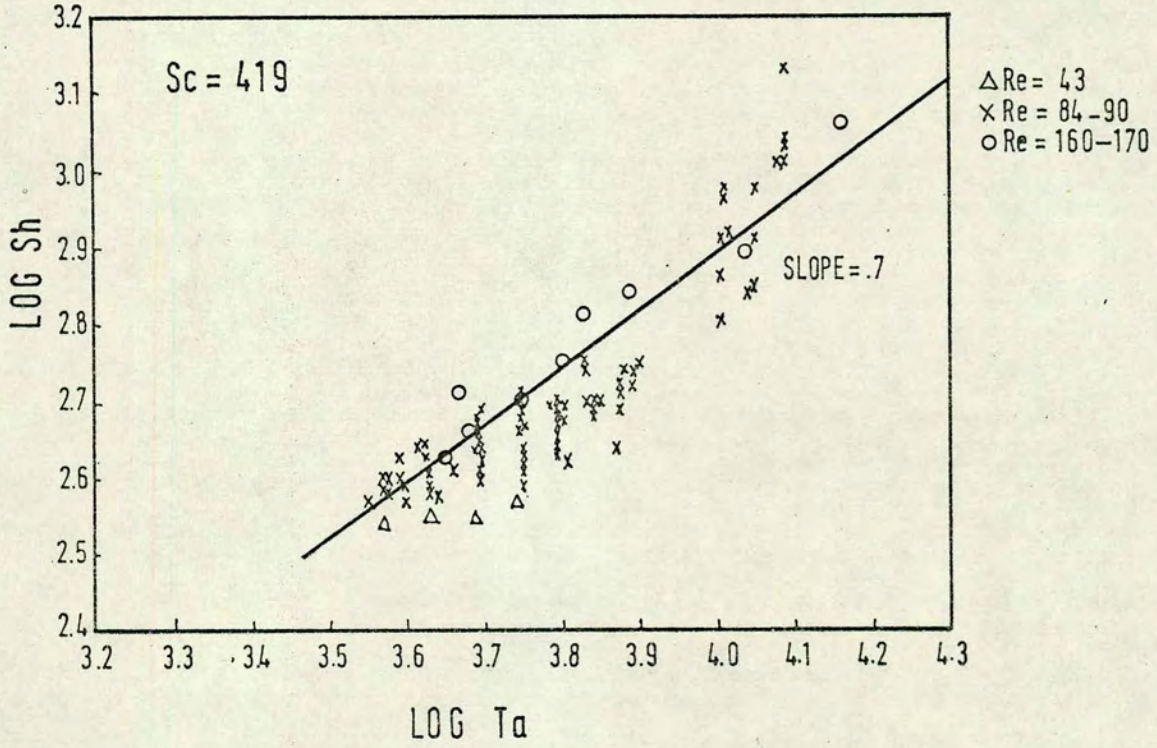

Fig.(5.5): Log Sh vs. Log Ta. Ta= 3000-16000.

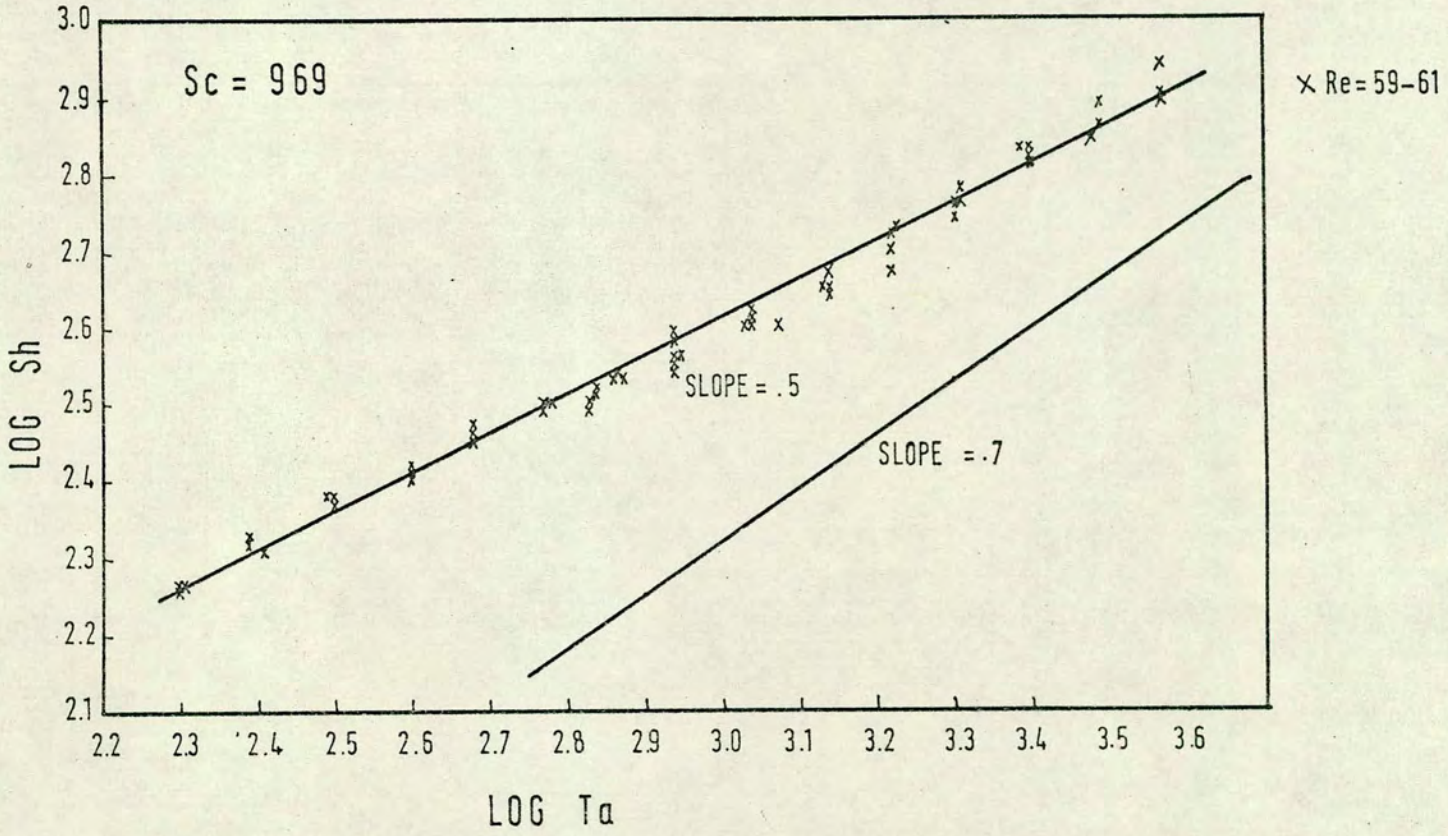

Fig.(5.6): Log Sh vs. Log Ta. Dilute Sucrose Solution. Ta=200-3500.

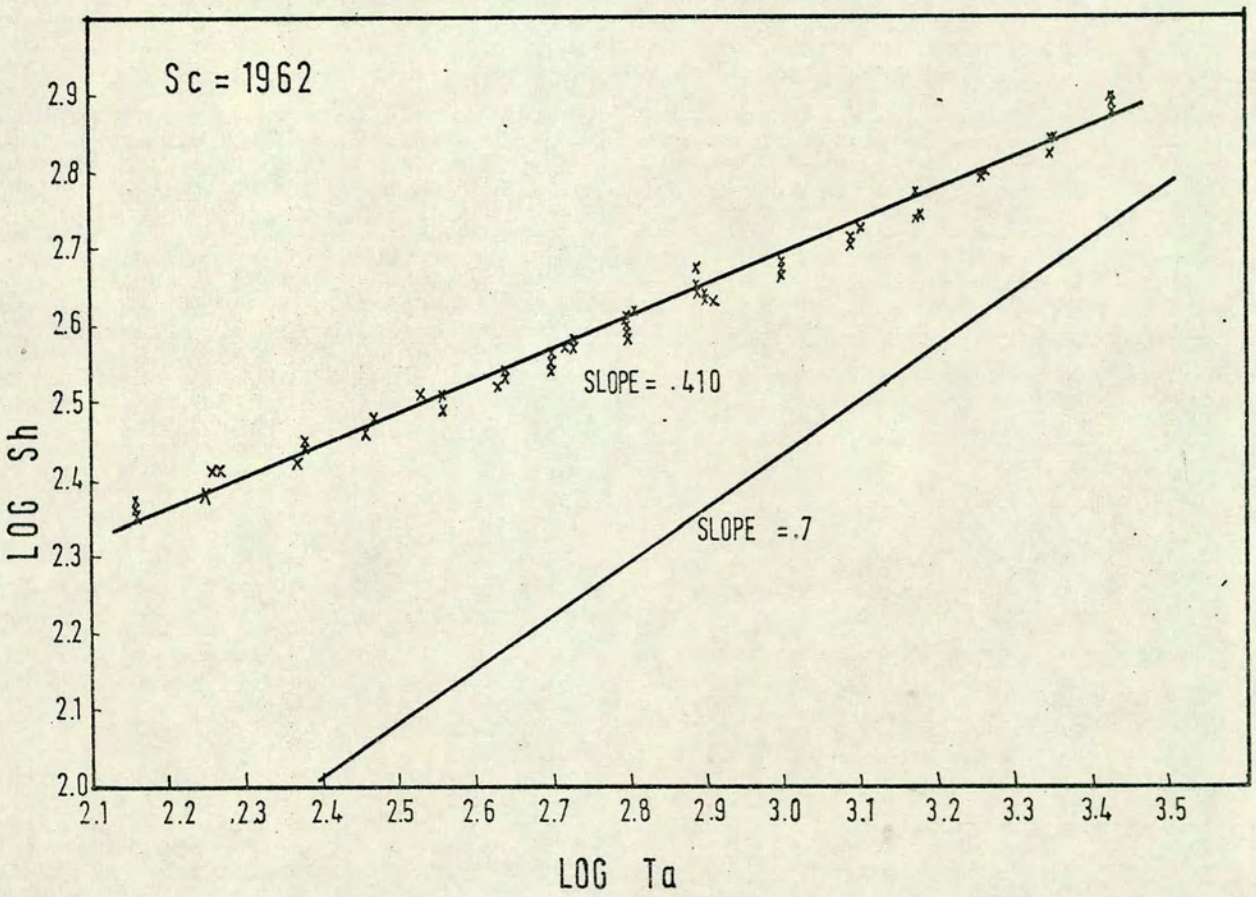

Fig.(5.7): Log Sh vs. Log Ta ; Concentrated Sucrose Solution Ta=130-3200.

5.1.5 Discussion

The relation $Sh \propto Ta^{.5}$ approximately characterising the present experimental data, obtained with a rotor that is not a circular cylinder, is in disagreement with the results obtained with a rotor of true circular section using an ethyl salicylate-water system having a similar Sc number. Furthermore, these oxygenation results are not in harmony with the mechanism of mass transfer, proposed in Chapter 3, for a high Sc system between smooth coaxial cylinders in the laminar and vortex region.

The following explanations of this disagreement are possible: a) The occurrance of a systematic error in the experiments with the oxygenator; b) The Taylor number index depends on some other dimensional characteristic of the coaxial cylinders system not previously identified; and c) The longitudinal "rib" added to the rotor, formed by the taped seam of the porous covering, alters the mass transfer characteristics of the system by modifying the character of the fluid motion. These three possibilities will now be reviewed in detail in the light of the present experimental data.

5.1.6 Possible Sources of Systematic Error

In the present experiments the results could have been affected by three sources of systematic error;

a) Uncovering of the mass transfer area of the rotor, due to the centrifugal action on the fluid. To minimize this effect the mass transfer area ended 2 cm below the outlet; furthermore, the liquid level in the annulus was allowed to rise several cms. above the outlet to ensure that the exit tubing was filled with liquid, and sufficient head of water was available to drive the fluid through the outlet lines.

These measures allowed water to creep up to 10 cms higher on the outer annular surface than the rotor surface with no appreciable reduction of the mass transfer area. This allowance was enough to eliminate any such reduction by a centrifugal effect. Subsequently, visual experiments using a perspex cylinder with a slightly larger diameter of 14.6 cm, secured in position after being filled with water, showed that no uncovering of the mass transfer surface occurred except at high rotor velocities corresponding to Ta ≃ 6000 in the oxygenator, despite the fact that in these visual experiments the larger annular gap would accentuate this effect.

b) The visual experiments also showed that bubble entrainment is a major problem at higher rotor speeds, corresponding to approximately Ta ≃ 4000 in the oxygenator. It is nevertheless unlikely that air bubble entrainment is an important source of systematic error as the experimental outlet O_2 concentrations in the liquid corresponded to oxygen partial pressures higher than those prevailing in air. As to the possibility of oxygen bubbles being formed across the membrane, visual experiments, both with stationary and rotating inner cylinders, failed to detect any such bubble formation.

Furthermore, the experimental data for a stationary annulus can be used as evidence that oxygen microbubble formation across the membrane was not a significant cause of error in the present results. The value of the Sh number obtained on extrapolation of the line of eq. 3.10, obtained for mass transfer in the absence of bubbles, to the critical Taylor number is presumably that for pure Couette flow, i.e. for laminar circumferential flow in the absence of vortices. As such this extrapolated Sh value should be the same as that measured for axial flow alone in a stationary annulus in

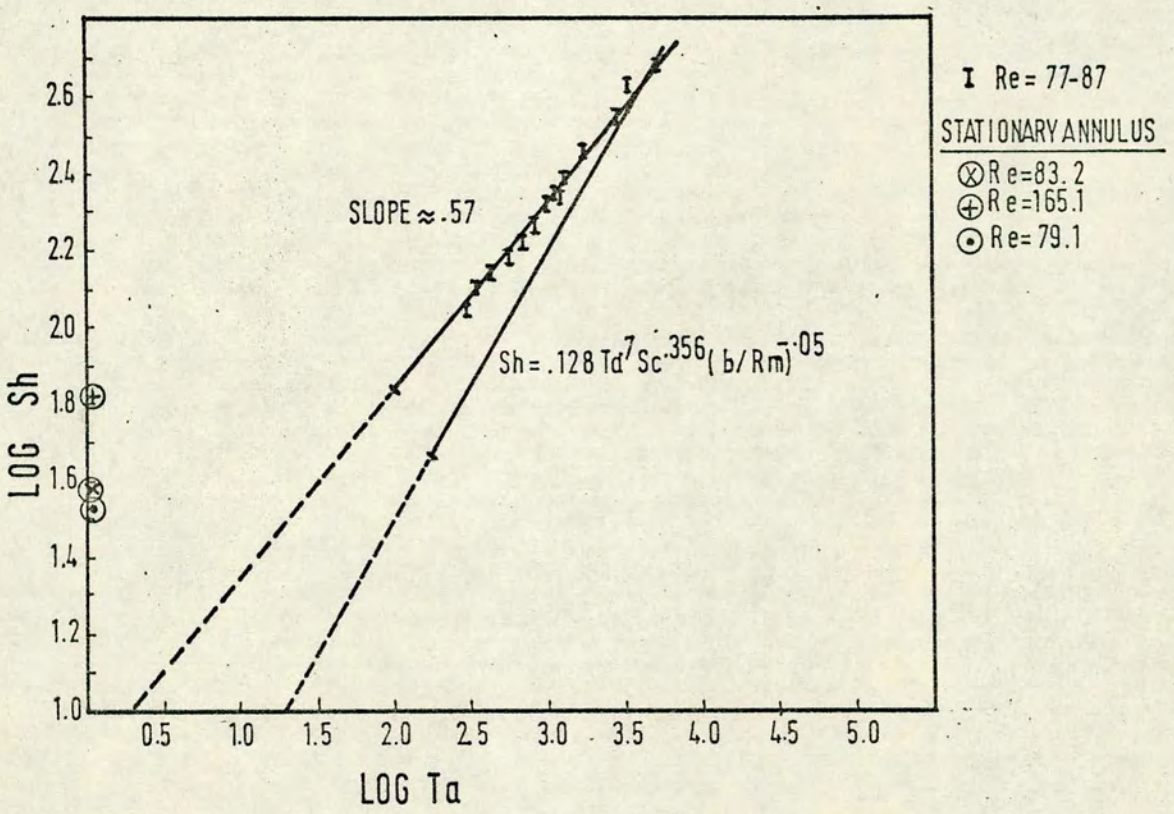

Fig.(5.8): Log Sh vs. Log Ta Including Experimental Data for the Stationary Annulus.

circumstances where the fluid stream is laminar and undisturbed by bubbles or other extraneous agencies. The expected agreement between measured and estimated Sh values is in fact observed, indicating that no bubbles disturb the fluid stream.

c) A third source of systematic error arises from the possible clogging of the mass transfer area by the entrainment of liquid in the foam underlayer to the membrane. As such liquid would be essentially stationary, and therefore create a resistance to mass transfer, the overall level of mass transfer would have been lower than in this case. Furthermore, frequent inspection of the membrane showed it to be intact, and its underlayer dry.

5.1.7 Possible Dependance of the Index of the Taylor Number on Some Other Characteristic of the Coaxial Cylinder System.

On the provisional assumption that the irregularity of the rotor does not affect the mass transfer rate in the annulus, we examined other special features of the present system which might be associated with the unexpected Sh vs. Ta relationship. The present experiments can be categorised, together with previously reported mass transfer data, according to the prevailing experimental circumstances and experimentally determined value of the Ta index, as shown in Table 5.1.

From inspection of this table the following hypotheses can be made concerning the possible dependance of the Ta index on dimensional or operational characteristics of coaxial cylinder systems.

a) Dependance of the Ta index upon Sc number. This hypothesis proposed in Chapter 3, is supported by all previous mass transfer data, as well as heat and momentum transfer studies done on the rotating

A	B
$Sh \propto Ta^{.5}$	$Sh \propto Ta^{.7}$
1. Oxygenator $b/Ro \simeq .1$; L/b Large Reϕ Large; Sc = 419-1962 Good entry (axial)	1. Ester Experiments $b/Ro \simeq .24$; L/b Large Reϕ small; Sc = 1260 Side entry.
2. Flower et al. (108) $b/Ro \simeq .3$ and .1; L/b Large Reϕ small; Sc = .7-3.0 Good entry (weir).	2. Eisenberg et al. (120) b/Ro mostly > .3 L/b small, Reϕ Large Sc = 800-2000 No axial flow
	3. Sherwood & Ryan (139) $b/Ro > .4$, L/b small Reϕ Large, Sc $\simeq$ 2000 No axial flow.

Table 5.1 Mass Transfer Experiments Classified According to the Index on the Ta Number.

coaxial cylinders system. The experimental data obtained with the oxygenator does not fit this model, since the index of the Taylor number would be expected to be ≃ .7, in such high Sc number system.

b) The Ta index $f(^{b}/Ro)$. This hypothesis is consistent with 1A and 1B, that is, a large $(^{b}/Ro)$ corresponds to a Ta index of .7, and a small $(^{b}/Ro)$ corresponds to a Ta index of .5. However, the experimental data of set 2A, taken with both large and small annular gaps does not provide evidence of such dependance. Furthermore, this hypothesis is in conflict with the work of Flower et al. (108), who demonstrated that for $^{b}/Ro < .4$, the state of the fluid in the annulus is independant of $(^{b}/Ro)$ as a separate dimensionless group when the Ta number is formulated as:

$$Ta = \frac{V\phi b\rho}{\mu}\sqrt{^{b}/Ro}$$

Sets 2B and 3B, are in agreement with this hypothesis, but the large $(^{b}/Ro)$ studied makes it doubtful whether the state of the fluid can be fully described in the manner proposed by Flower et al. for $(^{b}/Ro) < .4$, and makes uncertain the relevance of Sherwood and Ryan's data for this investigation.

c) Sets 1B, 2B and 3B are consistent with the hypothesis that the Ta index $f(^{b}/Ro,Sc)$, but 1A and 2A seem to be in contradiction; in 1A, $^{b}/Ro$ is small and Sc large, while in 2A, $^{b}/Ro$ is both small and large, and Sc is small.

d) Sets 1A and 2A are consistent with the hypothesis that the Ta index $f(^{L}/b)$. This assumption is inconsistent with 1B, and with the analysis of Flower et al. on the dimensionless group affecting the state of the fluid in the annulus.

e) Dependance of the Ta index on Sc and Reϕ; this is consistent with 2A, 1B, 2B and 3B (Reϕ small and large, Sc large, or Reϕ small, Sc small), but inconsistent with 1A (both Reϕ and Sc large).

f) The mass transfer coefficient is a function of Reϕ alone. This supposition was originated by Eisenberg et al. on the basis of their results in the case of no axial flow. While the slope of the curves Sh vs. Reϕ obtained by using the data in 1A, 2A and 2B, is the same as the slope of the curves Sh vs. Ta, (Fig.5.9), the dependance of the Ta index on Reϕ alone is consistent with 1A and 1B but not consistent with 2A. Therefore, the state of the fluid is not dependant on the Reϕ alone, but on a dimensionless group including the Reϕ.

g) Sets 1A, 1B and 2A are consistent with the hypothesis that the Ta index varies with fluid entry conditions. In this case, 1A and 2A have good entry geometries, ensuring good fluid distribution, while 1B has an asymmetrical side entry. However, the length of the annulus in relation to the small gap width in all these experimental apparatus, and the low axial Re in 1A and 1B would minimize entrance effects; furthermore, the agreement between the experimental data of 2A and the investigation of Eisenberg, Tobias and Wilke for a system with no axial flow, contradicts the hypothesis that entrance effects are significant in the ester apparatus.

In conclusion, none of the possible assumptions of Ta index dependance on some dimensional or operational characteristic of the system is consistent with all the experimental results, if the provisional assumption is made that the same flow regime prevails in all these cases.

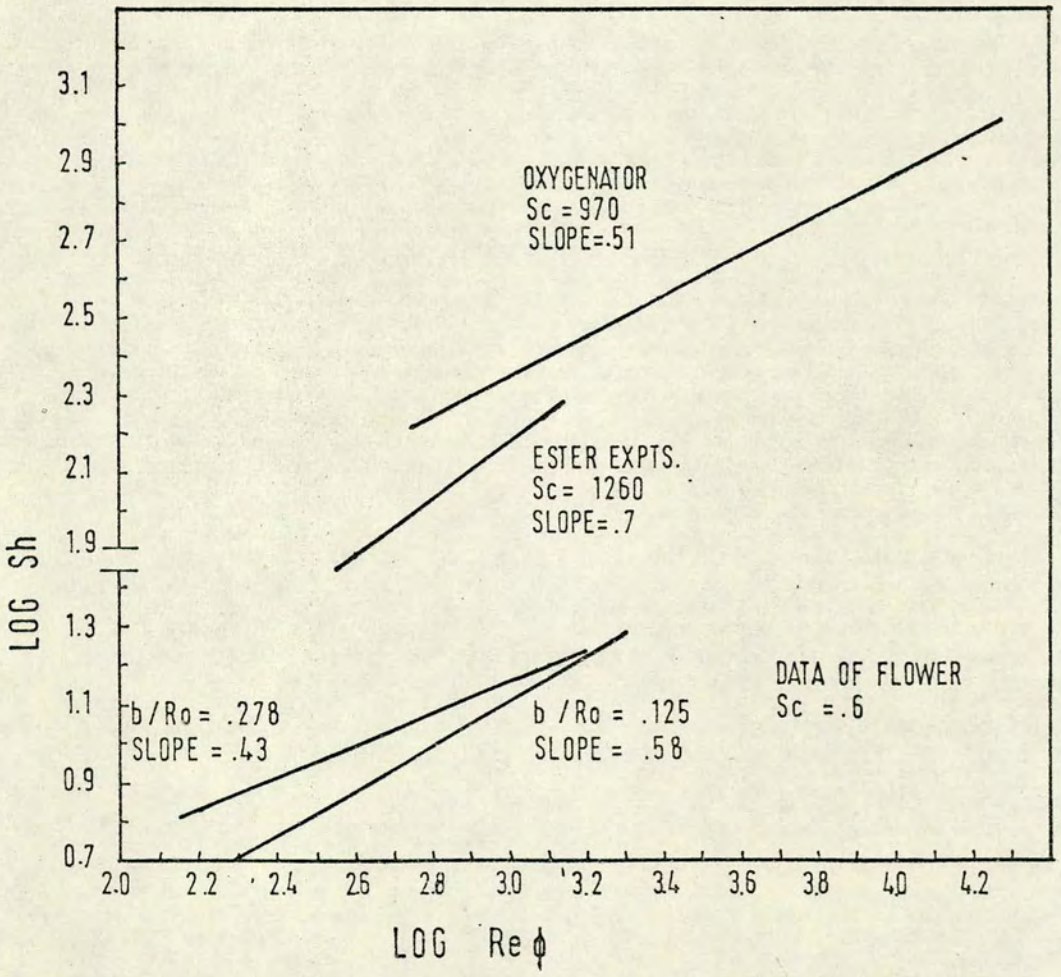

Fig. (5.9): Log Sh vs. Log Re_o.

5.1.8 Ester Experiments with a Rotor of Non-Circular Crossection.

The hypothesis that the non-circular crossection of the rotor in the oxygenator influences the rate of mass transfer in the manner shown by the experimental results, is best tested by modifying the rotor of the experimental apparatus described in Chapter 3. For this purpose, a section of 1.5 mm OD hypodermic tubing was fixed lengthwise to the entire polymer coating of the rotor. Although this irregularity of the rotor was more abrupt than in the oxygenator, the ratio height of rib/annular gap was similar.

Two separate runs were performed following the same experimental procedure as in Chapter 3. The experimental results are reported in Fig.5.10, and show a very different dependance of Sh upon Ta, viz. $Sh \propto Ta^{.35}$, compared with the ester mass transfer from a smooth cylindrical rotor, which showed a $Sh \propto Ta^{.7}$ relation.

Apart from the different Ta index, the overall rate of mass transfer is also much higher in these experiments, up to Ta = 725, than those expected from eq. 3.10 which closely correlated the experimental data for smooth cylinders.

The general similarity between the experimental data obtained with an irregular rotor in the ester apparatus, and the data obtained with the oxygenator, fully supports the hypothesis that even a smooth longitudinal "rib" like that in the oxygenator rotor disturbs the pattern of fluid flow and alters the mass transfer mechanism. The prevailing flow pattern in the oxygenator is therefore apparently no longer a purely laminar and vortex flow.

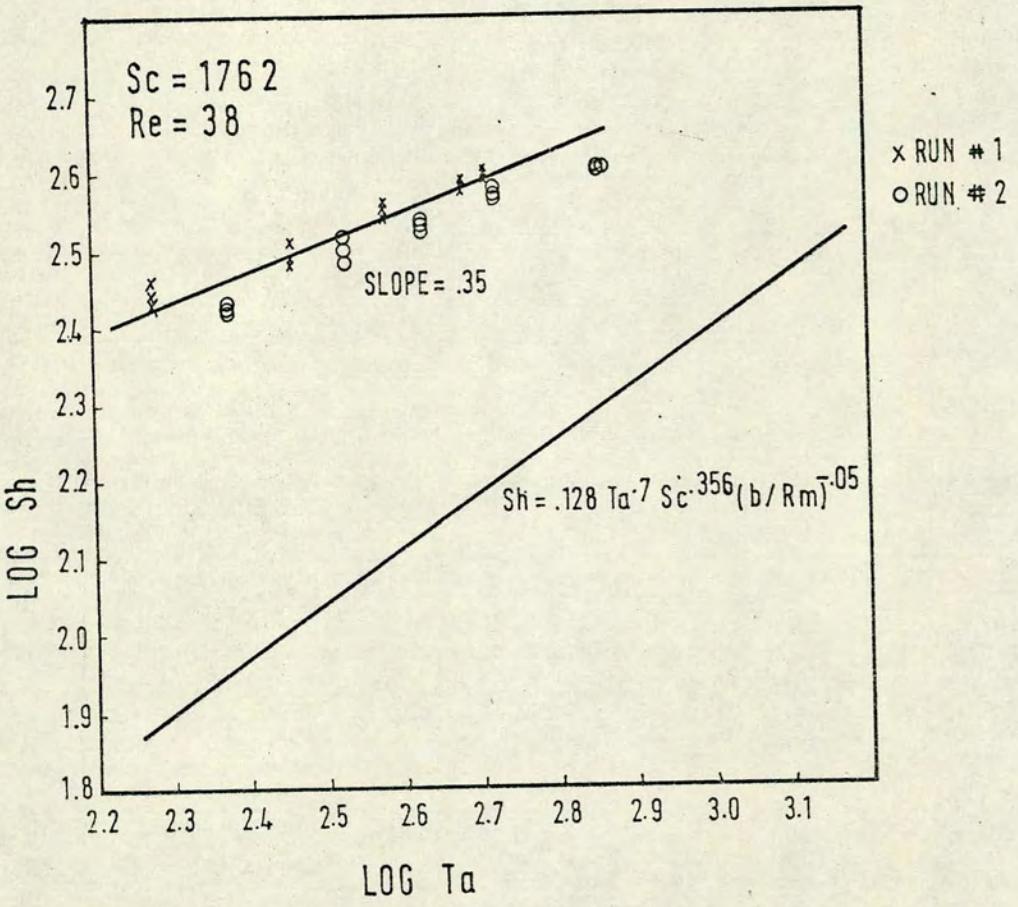

Fig.(510): Log Sh vs. Log Ta. Ester Experiments with an Irregular Rotor.

5.1.9 Hypothesis on the Influence of a Rotor of non Circular Section on the State of the Fluid in the Annulus

All the available evidence therefore points to a different flow regime than pure laminar and vortex flow in the annulus; as a consequence it can be concluded that the smooth departure of the rotor from cylindrical symmetry does affect mass transfer mechanically. Visual experiments using the perspex cylinder, and adding permanganate to the water in the annulus, clearly showed the characteristic bands due to the presence of Taylor vortices. However it was impossible to distinguish the character of the disturbance to these bands by the rapidly rotating longitudinal rib, because of the speed of the motion. On this evidence, it is reasonable to postulate that mass transfer in the present case is enhanced by the disturbance of the boundary layer by the longitudinal rib, and outside the boundary layer, mass transfer occurs by the convective action of the vortices. The added disturbance of the boundary layer would therefore result in higher rates of mass transfer than those predicted from eq. 3.10, which correlates data supposedly corresponding to purely diffusional transport across the thin boundary layer.

This proposed relative importance of the disturbed boundary layer in the overall mass transport mechanism is in line with the decreased influence of the rotor speed on the mass transfer coefficient. This contrasts with the strong influence of the rotor speed on mass transfer between cylinders of circular section, in low Sc systems, where the vortices are the main agent for mass transfer. Similarly, the hypothesis is in line with the small but direct influence of the axial Re on the mass transfer rate.

Within the disturbed boundary layer, it is reasonable to expect a strong dependance of the mass transfer coefficient with the local Re, namely, the resultant of the Re_ϕ and Re_z. The important role played by the disturbed boundary layer in affecting the overall mass transfer coefficient would then result in this strong local direct dependance of mass transfer on Re being expressed in the overall relation as a weak direct $Sh \propto Re_z$ dependance.

As the rotor velocity increases, for the same axial Reynolds number, the angle between the resultant velocity and the azimuthal plane becomes shallower. In effect, a quasi-stagnant fluid effect would be obtained with the boundary layer close to the surface not being renewed as quickly. Within this boundary layer, the solute concentration would build up, and the concentration driving force for mass transfer would be decreased, thus reducing the overall level of mass transfer in the manner observed in the present experiments at high values of the Ta number, and consequently the Re_ϕ.

In conclusion, the present experiments do show that enhanced mass transport is possible by adding longitudinal ribs to the rotor; this in turn is of great practical importance in the construction of oxygenators based on the concentric cylinder system. Higher rates of mass transfer would be obtainable at low Taylor numbers, allowing the use of lower rotor velocities, with all the mechanical and operational advantages this implies.

5.2 Blood Experiments

5.2.1 Experimental Method and Procedure

The principal objection to prolonged circulation of a batch of blood in a test circuit like the present one, is the deterioration of the state of blood as time passes. Increasing hemolysis means that the free hemoglobin concentration must be measured, together with the inlet and outlet O_2 concentrations, in order to obtain reliable mass transfer readings. Therefore, it was proposed to use a volume of blood similar to that required to prime the circuit if the conventional test method were used, and to adopt a once-through method for testing the oxygenator. This technique has the added advantage of being better suited than a closed test circuit for use in a laboratory not equipped to handle blood.

The oxygenator was primed with tap water, using the open circuit described in Section 5.1.2. When all the readings had stabilized, the flow of water was changed over to a flow of blood by operating a three-way stopcock at the oxygenator inlet upstream of the oxygen meter and thermometer assemblies. Fresh ox blood, obtained from the slaughterhouse and collected in acid citrate dextrose bottles, was placed in a reservoir; once the blood flow was started, a previously calibrated roller pump served to measure the flow rate as well as to drive the blood through the oxygenator.

The volume of blood needed for each shot was determined by the time required for the oxygen meters to give stable readings; typically, about ¾ liter of blood per reading was necessary.

In order to evaluate the mass transfer data, it was also necessary to know the blood hematocrit and hemolysis level, apart from the inlet and outlet oxygen concentrations, temperatures and blood flow rate. The experimental blood was buffered to a pH=6.8 by adding crushed buffer tablets.

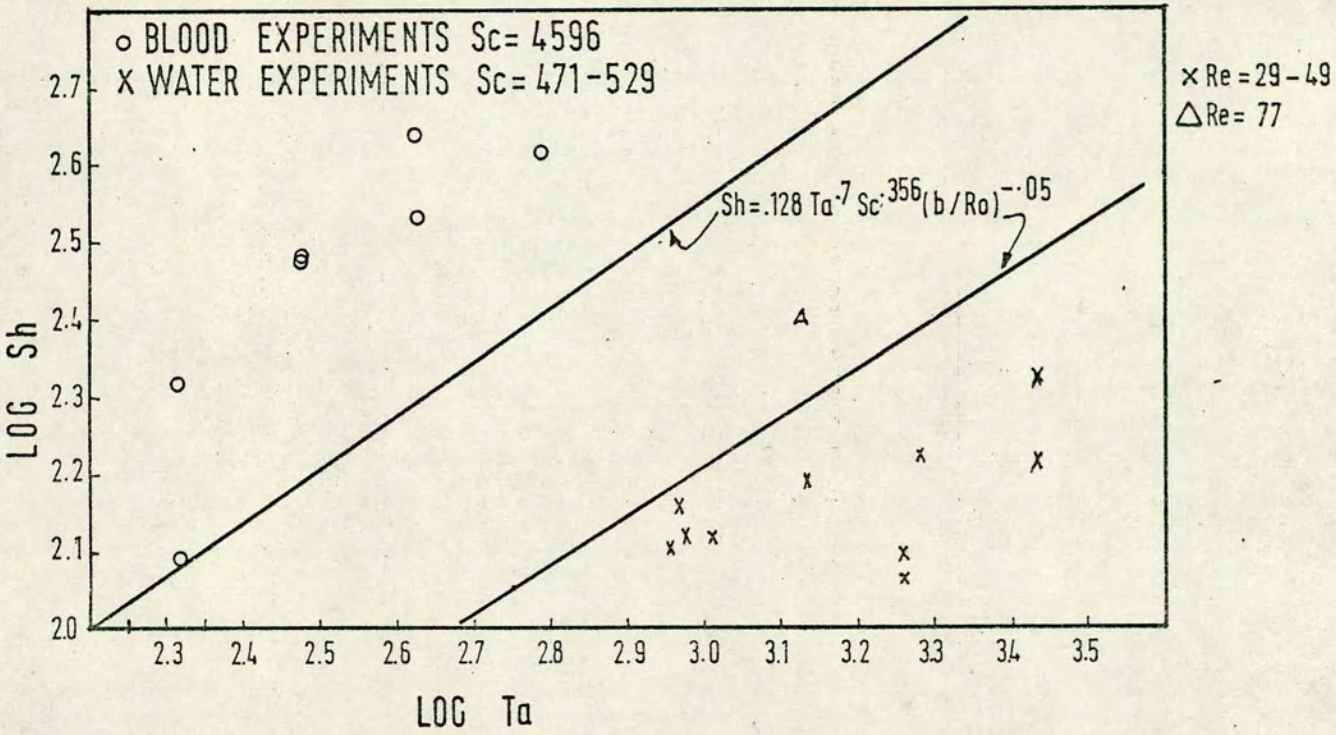

Fig. (5.11): Log Sh vs. Log Ta, Experimental Data Using Ox Blood.

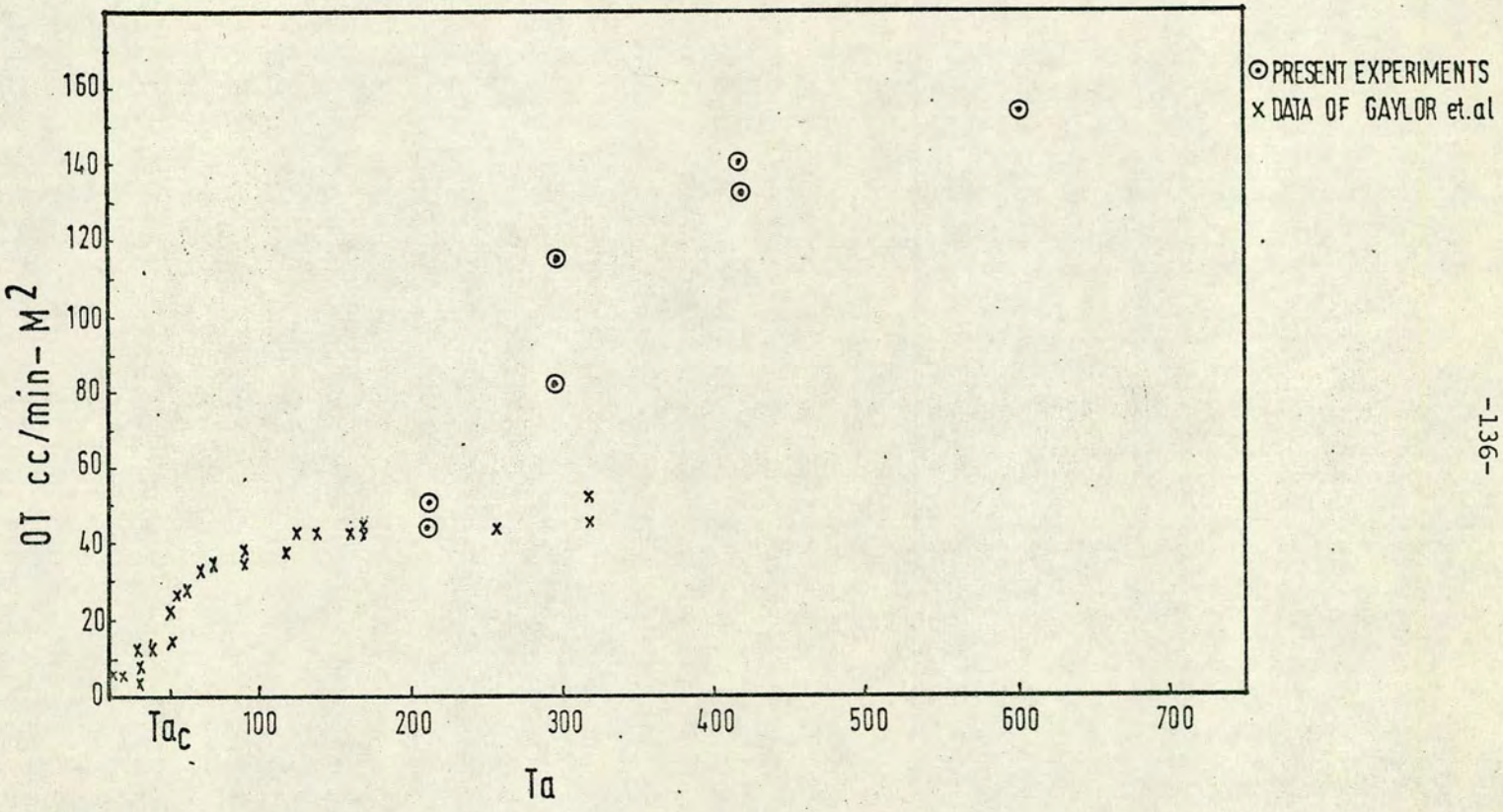

Fig. (5.12): Oxygen Uptake by Ox Blood as a Function of the Taylor Number.

The hematocrit was determined by spinning in a centrifuge a known volume of blood until there was no more erythrocyte sedimentation. The plasma layer was then pipetted and its volume measured giving a reasonably accurate hematocrit measurement. Samples of blood were also collected at several points during the experiment to measure hemolysis; in all cases the level of hemolysis was low.

5.2.2 Results and Discussion

For the Ta range studied, $200 < Ta < 625$, there was a steadily increasing rate of oxygen uptake by blood. The maximum O_2 transfer rate obtained was 150 cc/min m^2, or considerably higher than the O_2 transfer rates obtained with laminar flow oxygenators with much narrower blood passages. From Fig. 5.11, it can be seen that over the Ta range for which a comparison with Gaylor's data can be made, most of the present oxygenation results lie well above Gaylor's. Part of the discrepancy is perhaps due to the irregularity of the rotor in our experiments; there is, however, no evidence in these experiments of a levelling-off of the oxygen uptake rate above Ta = 150 such as was noticed in (140).

The general position of the points in respect to the line calculated from eq. 3.10 for transfer from a smooth rotor does not disagree with the experimental results of section 5.1, and is therefore consistent with the assumption that blood can be treated as a macroscopically homogeneous fluid with macroscopically averaged physical properties. The scatter of the experimental points, due to the rough experimental method, however, does not allow a more precise and detailed analysis.

Chapter 6

6.1 Conclusions

The following conclusions can be drawn from the present experimental work, and are of importance to the design and construction of membrane blood oxygenators based on the coaxial cylinder principle.

a) In a high Sc number system, like that involved in the oxygenation of blood, the mass transfer coefficient depends more strongly on rotor velocity than in a low Sc system. The explanation here proposed is that in a high Sc number system, the concentration boundary layer is so thin as to be effectively outside the vortical core of the annular stream, whereas in a system of low Sc there exists no such resistive fluid layer relatively inaccessible to the vortices. This view is supported by the experimental data, as well as by previously published data on mass transfer, velocity and temperature profiles in the annulus between rotating coaxial cylinders.

b) The close agreement between the results of preliminary work described in this thesis, on physical mass transfer rate determination to an axial fluid stream between rotating coaxial cylinders, and the results of Eisenberg, Tobias and Wilke (120), on physical mass transfer to a stagnant fluid between rotating cylinders, allows the use of the correlation proposed by Eisenberg et al. as the main design equation for a membrane blood oxygenator, in which the membrane-covered surfaces are truly circular coaxial cylinders, of which the inner rotates. Furthermore, the correlation of Eisenberg et al. was established over wider ranges of $^{b}/Ro$, Sc, and $V\phi$, than those examined in these preliminary experiments; their results thus furnish a basis for extrapolating the results with the ester transfer apparatus described above, to configurations not covered by the present experiments.

c) For such an oxygenator consisting of truly circular coaxial cylinders, the constraints placed on the maximum allowable shear stress tolerable by blood flowing through the annulus between the cylinders, as well as the maximum allowable pressure drop across the oxygenator, preclude the use of very narrow annular gaps in the oxygenator. Therefore, wider annuli (.4-.6 cm) are necessary; and correspondingly higher Taylor numbers (3000-5000) are required to maintain high rates of mass transfer.

d) The design considerations are significantly different if the cylinders are not truly circular. Addition of a thin longitudinal "rib" of smooth section to the circular rotor, for instance, protruding approximately to one third of the annular gap width, has been found to enhance substantially the mass transfer rate in comparison to the predicted results for a smooth rotor of circular section, for Ta numbers up to 4000. In the light of point c) in this discussion, these findings are of great interest for oxygenator design as much lower rotor velocities are required to obtain high rates of mass transfer than if both cylinders have a truly circular section. Two further experimental observations with the modified rotor including a longitudinal "rib" are of practical interest in oxygenator design;

i) Above Ta $\simeq$ 4000 there is little advantage in using a modified rotor, as opposed to a rotor of circular section, since the mass transfer rate is not appreciably enhanced, and may actually be decreased, as a result of the disturbed flow pattern in the annulus.

ii) The mass transfer coefficient for the non-circular rotor is weakly but directly dependant on the axial Re number. When both cylinders are of circular crossection, on the other hand, and the flow is a laminar and vortex flow, the evidence points to a weak inverse Sh - Re_z relation.

The mass transfer data obtained with the oxygenator featuring a modified rotor, as well as the experimental observations with the modified ester apparatus having a longitudinal "rib" added to the rotor, support the hypothesis of a different flow regime in the annulus, with higher mass transfer rates brought about by the influence of the longitudinal fin on the boundary layer at the rotor surface. Further investigation of the effect of such fins with different fin height/ annular gap ratios, of the effect of these fins on the fluid flow pattern, and of the effect of multiple longitudinal "ribs" added to the rotor and stator surfaces, would be of interest for the further development of coaxial cylinder oxygenators. The use of fins of smooth section either on the rotor or stator surfaces is also of interest in other areas, i.e. electric motors, where high rates of heat transfer to the cooling fluid in the space between the rotor and stator windings is sometimes required.

From the operational point of view, the following improvements would be desirable on the existing apparatus:

a) The use of both annular walls for oxygenation, allowing the size of the apparatus to be halved for a given oxygenation duty. This would entail a modified outer cylinder, and the lining of its concave inner surface with the foam backed Goretex membrane.

b) The provision of a seal between the upper ends of the inner and outer cylinders of the oxygenator. The mass transfer experiments with the prototype have shown that bubble entrainment is a major problem, particularly athigh rotor speeds. The entrainment of bubbles would be unacceptable in an oxygenator tested in-vivo.

The oxygenator is apparently best placed to gain acceptance in the field of long term bypass and cardiopulmonary assist, where the inherent advantage of a small mass transfer area, and therefore, potentially reduced blood trauma, outweighs the increased complexity of the apparatus. However, the limited experience available at present with long term bypass and assist procedures, does not allow a critical evaluation of existing oxygenators, therefore, there is no basis of comparison for the blood handling characteristic of the coaxial cylinders oxygenator, such as may be found from an extensive in-vivo evaluation.

As a research tool, the fundamental characteristics of this oxygenator, viz. the high rates of mass transfer obtainable by increasing the rotor velocity, and the negligible resistance of the Goretex membrane at the mass transfer rates envisaged, allow fundamental studies of blood oxygenation to be carried out. In particular, it is of interest for future oxygenator development to establish whether there is an upper limit to the rates of oxygen uptake by blood. Such an upper limit was tentatively postulated by Hopf (141) on the basis of results with the toroidal flow oxygenator. Hopf predicted that at levels of oxygen uptake by blood in the vicinity of 300 cc/min m^2, the main resistance to oxygen transfer would lie, not in the plasma phase, but in the red cell membrane. If there is such a limit, further improvement of oxygenator mass transfer rates would be futile.

The coaxial cylinder oxygenator, is suited for production and full disposability of all parts in contact with blood. The simple and unobstructive blood path allows easy sterilization, and the coaxial cylinders can be quickly assembled.

APPENDICES

Appendix 1

1.1) Literature Values for the Diffusivity of Oxygen in Whole Blood

1.1.1) 1.38×10^{-5} cm^2/sec (92),

obtained from the expression

$$D_{AB} = 1.89 \times 10^{-5}\left(\frac{100 - 0.648H}{100 + 0.531H}\right)$$

derived from heterogeneous media theory.

1.1.2) $.89 \times 10^{-5}$ cm^2/sec (93), obtained experimentally.

1.1.3) 1.125×10^{-5} cm^2/sec (94), obtained from heterogeneous media theory.

Hematocrit 42%

Hemoglobin 15g %.

1.1.4) 1.28×10^{-5} cm^2/sec (137),

obtained from heterogeneous media theory, allowing for the change in diffusivity with O_2 concentration. The value above represents the average value for the diffusivity of O_2 in 45% hematocrit blood at $38^{\circ}C$.

Inlet PO_2 = 40 mmHg.

Outlet PO_2 = 100 mmHg.

1.1.5) 1.08×10^{-5} cm^2/sec for blood with 45% Hematocrit.

Calculated from the expression of Buckles et al.(92), derived from heterogeneous media theory.

Appendix 1

1.2 Oxygen Uptake in Round Capillaries

Conditions: To raise a venous blood-O_2 saturation of 70% to an arterial saturation of 95%

Blood hematocrit - 45%

Maximum allowable ΔP = 50mm Hg

From Weissman and Mockros (93), the dimensionless distance required to effect the required venous-arterial saturation difference is

$$(1.2.1) \qquad Z^* = \frac{\pi D_{AB} Z}{2Q} = .25$$

since $Q = V_z \pi d^2/4$

$$(1.2.2) \qquad V_z = 2\pi D_{AB} Z \Big/ .25\pi d^2$$

The Poiseuille equation for pressure drop through tubes can be rearranged to:

$$(1.2.3) \qquad V_z = - \frac{\Delta P \ g_c \ d^2}{32 \mu Z}$$

equating (1.1.2) and (1.1.3)

$$(1.2.4) \qquad \frac{d^4}{Z^2} = \frac{67 D \mu}{.25 \Delta P g_c}$$

solving eq. 1.2.4 for Z, given values of d and substituting d and Z into 1.2.3 to solve for V_z, it then becomes possible to find the maximum allowable flow rate per capillary:

$$(1.2.5) \qquad Q_T = V_z \pi d^2/4$$

and the number of tubes required

$$(1.2.6) \qquad N_T = Q/Q_T$$

The total mass transfer area becomes

(1.2.7) $A = \Pi\ d\ Z\ N_T$

and the O_2 transfer rate is

(1.2.8) $OT = \text{Oxygen Requirements}/_A$

where the units of OT are cc/m^2 min.

Appendix 2

2.1 Dimensional Analysis

Let $h_D = f(V\phi, b, R, \mu, \rho, D_{AB}, V_z)$, then b, ρ, μ can not be combined in any manner to form a dimensionless group. From Buckingham's Π theorem the number of dimensionless groups is then equal to the total number of variables less those that can not be combined in any way to form a dimensionless group; in this case there are ultimately 4 dimensionless groups

$$\Pi = b^a \rho^b \mu^c V\phi^d$$

$$L^a \left(\frac{M}{L^3}\right)^b \left(\frac{M}{LT}\right)^c \left(\frac{L}{T}\right)^d \quad \text{for } L = 0 = a-3b-c+d$$

$$M = 0 = b+c$$

$$T = 0 + -c-d$$

letting $c = -1$, then $d = +1$, $b = +1$, and $a = +1$

$$\therefore \quad \Pi_1 = \frac{V\phi\rho b}{\mu}$$

Similarly $\Pi_2 = b^a \rho^b \mu^c V_z^{\,d} = \dfrac{b\rho V_z}{\mu}$

$$\Pi_3 = b^a \rho^b \mu^c R^a = \frac{b}{R}$$

$$\Pi_4 = b^a \rho^b \mu^c D_{AB} = \frac{\mu}{\rho D_{AB}}$$

Combining π_5 and π_4 to form the dimensionless group π_6 we have $\dfrac{h_D b}{D_{AB}} = f\left(\dfrac{bV\phi\rho}{u}, \dfrac{b}{R}, \dfrac{b\rho Vz}{u}, \dfrac{u}{\rho D_{AB}}\right)$, furthermore from experiment we know that these groups can be combined to form this relation

$Sh = f(T_A, Re_z, Sc)$.

2.2 Density and Viscosity of Water

The coaxial cylinder experiments were performed at $20^\circ C \pm .5^\circ C$

$T^\circ C$	ρ-gm/cc	μ-gm/cm sec.
19	.9984	1.0299
20	.9982	1.005
21	.9980	.981

2.3 Dimensions of Experimental Equipment

Mass transfer experiments from:

	Inner Wall	Outer Wall	Both Walls
Area of annulus cm^2	7.655	7.345	6.88
L cm	45	45	45
R_o cm	2.5	2.45	2.45
R_i cm	1.95±.01	1.914±.01	1.952±.01
b cm	0.54±.01	0.53±.01	0.50±.01
Mass Transfer Area cm^2	551.6	692.4	1244

2.4 Experimental Flow Rates and Re_z (Metric size 7 rotameter)

Rot. reading	Flow Rate(cc/min)	Re_z
1.6	138	33.3
2.5	159	38
3.2	179	42
4.6	214	52
5.8	249	60
6.5	269	65
7.1	287	69
8.7	335	81
9.5	363	88
11.2	415	99

2.5 Experimental Solubility Data

Ethyl salicylate in distilled water.

Run	Temp.(°C)	Solubility (α)gmES/ccH_2OX10^4
1	24	3.59
2	24.3	3.67
3	24	3.595
4	24	3.366
5	24	3.322
6	20.7	2.82
7	22.6	3.29
8	22.6	3.264
9	20.2	3.016
10	19	2.79
11	23.9	3.706
12	21.5	3.175
13	21.8	3.05
14	21.5	3.159
15	21.6	2.935
16	24	3.42

Methyl salicylate in distilled water.

1	30°C	7.36
2	30°C	7.48

Literature value 7.4×10^{-4} gmMS/ccH_2O (123)

2.6 Diffusion Coefficient of Ethyl Salicylate in Water Calculated from the Wilke-Chang Equation.

$$\frac{D_{AB}\mu}{T} = \frac{7.4 \times 10^{-8}(XM)^{0.5}}{V_o^{0.6}}$$

V_o = 185.6 = molecular volume

X = 2.6

M = Molecular weight of solvent = 18

T = ^oK

μ = viscosity, centipoise

T ^oC	$D_{AB} \times 10^6$ $\frac{cm^2}{sec}$
19	6.24
20	6.43
21	6.61
22	6.79
23	6.97
24	7.16

2.7 Experimental Determination of the Diffusion Coefficient of Ethyl Salicylate in Water

Experimental data

	Re_z	Temp.(^oC)	Conc. gm ES/ccH_2Ox10^5		$D_{AB}x10^6$ $\frac{cm}{sec}^2$
1)	33.3	21.6	Max. 1.098		
			Min. 1.086	10 samples	8.79
			Ave. 1.096		
2)	35.6	23	Max. 1.354		
			Min. 1.145	20 samples	9.97
			Ave. 1.271		
3)	54.69	23	Max. 0.936		
			Min. 0.935	5 samples	9.910
			Ave. 0.935		
4)	45.7	21.6	Max. 1.03		
			Min. 0.952	5 samples	9.1
			Ave. 0.988		
5)	63.6	23	Max. 0.919		
			Min. 0.79	5 samples	9.95
			Ave. 0.85		
6)	69.5	23	Max. 0.86		
			Min. 0.80	5 samples	9.92
			Ave. 0.82		

The expression for mass transfer in a stationary annulus analogous to the equation of Lundberg et al (124) for heat transfer from the inner wall with the outer wall insulated, is

$$2.7.1) \quad \phi_{Mi} = \frac{C_o}{C_s} = \left(\frac{6R^*}{1+R^*}\right) 2.2396\,(1-R^*)\left[\frac{(B/R^*)-2R^*}{18(1-R^*)^2 M}\right]^{\frac{1}{3}} \overline{X}^{-\frac{2}{3}}$$

where $\overline{X} = \frac{L}{d_h ReSc}$; $R^* = \frac{R_i}{R_o}$; $B = (R^{*2}-1)/\ln R^*$; and $M = 1+R^{*2}-B$

Sample calculation using data from run 2 at 23°C

$$\frac{C_o}{C_s} = \frac{1.271 \times 10^{-5}\ \text{gm/cc}}{3.35 \times 10^{-4}\ \text{gm/cc}} = \phi_{Mi} = .03793$$

$L = 45\text{cm}$, $d_h = 1.096\text{cm}$, $Re_z = 35.6$, $\mu = .009358\text{gm/cm sec}$;

$\rho = .9976\text{gm/cc}$; $\overline{X} = 122.88\ D_{AB}$

and eq. (2.8.1) becomes

$$.03793 = 3.257\,(122.9)^{\frac{2}{3}}\, D_{AB}^{\frac{2}{3}}$$

$$D_{AB} = 9.97 \times 10^{-6}\ \text{cm}^2/\text{sec}$$

2.8 Silicoloid 201 Rubber Swelling Data

Sample Time (Min.)	1	2	3	4	5	6	7	8	9	10	Ave±
1	3.0	3.35	3.12	3.01	3.12	3.01	3.02	3.22	3.21	2.94	3.1±8%
2	4.75	4.92	4.87	4.46	4.68	4.52	4.72	4.79	4.79	4.50	4.7±5%
3	5.81	6.05	6.00	5.39	5.69	5.40	5.72	5.68	5.71	5.56	5.7±6%
4	7.14	7.29	7.21	6.52	6.91	6.71	6.90	6.91	7.01	6.90	6.95±6%
5	7.98	8.10	8.07	7.67	7.81	7.68	7.82	7.88	7.93	7.76	7.87±3%
6	8.51	8.72	8.60	8.12	8.38	8.19	8.40	8.41	8.45	8.54	8.43±4%
7	9.88	10.16	9.81	9.05	9.59	9.21	9.57	9.80	9.63	9.40	9.61±6%

Sample Time (Min.)	1	2	3	4	5	6	7	8	9	10	Ave±
8	10.41	10.52	10.42	9.55	10.05	9.88	10.21	10.31	10.19	10.46	10.2±6%
9	10.99	11.11	11.10	9.84	10.69	10.29	10.74	10.81	10.59	10.84	10.7±8%
10	11.65	11.55	11.6	10.56	11.37	11.05	11.21	11.40	11.29	11.31	11.3±6%
30	17.2	16.4	17.0	15.6	16.25	16.0	16.2	16.3	16.16	15.88	16.3±6%
75	18.2	18.3	17.9	17.3	17.91	17.8	17.9	17.9	17.95	17.9	17.9±4%
80	18.3	18.2	17.9	17.45	18.06	18.0	18.0	18.03	17.92	18.14	18.0±3%
90	18.3	18.1	17.9	17.5	18.05	17.95	17.97	18.05	17.75	18.16	17.96±3%

2.9 Data for "Constant Rate" Period Measurement

Re_z = 33.4 T = 20 ± 5°C

Ta = 680.2

Sample	Time(Min)	u.v.Abs.	Conc. x 10^5 gm/cc
1	5	.478	7.74
2	5	.477	7.71
3	5	.477	7.71
4	10	.469	7.45
5	10	.470	7.48
6	10	.470	7.48
7	15	.466	7.35
8	15	.466	7.32
9	15	.465	7.32
10	20	.462	7.23
11	20	.462	7.23
12	20	.462	7.23
13	25	.458	7.1
14	25	.458	7.1
15	25	.459	7.13
16	30	.454	6.97
17	30	.455	7.0
18	30	.455	7.0
19.	35	.455	7.0
20	35	.454	6.97
21	35	.453	6.94

Sample	Time(Min)	u.v. Abs.	Conc. x 10^5 gm/cc
22	40	.456	7.03
23	40	.454	6.97
24	40	.453	7.03
25	45	.449	6.81
26	45	.449	6.81

2.10 Mass Transfer Experimental Data

T = 20 ±.5°C a) Inner Wall Transferring

Re_z	RPM	Ta	Co x 10^5 gm/cc	Sh
33.34	40	209	3.58	76.4
			3.58	76.4
			3.58	76.4
38.8			3.06	75.3
			3.06	75.3
			3.06	75.3
42.6			2.52	67.4
			2.71	72.7
			2.71	72.7
51.20			2.42	77.6
			2.58	83
			2.59	83.3
49.30			2.39	88.6
			2.39	88.6
			2.35	87.3
			2.35	87.3
			2.19	81
			2.29	84.9
65.02			2.1	84.9
			2.07	83.7
			2.04	82.5
			2.19	88.8
			2.13	86.3
			2.19	88.9
68.6			-	-
			-	-
			-	-
80.9			1.61	80.6
			1.77	88.9
			1.70	85.1

Re_z	RPM	Ta	Co x 10^5 gm/cc	Sh
86.9	40	209	1.48	79.2
			1.74	93.5
			1.65	88.6
33.3	50	261	4.38	94.9
			4.52	98.2
38.8			4.16	104.5
			4.06	101.8
			3.88	96.98
42.63			3.71	101.3
			3.63	99.2
			3.63	99.2
51.20			2.61	84.0
			2.74	88.4
			2.84	88.4
59.3			2.45	91.0
			2.58	96.1
			2.68	100.0
			2.52	93.8
			2.45	91.0
			2.39	88.6
65			2.29	93.0
			2.26	91.8
			2.32	94.4
			2.45	99.83
			2.39	97.15
			2.23	90.5
68.6			2.20	94.1
			2.19	93.7
			2.16	92.4
81			1.97	99.1
			2.10	105.9
			2.06	103.8
87			1.84	99.1
			1.84	99.1
			1.84	99.1

Re_z	RPM	Ta	Co x 10^5 gm/cc	Sh
99	50	261	1.55	94.5
			1.55	94.5
			1.67	102.0
33.3	60	314	5.35	118.3
			5.45	120.7
			5.42	119.9
38.8			4.81	122.4
			4.81	122.4
			4.71	119.7
42.6			3.87	105.3
			3.87	105.3
			3.81	104.4
51.2			3.19	103.9
			3.29	107.2
			3.36	106
59.3			2.62	97.7
			2.62	97.7
			2.65	98.8
			2.58	96.1
			2.62	97.7
			2.63	97.7
65			2.39	97.2
			2.39	97.2
			2.36	95.8
			2.32	94.3
			2.32	94.3
			2.32	94.3
68.6			2.29	98.2
			2.29	98.2
			2.36	101.3
81			2.16	109
			2.19	110.8
			2.19	110.8
87			1.94	104.7

Re_z	RPM	Ta	Co x 10^5 gm/cc	Sh
87	60	314	1.94	104.7
			1.94	104.7
98			1.62	98.8
			1.62	98.8
			1.65	100.7
33.3	70	366	5.35	118.2
			5.71	127.1
			5.35	118.2
38.8			5.26	135.1
			5.1	130.5
			4.98	127.2
42.6			4.1	112.9
			4.23	116.8
			4.23	116.8
51.2			3.16	102.7
			3.18	103.4
			3.23	105.2
59.3			3.03	113.8
			3.16	119
			3.0	112.6
			2.73	113.8
			3.0	112.6
			3.03	113.8
65			2.55	104.1
			2.58	105.4
			2.58	105.4
			2.58	105.4
			2.58	105.4
			2.55	104.1
68.6			2.48	106.7
			2.42	103.9
			2.45	105.3
81			2.23	112.7
			2.23	112.7
			2.23	112.7

Re_z	RPM	Ta	Co x 10^5 gm/cc	Sh
87	70	366	2.16	117.
			2.10	113.7
			2.10	113.7
99			1.96	120.3
			1.96	120.3
			2.0	122.8
33.3	80	419	5.74	127.9
			5.68	126.4
			5.80	129.4
38.8			5.19	133.1
			5.16	132.3
			5.13	131.4
42.6			4.35	120.5
			4.32	119.6
			4.32	116.9
51.20			3.67	119.5
			3.62	118.7
			3.74	122.9
59.30			3.19	120.2
			3.19	120.2
			3.16	119
			3.25	122.6
			3.25	122.6
			3.32	125.4
65			2.87	116.6
			2.91	119.6
			2.87	117.9
			2.93	120.5
			2.93	120.5
			2.96	121.8
68.6			2.71	117.1
			2.71	117.1
			2.81	121.6
81			2.39	121.2
			2.32	117.5

Re_z	RPM	T_a	Co x 10^5 gm/cc	Sh
87	80	419	2.13	115.4
			2.13	115.4
			2.19	118.7
99			1.9	116.5
			1.9	116.5
			1.93	118.4
33.3	90	471	6.38	144
			6.35	143.3
			6.32	142.5
38.8			5.74	148.9
			5.74	148.9
			5.63	145.7
42.6			5.00	140.3
			5.13	144.3
			4.93	138.1
51.20			4.54	151.6
			4.48	149.4
			4.42	147.3
59.3			3.61	137.1
			3.71	141.2
			3.71	141.2
			3.74	142.4
			3.74	142.4
			3.74	142.4
65			3.23	133.5
			3.23	133.5
			3.29	136.2
			3.38	140.1
			3.38	140.1
			3.32	137.5
68.6			3.16	137.6
			3.09	134.4
			3.09	134.4

Re_z	RPM	Ta	Co x 10^5 gm/cc	Sh
81.0	90	471	2.71	138.2
			2.68	136.6
			2.68	136.6
87			2.38	129.5
			2.48	135.2
			2.48	131.8
99			2.16	133.1
			2.16	133.1
			2.13	131.2
33.3	100	523	6.87	156.7
			6.90	157.5
			6.90	157.5
38.8			6.03	157.3
			6.10	159.4
			6.10	159.4
42.6			5.26	148.3
			5.26	148.3
			5.19	146.2
51.2			4.93	165.9
			4.87	163.7
			4.84	162.6
59.3			3.84	146.5
			3.84	146.5
			3.81	145.3
			3.84	146.5
			3.84	146.5
			3.75	142.8
65			3.42	141.9
			3.42	141.9
			3.38	140.2
			3.45	143.2
			3.42	141.9
			3.38	140.2
68.6			3.06	133
			3.03	131.7
			2.97	128.9

Re_z	RPM	Ta	Co x 10^5 gm/cc	Sh
81	100	523	2.74	139.8
			2.81	143.6
			2.81	143.6
87			2.64	144.3
			2.62	143.2
			2.52	137.5
98.8			2.26	139.5
			2.26	139.5
			2.17	133.7
33.4	130	680	7.77	180.8
			7.96	186.0
			7.90	184.4
38.8			6.80	180.4
			6.80	180.4
			6.96	185.2
42.6			6.48	187.5
			6.48	187.5
			6.30	181.6
51.2			5.16	174.5
			5.16	174.5
			5.19	175.6
59.3			4.77	185.3
			4.60	178.1
			4.69	181.9
			4.71	182.8
			4.71	182.8
			4.71	182.8
65			4.19	176.7
			4.19	176.7
			4.12	173.5
			4.20	177.1
			4.16	175.3
			4.16	175.3
68.6			3.93	173.7

Re_z	RPM	Ta	Co x 10^5 gm/cc	Sh
68.6	130	680	3.84	169.5
			3.87	170.9
81			3.22	165.8
			3.26	167.9
			3.29	169.6
87			2.91	159.9
			2.97	163.4
			2.94	161.6
98.8			2.39	147.9
			2.45	151.8
			2.36	145.9

b) Outer Wall Transferring

Re_z	RPM	Ta	Co x 10^5 gm/cc	Sh
34	40	200.6	5.32	91.6
			5.42	93.5
			5.32	91.6
43.5			4.29	92.5
			4.41	95.3
			4.29	92.5
52.2			3.80	97.5
			3.77	96.7
			3.71	95
60.5			2.87	83.8
			3.22	94.6
			2.97	86.85
66.3			2.65	84.45
			2.52	80.11
			2.52	80.11
			2.23	74.4
			2.23	74.4
			2.10	69.9

Re_z	RPM	T_a	Co x 10^5 gm/cc	Sh
88.6	40	200.6	1.84	77.2
			1.81	75.9
			1.84	77.2
100.8			1.42	67.3
			1.42	67.3
			1.36	67.3
33.4	60	300.9	6.74	119.5
			6.81	120.9
			6.71	118.9
43.4			5.97	133.1
			5.94	132.4
			5.90	131.4
52.2			4.65	121.3
			4.55	118.6
			4.55	118.6
60.5			3.87	115.1
			3.81	113.2
			3.81	113.2
66.3			3.19	102.7
			3.23	104.1
			3.13	100.6
69.9			2.81	94.7
			2.87	96.9
			2.74	92.3
88.6			2.03	85.5
			2.16	91.2
			2.29	96.9
100.8			1.68	79.9
			1.68	79.9
			1.64	77.9
33.4	80	401	7.96	144.9
			7.84	142.3
			8.10	147.9

Re_z	RPM	Ta	Co x 10^5 gm/cc	Sh
43.5	80	401	6.89	152.1
			6.94	157.7
			6.94	157.7
52.2			6.45	144.5
			6.54	147.3
			6.49	145.6
60.5			6.00	146.2
			5.64	143.8
			5.40	135.6
66.3			4.19	137.5
			4.10	134.3
			4.19	137.5
69.9			3.77	129.5
			3.71	127.3
			3.71	127.3
88.6			2.61	111.1
			2.74	116.9
			2.74	116.9
100.8			2.16	103.7
			2.19	105.2
			2.10	100.7
33.4	100	501.5	9.58	171
			9.74	174.8
			9.58	171
43.5			8.06	178
			8.09	178.8
			7.97	175.6
52.2			6.45	174.5
			6.41	173.3
			6.45	174.5
60.5			5.29	161.8
			5.42	166.3
			5.52	169.7

Re_z	RPM	Ta	Co x 10^5 gm/cc	Sh
66.3	100	501.5	4.65	154
			4.77	158.3
			4.65	154
69.9			4.00	138
			4.03	139.1
			3.90	134.3
88.6			3.03	130
			2.97	127.3
			2.97	127.3
100.8			2.61	126.4
			2.71	131.4
			2.61	126.4
33.4	130	652	11.36	224.4
			11.03	216
			11.09	217.5
43.5			8.90	211.6
			8.42	198
			8.82	200
52.2			6.80	185
			7.26	199.8
			7.10	195
60.5			5.80	179.3
			5.90	182.8
			5.97	185.2
66.3			5.45	183.4
			5.40	181.5
			5.32	178.6
69.9			4.87	170.9
			4.97	174.7
			4.84	169.7
88.6			4.03	176.3
			4.00	174.8
			3.74	172
100.8			3.45	169.7
			3.32	162.9
			3.39	166.5

c) Mass Transfer from Both Walls

Re_z	RPM	Ta	Co x 10^5 gm/cc	Sh
33.7	60	275	9.87	97.1
			9.84	96.7
			9.87	97.1
43.1			8.55	104.3
			8.03	96.8
			8.13	98.2
51.8			6.94	98.1
			6.77	95.4
			6.81	96.0
59.9			5.67	90.4
			5.58	88.8
			5.67	90.4
65.7			5.13	88.7
			4.90	84.3
			5.00	86.2
69.4			4.77	86.4
			4.87	88.4
			4.81	87.2
87.9			4.29	97.5
			4.13	93.6
			4.32	98.3
99.9			3.42	86.9
			3.42	86.9
			3.32	84.2
33.7	80	366.5	11.70	120.5
			11.58	119.1
			11.61	119.2
43.1			9.90	126
			9.74	122
			9.84	123.8

Re_z	RPM	Ta	Co x 10^5 gm/cc	Sh
51.8	80	366.5	7.96	115.1
			8.10	117.5
			7.97	115.1
59.9			7.07	116.1
			7.00	114.8
			7.07	116.1
65.8			6.45	114.6
			6.52	116
			6.45	114.6
69.4			6.35	118.8
			6.23	116.3
			6.19	115.4
87.9			4.87	112
			4.93	113.5
			5.06	116.8
99.9			4.58	119
			4.64	120.8
			4.51	117
33.7	100	458	14.9	168.9
			15.3	175.1
			14.8	167.2
43.1			11.9	158.3
			11.9	157.1
			11.9	157.1
51.8			10.3	157.1
			10.10	153.5
			10.10	153.5
59.9			8.83	150.8
			8.83	150.8
			8.59	145.9
65.7			-	-
			-	-
			-	-
69.4			7.74	149.2

Re_z	RPM	Ta	Co x 10^5 gm/cc	Sh
69.4	100	458	7.87	152.1
			7.74	149.2
87.9			5.84	136.9
			6.10	143.8
			5.84	136.9
99.9			5.22	137.4
			5.41	143
			5.31	140

Appendix 3

Principle of Construction of Figure 4.1. A Chart to Estimate the Oxygenation Area Required for a Coaxial Cylinders Oxygenator when the Parameters Ta, b, and Ro are Specified.

Supposing that the equation to be solved by the designer is of the form

$$Y = K.\ X_1^{\ a}\ X_2^{\ b}\ .....X_n^{\ z}$$

where a, b, ... z are all <1, and K is a constant.

Therefore, if the value of K is plotted on the logarithmic scale of a semi-log paper, and starting from this point on that scale representing K, a logarithmic scale of X_1, inclined to the main log scale by an angle whose cosine is a, can be drawn. From the terminus of this line, another logarithmic scale representing the range of X_2 can be drawn at an angle whose cosine is b to the main logarithmic scale, and so on.

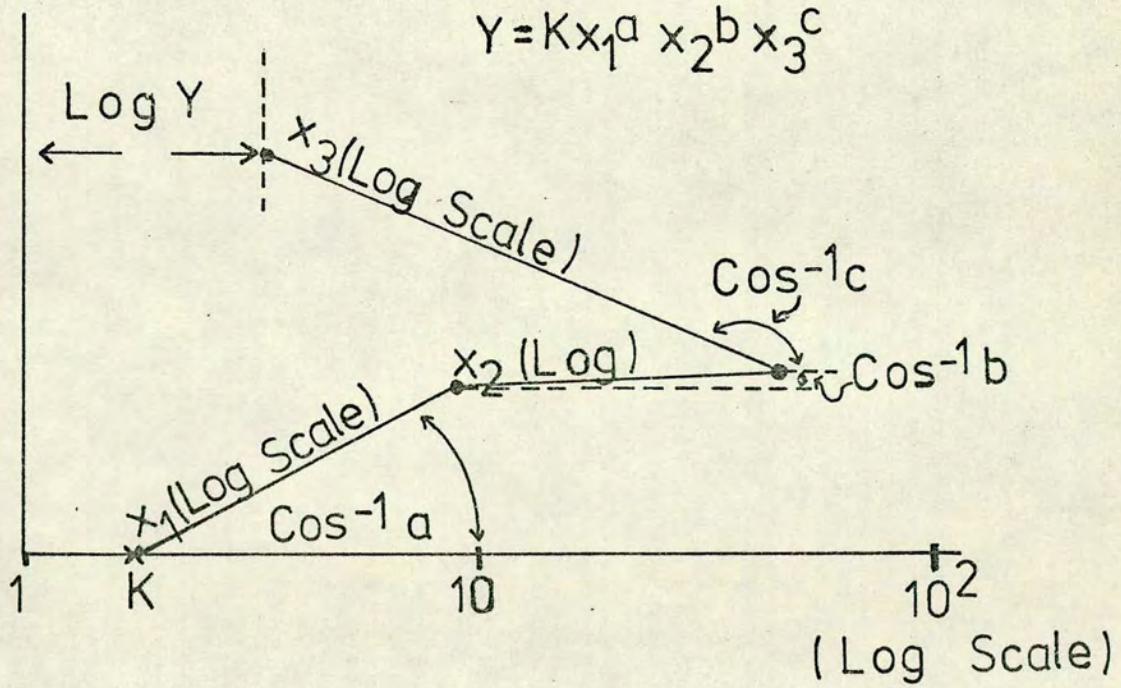

The distance from the terminus of the final line in the chain to 1 on the logarithmic scale, then represents Y on the main logarithmic scale.

Example:

The main design equation for the coaxial cylinders oxygenator is:

3.1) $$Sh = \frac{h_D 2b}{D_{AB}} = .128\ Ta^{.7}\ Sc^{.356}\left(b/_{Ro}\right)^{-.05}$$

3.2) and $$A = \frac{Q}{h_D}\ \ln 6,$$

3.3) then $$A = \frac{Q\ 2b(\ln 6)}{D_{AB}(1.28\ Ta^{.7}\ Sc^{.356}(b/_{Ro})^{-.05})}$$

Where $Q = 16.66$ cc/sec

$u = .0291$ poise

$\rho = 1.05$ gm/cc

$D_{AB} = 1.08 \times 10^{-5}$ cm^2/sec.

3.3) then becomes

3.4) $$A = 2.77 \times 10^{6}\ Ta^{-.7}\ b^{1.05}\ Ro^{-.05},$$

which is in the form

$$Y = KX_1^{a}X_2^{b}X_3^{c}$$

since the cosine of an angle cannot be greater than 1, assume that the power of b is 1 instead of 1.05.

K is then equal to 2.77×10^6; from this point, a line 10^4 log scale units, representing the Ta range from 1 to 10,000, is drawn at an angle whose cosine is .7 or $\simeq 45^{o}$.

From its terminus, a line representing Ro = 1-20 cm in log scale units, is drawn at an angle $\cos^{-1}(.05) \simeq 87^{o}$. A line parallel to the main log scale ($\cos^{-1}(1) = 0$) is then drawn for b, with a log scale from .1 to 1 cm.

To find the required mass transfer area for an oxygenator operating at Ta = 3000, with an outer radius Ro = 6 cm and an annular gap b = .5 cm, the distances on the main log scale, between b = .1 and .5, Ro = 1 and 6, and Ta = 10,000 and 3000, are measured adding the combined distances to the distance between the terminal point of the chain and 1, as measured on the main log scale; the resulting value on this scale is the mass transfer area A in cm^2, in this case 5800 cm^2.

Appendix 4

4.1 Physical Properties of O_2-Water Systems

T^oC	Viscosity(poise)	Density(gm/cc)
17	0.010828	.9989
18	0.010559	.998
19	0.010299	.9986
20	0.010050	.9984

T^oC	Diffusivity(cm^2/sec)	Solubility of O_2 in Water at 760 mm Hg
17	2.05×10^{-5}	46.075 (ppm)
18	2.12×10^{-5}	45.125
19	2.19×10^{-5}	44.65
20	2.26×10^{-5}	43.70

T^oC	Sc
17	472
18	448
19	434
20	419

4.2 Physical Data for a .4M Sucrose-Water Solution

Viscosity Data: Measured with an Ostwald viscometer.

Tap water at 20°C, Average of 8 readings - 8 sec

.4M sucrose solution at 20°C, average of 8 readings - 12.1 sec

The viscosity of tap water at 20°C is .010050 poise

∴ the viscosity of a .4M sucrose solution at 20°C is ≃ .0152 poise

The viscosity of 20% wt. sucrose solution (.584M) = .0197 poise (138)

Density Data: % wt sucrose at 20°C ρ (gm/cc)

13	-	1.050
14	-	1.054
extrapolating 13.68 (.4M)	-	1.053

Diffusivity:

$$\frac{D_{AB}\mu}{T} = \text{constant}$$

for water at 20°C $D_{AB} = 2.26 \times 10^{-5} cm^2/sec$

$$\frac{D_{AB}\mu}{T} = 7.78 \times 10^{-10}$$

Therefore for a .4M sucrose solution at 20°C

$$D_{AB} = \frac{7.78 \times 10^{-10}(293)}{.0152} = 1.49 \times 10^{-5} cm^2/sec$$

Solubility of O_2 in .4M Sucrose-Water Solution: The solubility of O_2 in a .4M sucrose solution was measured by bubbling air through a solution contained in a beaker, and recording the concentration of oxygen in the solution near equilibrium. The oxygen meters used in the mass transfer experiments (Beckman Fieldlab^R Oxygen Analyzer, EIL Oxygen Meter) were also used here.

Measured Values:

Solubility of O_2 in water at 20°C - 9.2 ppm at 161 mm Hg

Solubility of O_2 in .4M sucrose solution at 20°C

8 ppm at 161 mm Hg

$\therefore$ Solubility of O_2 in a .4M sucrose solution at 20°C and 760 mm Hg is 38 ppm

$$\therefore \quad \frac{\alpha\ O_2 \text{.sucrose}}{\alpha\ O_2\ \text{water}} = .874$$

Solubility of O_2 in a .4M sucrose solution at 15°C and 760 mm Hg - 42.4 ppm (138)

$$\therefore \quad \frac{\alpha\ O_2\ \text{sucrose}}{\alpha\ O_2\ \text{water}} = .875$$

Schmidt Number for O_2-.4M Sucrose-Water Solution System

$$\frac{\mu}{\rho D_{AB}} = \frac{.0152}{1.053\ (1.49 \times 10^{-5})} = 969$$

4.3 Physical Data for Concentrated Sugar Solution

Viscosity Data:

Tap water at 17°C, average of 8 measurements

= 15.9 sec

$\therefore$ Viscosity of sucrose solution at 17°C =

$$\frac{15.9}{8} \times .010828 = .0215 \text{ poise}$$

Diffusivity Data:

Diffusion coefficient at 17°C for O_2-H_2O system 2.05×10^{-5} cm^2/sec

$$\frac{D_{AB}\mu}{T} = \text{constant} = 7.54 \times 10^{-10}$$

for the concentrated sucrose solution

$$D_{AB} = 7.54 \times 10^{-10}\ (290)/_{.0215} = 1.01 \times 10^{-5} cm^2/sec$$

Solubility Data

Eight separate readings were taken in Oxygen-saturated sucrose solutions at 17°C

Measured values - 8.3 ± .15 PPM at 157 mm Hg or 8.44 ± .15 PPM at 760 mm Hg

Solubility of Oxygen in the concentrated sucrose solution at 17°C and 160 mm Hg - 40.09 ± .7 PPM

Density of Concentrated Sucrose (.21 wt %) = 1.085 (138)

Schmidt Number of O_2-Concentrated Sucrose Solution System

$$Sc = \frac{\mu}{D_{AB}} \quad \frac{.0215}{1.085\ (1.01 \times 10^{-5})} = 1962$$

4.4 Sample Calculation Using the Experimental Mass Transfer Data

Given: 1) T in = 17°C

T out = 17°C — Measured

Q = 970 cc/min — experimentally

C_i = 1.358 PPM

C_o = 18.9 PPM

RPM = 346.9

2) R_i = 5.85 cm

R_o = 6.45 cm — Measured with Calipers before The experiment

b = .6 cm

A = 748.07 cm^2

3) μ = .010828 poise at 17°

ρ = .9989 gm/cc^3 at 17°

D_{AB} = 2.05 x 10^{-5} cm^2/sec at 17°

C_s = 45.54 PPM at 751.25 mm Hg and 17°C

Obtained from the literature or measured in the case of the sucrose-water solutions

then $V_\phi = RPM\ (2\pi R_i)/60 = 212.4$ cm/sec

and $Ta = \frac{V_\phi b \rho}{\mu} \sqrt{b/R_o} = 3586$

The mass transfer coefficient then becomes

$$h_D = \frac{Q}{A} \left(\ln \frac{C_s - C_i}{C_s - C_o} \right)$$

and $Sh = \frac{h_D 2b}{D_{AB}} = 606$

Finally the axial Reynolds number is

$$Rez = \frac{Q\ 2b\ \rho}{60\pi(R_o^2 - R_i^2)\mu} = 77.2$$

4.5

Experimental Data

Oxygenation of Tap Water

Area (cm^2)	Atmospheric Pressure (mm Hg)	RPM	H_2O Flow (cc/min)	T in (^oC)	T out (^oC)	O_2 in (PPM)	O_2 out (PPM)	Sc	Re_z	Ta	Sh
748.07	751.25	346.9	970	17	17	1.358	18.9	471.3	77.23	3586	606
"	"	346.9	970	"	"	1.30	18.9	"	77.23	3586	573
"	"	438	950	"	"	1.04	18.6	"	75.64	4528	555
"	"	549.7	950	"	"	1.02	19.8	"	75.64	5682	606
"	"	346.9	940	"	"	.99	16.5	"	74.84	3585	468
"	"	438	940	"	"	.99	18.5	"	74.84	4528	546
"	"	549.7	940	"	"	.99	18.3	"	74.84	5682	538
"	774.90	346.9	1020	20	20	.47	13.7	419.4	87.45	3861	405
"	"	417.4	1010	"	"	.457	14.0	"	86.6	4646	412.7
"	"	438	990	"	"	.457	14.7	"	84.88	4876	430.1
"	"	496.8	990	"	"	.457	13.7	"	84.88	5530	396
"	"	558.6	990	"	"	.508	15.5	"	84.88	6217	458.8

Area (cm^2)	Atmospheric Pressure (mm Hg)	RPM	H_2O Flow (cc/min)	T in (^oC)	T out (^oC)	O_2 in (PPM)	O_2 out (PPM)	Sc	Re_z	Ta	Sh
748.07	774.90	602.6	970	20	20	.417	15.2	419.4	83.2	6708	440.6
"	"	679	980	"	"	.589	17.8	"	84	7559	542.6
"	"	923	980	"	"	.529	25.5	"	84	10275	914
"	"	346	1030	"	"	.518	13.0	"	88.3	3861	382.4
"	"	388	1030	"	"	.518	13.8	"	88.3	4319	411.8
"	"	441	1030	"	"	.508	14.4	"	88.3	4908	434.4
"	"	496.8	1030	"	"	.508	15.0	"	88.3	5530	457.5
"	"	555.3	1020	"	"	.508	15.8	"	87.5	6181	484.2
"	"	629.1	1020	"	"	.508	16.4	"	87.4	7003	508.2
"	"	693.8	1020	"	"	.406	17.5	"	87.4	7723	556.4
"	"	926	1020	"	"	.406	25.5	"	87.4	10308	954.6
"	"	346.9	1020	"	"	.427	13.5	"	87.4	3861	399.2
"	"	388	1020	"	"	.427	14.0	"	87.4	4319	416.6
"	"	443.9	1010	"	"	.416	14.7	"	86.6	4941	439.9

Area (cm^2)	Atmospheric Pressure (mm Hg)	RPM	H_2O Flow (cc/min)	T in (°C)	T out (°C)	O_2 in (PPM)	O_2 out (PPM)	Sc	Re_z	Ta	Sh
748.07	774.90	496.8	1010	20	20	.416	15.5	419.4	86.6	5530	470.4
"	"	555.6	1000	"	"	.416	15.5	"	85.7	6185	465.7
"	"	629.1	1000	"	"	.416	15.8	"	85.7	7003	477.3
"	"	705.5	1000	"	"	.416	17.5	"	85.7	7854	545.2
"	"	926	1000	"	"	.416	23.5	"	85.7	10308	825
"	"	349.8	990	"	"	.416	14	"	84.8	3870	4055
"	"	443.9	990	"	"	.416	15.2	419.4	84.88	4941	449.7
"	"	496.8	990	"	"	.416	15.7	"	84.88	5529	468.7
"	"	496.8	990	"	"	.427	15.8	"	84.88	5529	472.3
"	"	555.6	990	"	"	.406	16	"	84.88	6185	480.5
"	"	629.1	990	"	"	.406	16.2	"	84.88	7003	488.23
"	"	705.5	990	"	"	.406	17.4	"	84.88	7690	534.9
"	"	926	990	"	"	.406	21.5	"	84.88	10308	716.4
"	"	352.8	1040	"	"	.762	13.1	"	89.2	3910	383.3
"	"	388	1020	"	"	.783	13.7	"	87.5	4320	397.3

Area (cm^2)	Atmospheric Pressure (mm Hg)	RPM	H_2O Flow (cc/min)	T in (°C)	T out (°C)	O_2 in (PPM)	O_2 out (PPM)	Sc	Re_z	Ta	Sh
748.07	774.90	438.	1020	20	20	.711	14.0	419.4	87.5	4876	410.3
"	"	496.8	1010	"	"	.711	14.8	"	86.6	5530	436
"	"	558.6	1010	"	"	.691	15.8	"	86.6	6218	475
"	"	349.9	990	"	"	.508	12.5	"	84.9	3894	366.7
"	"	393.9	980	"	"	.508	13.3	"	84	4385	374.5
"	"	440.9	980	"	"	.508	14.4	"	84	4908	414.6
"	"	496.8	970	"	"	.498	15.0	"	83.2	5530	431.3
"	"	569.7	980	"	"	.437	16.2	"	84	6341	482.5
"	"	617.3	970	"	"	.508	18.8	"	83.2	6872	579.8
"	"	955.4	960	"	"	.630	24.5	"	82.3	10635	838.3
"	750.45	343.9	1010	"	"	.545	12.5	"	86.6	3829	370.5
"	"	388	1030	"	"	.524	13	"	88.3	4319	397.3
"	"	440.9	1020	"	"	.524	13.6	"	87.5	4909	416.3
"	"	502.4	1020	"	"	.514	14.2	"	87.5	5592	449
"	"	569.6	1020	"	"	.494	15.2	"	87.5	6342	480.4

Area (cm^2)	Atmospheric Pressure (mm Hg)	RPM	H_2O Flow (cc/min)	T in (°C)	T out (°C)	O_2 in (PPM)	O_2 out (PPM)	Sc	Re_z	Ta	Sh
636.39	759.6	346.9	1060	20	20	.829	11.2	419.4	90.9	3861	384.7
"	"	382.2	1040	"	"	.622	11.3	"	89.2	4254	388.3
"	"	440.9	1030	"	"	.622	11.9	"	86.6	4908	401.8
"	"	493.9	1010	"	"	.622	12.3	"	86.6	5498	418.5
"	"	558.6	1010	"	"	.601	12.6	"	86.6	6217	431.9
"	"	617.3	1010	"	"	.622	14.4	"	86.6	6871	510.2
"	"	676.2	990	"	"	.539	14.2	"	84.9	7526	493.7
"	"	1029	950	"	"	.778	21.5	"	81.4	11453	821
636.4	"	1111.2	970	"	"	.829	29	"	83.2	12370	1361
"	"	349.8	960	"	"	.466	12.7	"	82.3	3894	418.5
"	"	385.1	950	"	"	.435	12.6	"	81.5	4287	411
"	"	443.9	1100	"	"	.435	13.1	"	94.3	4942	499.3
"	"	496.8	1150	"	"	.622	12.6	"	98.6	5530	492
"	"	552.7	1130	"	"	.622	13.3	"	96.9	6152	516.2
"	"	620.3	1130	"	"	.726	14.3	"	96.9	6905	562.2

Area (cm^2)	Atmospheric Pressure (mm Hg)	RPM	H_2O Flow (cc/min)	T in (^oC)	T out (^oC)	O_2 in (PPM)	O_2 out (PPM)	Sc	Re_z	Ta	Sh
636.4	759.6	682	1130	20	20	.622	14.4	419.4	96.9	7592	570.8
"	"	1017.2	1130	"	"	.829	17	"	96.9	11323	702
"	"	346.8	1140	"	"	.580	11	"	96.9	3861	409.6
"	"	382.2	1120	"	"	.601	11.8	"	96	4254	441.6
"	"	440.9	1100	"	"	.591	12.3	"	94.3	4909	456.9
"	"	496.8	1100	"	"	.591	13.4	"	94.3	5530	508.3
"	"	569.6	1100	"	"	.591	13.4	"	94.3	6342	508.3
"	"	617.3	1100	"	"	.622	14.3	"	94.3	6871	550.7
"	"	687.9	1090	"	"	.612	14.4	"	93.5	7657	550.9
"	"	1029	1090	"	"	.726	16.2	"	93.5	11453	638
"	"	341	1080	"	"	.425	11.2	"	92.6	3796	405.3
"	"	1096.5	1130	"	"	.850	22.3	"	96.9	12205	1028.6
"	"	-	-	-	-	-	-	-	-	-	-
"	769.65	341	1060	20	20	.532	12.2	"	90.1	3796	430.9
"	"	376.8	1060	"	"	.552	12.7	"	90.1	4189	452.1

Area (cm^2)	Atmospheric Pressure (mm Hg)	RPM	H_2O Flow (cc/min)	T in (°C)	T out (°C)	O_2 in (PPM)	O_2 out (PPM)	Sc	Re_z	Ta	Sh
636.4	769.65	435	1050	20	20	.573	13.5	419.4	90	4843	482.5
"	"	496	1040	"	"	.583	14.6	"	89.2	5530	527.2
"	"	598.7	1020	"	"	.430	14.3	"	87.5	6664	508.3
"	"	602.6	1010	"	"	.450	14.6	"	86.6	6709	516
"	"	670.3	1010	"	"	.450	14.9	"	86.6	7461	529.5
"	"	1014.3	950	"	"	.665	18.8	"	81.4	11289	669.3
"	"	1117.1	980	"	"	.716	26	"	84	12435	1116
"	"	341	1030	"	"	.481	12.1	"	88.3	3796	416.1
"	"	388	1040	"	"	.522	12.8	"	89.2	4319	448.9
"	"	443.9	1030	"	"	.511	13.4	"		4942	471
"	"	497	1030	"	"	.542	13.7	419.4	88.3	5530	483
"	"	555	1020	"	"	.481	14.2	"	87.5	6185	502.3
"	"	608.5	1020	"	"	.522	14.7	"	87.5	6774	523.4
"	"	690	1010	"	"	.532	15.5	"	86.6	7690	554.3
"	"	999.5	1020	"	"	.594	16.4	"	87.5	11126	600.4
"	"	1117	1000	"	"	.644	25.5	"	87	12434	1127

Area (cm^2)	Atmospheric Pressure (mm Hg)	RPM	H_2O Flow (cc/min)	T in (°C)	T out (°C)	O_2 in (PPM)	O_2 out (PPM)	Sc	Re_z	Ta	Sh
636.4	769.65	340.4	940	20	20	.563	12.2	419.4	80.6	3789	381.3
"	"	379.2	980	"	"	.563	13.2	"	84	4222	438.2
"	"	440.9	980	"	"	.460	14.1	"	84	4909	479
"	"	499.8	980	"	"	.409	14.4	"	84	5563	493.3
"	"	564	980	"	"	.409	14.6	"	84	6283	502
"	"	623	970	"	"	.409	14.8	"	83.2	6937	506
"	"	676	960	"	"	.409	15.2	"	82.3	7526	517
"	"	1017	960	"	"	.614	23.5	"	82.3	11322	935
"	"	339	500	"	"	.204	18.4	"	43	3781	349
"	"	388	500	"	"	.194	18.5	"	43	4320	352
"	"	441	500	"	"	.184	18.4	419.4	43	4909	350
"	"	496.8	500	"	"	.204	19.5	"	43	5530	377
"	"	430.5	1950	"	"	1.33	8.6	"	167.2	4792	473
"	"	397.5	1940	"	"	1.23	8.2	"	166	4425	449

Area (cm^2)	Atmospheric Pressure (mm Hg)	RPM	H_2O Flow (cc/min)	T in (°C)	T out (°C)	O_2 in (PPM)	O_2 out (PPM)	Sc	Re_z	Ta	Sh
636.39	769.65	426	1940	20	20	1.26	9.3	419.4	166	4745	526
"	"	500	1850	"	"	1.23	9.5	"	159	5563	517
"	"	559	1930	"	"	1.26	9.8	"	166	6217	560
"	"	617	1930	"	"	1.28	11.2	"	166	6872	663
"	"	690	1940	"	"	1.24	11.8	"	168	7690	717
"	"	1014	1940	"	"	1.330	12.6	"	168	11290	774
"	"	1300	1940	"	"	1.433	16.9	"	168	14470	1139
"	750.15	88.2	1000	18	18	.602	6.3	464	81.6	934	190.9
"	"	112.5	1000	"	"	.591	7.1	"	81.6	1191	220.3
"	"	139.3	1000	"	"	.550	8.2	"	81.6	1475	262.6
"	"	176.4	980	"	"	.575	9.0	"	79.9	1868	287.5
"	"	220.5	970	"	"	.510	9.7	"	79.1	2335	312.2
636.4	"	264.6	1020	"	"	.510	10.7	"	83.2	2802	369
"	"	323.4	1010	"	"	.510	11.7	"	82.4	3425	407
"	"	393.9	1010	"	"	.510	12.8	"	82.4	4172	454.3

Area (cm^2)	Atmospheric Pressure (mm Hg)	RPM	H_2O Flow (cc/min)	T in (^oC)	T out (^oC)	O_2 in (PPM)	O_2 out (PPM)	Sc	Re_z	Ta	Sh
"	"	88.2	990	18	18	.510	6.6	464	80.7	934	202.6
"	"	114.6	980	"	"	.489	7.4	"	79.9	1214	229.9
"	"	143.2	980	"	"	.459	8.1	"	79.9	1517	256.4
"	"	176.4	980	"	"	.428	9.0	"	79.9	1868	291
"	"	217.2	980	"	"	.428	10.3	"	79.9	2300	341.2
"	"	264.6	950	"	"	.408	11.4	"	77.5	2802	374
"	"	323.4	950	"	"	.408	12.4	"	77.5	3425	414
"	"	396.9	940	"	"	.398	13.3	"	76.7	4203	446.6
"	"	485	940	"	"	.398	15.3	"	76.7	5137	532
"	"	89.3	1050	"	"	.398	6.3	"	85.6	946	207.2
"	"	113.9	1030	"	"	.489	7.4	"	84	1207	241.6
"	"	141.1	1030	"	"	.418	7.9	"	84	1494	263
"	"	176	1030	"	"	.40	8.7	"	84	1868	294.9
"	"	214.7	1030	"	"	.40	9.8	"	84	2274	339
"	"	264.6	1020	"	"	.40	10.8	"	84	2802	380.4

Area (cm^2)	Atmospheric Pressure (mm Hg)	RPM	H_2O Flow (cc/min)	T in (°C)	T out (°C)	O_2 in (PPM)	O_2 out (PPM)	Sc	Re_z	Ta	Sh
636.4	750.15	323.4	1020	18	18	.398	11.9	464	83	3425	423.2
"	"	393.9	1010	"	"	.398	13.1	"	82.4	4172	471
"	"	481.8	1010	"	"	.398	15.9	"	82.4	5102	600.4
"	"	89.3	980	"	"	.388	6.5	"	79.9	946	200.7
"	"	109.3	970	"	"	.377	7.4	"	79.1	1157	231
"	"	140.1	960	"	"	.357	8.4	"	78.3	1484	265.2
"	"	176.4	950	"	"	.357	9.3	"	77.5	1868	295.3
"	"	217.4	950	"	"	.326	10.4	"	77.5	2303	337.6
"	"	264.6	950	"	"	.326	11.4	"	77.5	2802	376.4
"	"	323.4	950	"	"	.326	12.4	"	77.5	3425	416.4
"	"	393.6	940	"	"	.326	13.6	"	76.7	4168	461.2
"	"	476.2	930	"	"	.316	16.2	"	75.9	5043	568.7
"	"	88.2	1050	"	"	.388	6.5	"	85.6	934	215
"	"	111	1040	"	"	.388	7.1	"	84.8	1176	235.7

Area (cm^2)	Atmospheric Pressure (mm Hg)	RPM	H_2O Flow (cc/min)	T in (^oC)	T out (^oC)	O_2 in (PPM)	O_2 out (PPM)	Sc	Re_z	Ta	Sh
636.4	750.15	141.9	1040	18	18	.388	7.9	464	84.8	1503	266.6
"	"	176.4	1040	"	"	.388	8.6	"	84.8	1868	294.2
"	"	217.6	1040	"	"	.388	9.8	"	84.8	2304	342.7
"	"	264.6	1040	"	"	.388	10.7	"	84.8	2802	380.2
"	"	323.3	1030	"	"	.388	12	"	84	3425	432.2
"	"	393.6	1030	"	"	.388	13.2	"	84	4168	485.2
"	"	88.2	2150	"	"	1.02	4.4	"	175.4	934	238.9
"	"	113.5	2150	"	"	1.02	4.8	"	175.4	2102	268.6
"	"	141.8	2150	"	"	1.02	5.2	"	175.4	1501	298.5
"	"	176.4	2150	"	"	1.02	5.7	"	175.4	1868	
"	"	220.5	2150	"	"	1.02	6.2	"	175.4	2335	374.6
"	"	264.6	2150	"	"	1.02	6.7	"	175.4	2802	413.4
"	"	323.4	2150	"	"	1.02	7.5	"	175.4	3425	476.5
"	"	396.9	2150	"	"	1.02	8.3	"	175.4	4203	541
"	"	88.2	480	"	"	.306	10.9	"	39.2	934	180.6
"	"	111.7	470	"	"	.326	12.2	"	38.4	1183	202

Area (cm^2)	Atmospheric Pressure (mm Hg)	RPM	H_2O Flow (cc/min)	T in (^oC)	T out (^oC)	O_2 in (PPM)	O_2 out (PPM)	Sc	Re_z	Ta	Sh
636.4	750.15	141.1	470	18	18	.326	13.2	464	38.4	1494	222.3
"	"	176.4	"	"	"	.306	14.4	464	38.3	1868	247.8
"	"	217.5	"	"	"	.306	15.7	464	38.3	2303	276.4
"	"	264.6	"	"	"	.357	17.3	464	38.3	2802	312.3
"	"	323.4	"	"	"	.387	18.4	464	38.3	3425	338.5
"	"	387.	"	"	"	.408	19.9	464	38.3	4099	376.3
"	766.4		1080	"	"	.646	-	"			
"	"		1060	"	"	-	-	"			
"	"	41.5	1020	"	"	.546	4.9	"	83.2	439	142.8
"	"	52.9	1030	"	"	.547	5.3	"	84	560	158.2
"	"	64.7	1030	"	"	.556	5.6	"	84	685	168.5
"	"	77.9	1030	"	"	.546	6.1	"	84	825	186.7
"	"	94	1020	"	"	.527	6.6	"	83.2	996	203.4
"	"	111.7	1020	"	"	.527	7.1	"	83.2	1183	221.5
"	"	138.2	1020	"	"	.516	7.7	"	83.2	1464	243.9

Area (cm^2)	Atmospheric Pressure (mm Hg)	RPM	H_2O Flow (cc/min)	T in (^oC)	T out (^oC)	O_2 in (PPM)	O_2 out (PPM)	Sc	Re_z	Ta	Sh
636.4	766.4	25.9	1010	18	18	.497	3.9	464	82.4	275	109.2
"	"	30	1010	"	"	.497	4.4	"	82.4	339	125.9
"	"	41.1	1010	"	"	.497	4.8	"	82.4	436	139.5
"	"	52.9	990	"	"	.487	5.2	"	80.7	560	150.5
"	"	64.7	990	"	"	.477	5.7	"	80.7	685	167.8
"	"	76.6	990	"	"	.457	6.1	"	80.7	811.2	182.1
"	"	94	980	"	"	.457	6.7	"	79.9	996.3	220.9
"	"	114.6	980	"	"	.457	7.3	"	79.9	1214	221.9
"	"	138.2	980	"	"	.457	7.8	"	79.9	1463	239.7
"	"	25.9	970	"	"	.427	4.0	"	79.1	275	110.1
"	"	31.8	970	"	"	.407	4.5	"	79.1	337	126.9
"	"	41.6	970	"	"	.407	4.9	"	79.1	441	139.9
"	"	52.9	970	"	"	.407	5.3	"	79.1	560.4	153.1
"	"	64.7	970	"	"	.397	5.7	"	79.1	685	166.8
"	"	76.4	970	"	"	.397	6.2	"	79.1	809	183.6

Area (cm^2)	Atmospheric Pressure (mm Hg)	RPM	H_2O Flow (cc/min)	T in (^oC)	T out (^oC)	O_2 in (PPM)	O_2 out (PPM)	Sc	Re_z	Ta	Sh
636.4	766.4	94	970	18	18	.387	6.7	464	79.1	996	201
"	"	114.6	970	"	"	.378	7.3	"	79.1	1214	222
"	"	141.1	960	"	"	.348	8.0	"	78.3	1494	245
"	"	25.96	1020	"	"	.348	3.9	"	83.2	275	114.9
"	"	33.97	1020	"	"	.318	4.3	"	83.2	360	129.3
"	"	41.97	1020	"	"	.308	4.6	"	83.2	445	139.9
"	"	51.9	1020	"	"	.300	5.1	"	83.2	550	157.4
"	"	64.7	1010	"	"	.300	5.5	"	82.4	685	169.7
"	"	77.9	1010	"	"	.288	6.05	"	82.4	805	189.3
"	"	95.5	1010	"	"	.288	6.5	"	82.4	1012	205.2
"	"	115	1010	"	"	.288	7.1	"	82.4	1214	226.7
"	"	138.2	1000	"	"	.278	7.7	"	81.6	1463	246.4
"	"	26.9	990	"	"	.268	3.8	"	80.8	285	110.6
"	"	33.9	990	"	"	.268	4.25	"	80.8	360	125.4
"	"	41.9	990	"	"	.258	4.7	"	80.8	445	140.7

Area (cm^2)	Atmospheric Pressure (mm Hg)	RPM	H_2O Flow (cc/min)	T in (^oC)	T out (^oC)	O_2 in (PPM)	O_2 out (PPM)	Sc	Re_z	Ta	Sh
636:4	766.4	52.9	990	18	18	.258	5.05	464	80.8	560	152
"	"	61.7	980	"	"	.249	5.65	"	79.9	654	171.2
"	"	77.9	980	"	"	.249	6.1	"	79.9	825	186.5
"	"	94	950	"	"	.249	6.7	"	77.5	996	200.8
"	"	114.6	980	"	"	.238	7.3	"	79.9	1214	228.7
"	"	135.2	970	"	"	.238	7.9	"	79.9	1432	247.2
"	"	25.9	2010	"	"	.905	2.9	"	163.9	275	126.4
"	"	31.8	2010	"	"	.894	3.1	"	163.9	3373	140
"	"	41.97	2010	"	"	.897	3.4	"	163.96	445	159.8
"	"	51.4	2010	"	"	.894	3.6	"	163.9	545	172.9
"	"	64.7	2010	"	"	.894	3.8	"	163.9	685	186.1
"	"	77.9	2010	"	"	.894	4.1	"	163.9	825	206
"	"	94	2000	"	"	.894	4.4	"	163.9	996	225
"	"	114.7	2000	"	"	.894	4.7	"	163.9	1214	245.2

Area (cm^2)	Atmospheric Pressure (mm Hg)	RPM	H_2O Flow (cc/min)	T in (°C)	T out (°C)	O_2 in (PPM)	O_2 out (PPM)	Sc	Re_z	Ta	Sh
636.4	766.4	135.4	2000	18	18	.894	5.1	464	163.9	1434	272
"	"	25.97	500	"	"	.099	6.56	"	40.8	275	105.5
"	"	32	500	"	"	.079	7.2	"	40.8	339	117
"	"	41.9	500	"	"	.079	7.8	"	40.8	445	128
"	"	49.97	470	"	"	.079	9.0	"	38.3	529	141.2
"	"	64.7	490	"	"	.079	9.9	"	39.97	685	164
"	"	77.9	480	"	"	.069	10.6	"	39.2	825	173.9
"	"	97	480	"	"	.079	11.9	"	39.2	1027	198.8
"	"	114.7	480	"	"	.079	12.8	"	39.2	1214	216.7
"	"	139.6	500	"	"	.069	13.8	"	48.8	1479	247
"	777.8	0	1020	"	"	.493	1.75	"	83.2	0	39.13
"	"	0	460	"	"	.493	1.7	"	37.5	0	16.93
"	"	0	2030	"	"	.997	2.1	"	165.6	0	69
"	"	0	970	"	"	.346	1.5	"	79.1	0	34

4.6 Experimental Results

Oxygenation of .4M Sucrose Solution

Area (cm^2)	Atmospheric Pressure (mm Hg)	RPM	H_2O Flow (cc/min)	T in (^oC)	T out (^oC)	O_2 in (PPM)	O_2 out (PPM)	Sc	Re_z	Ta	Sh
636.4	766.15	88	1020	20	20	1.785	6.9	969	60.9	685	326
"	"	141	1020	"	"	1.656	7.4	"	61	881	366
"	"	114	1020	"	"	1.507	7.9	"	61	1095	411
"	"	176	1020	"	"	1.408	8.4	"	61	1369	452
"	"	215	1020	"	"	1.388	9.4	"	61	1666	526
"	"	265	1020	"	"	1.309	9.9	"	61	2054	568
"	"	323	1020	"	"	1.339	10.9	"	61	2510	643
"	"	391	1020	"	"	1.378	11.5	"	61	3034	689
"	"	479	1020	"	"	1.488	12.8	"	61	3720	789
"	"	88	1020	"	"	1.448	6.5	"	61	684	317
"	"	113	1020	"	"	1.388	6.9	"	61	881	348
"	"	141	1000	"	"	1.279	7.6	"	59.8	1095	396

Area (cm^2)	Atmospheric Pressure (mm Hg)	RPM	H_2O Flow (cc/min)	T in (^oC)	T out (^oC)	O_2 in (PPM)	O_2 out (PPM)	Sc	Re_z	Ta	Sh
636.4	766.15	176	1020	20	20	1.19	8.5	969	61	1369	472
"	"	218	"	"	"	1.19	9.5	"	"	1689	575
"	"	265	"	"	"	1.19	10.3	"	"	2054	606
"	"	324	"	"	"	1.21	11.3	"	"	2510	683
"	"	396	"	"	"	1.279	12.4	"	"	3081	768
"	"	479	"	"	"	1.399	13.6	"	"	3720	863
"	775.6	25.9	"	"	"	1.146	4.2	"	"	202	180
"	"	33	"	"	"	.970	4.4	"	"	256	205
"	"	41.2	"	"	"	.793	4.8	"	"	319	240
"	"	51.7	"	"	"	.872	5.1	"	"	402	254
"	"	61.7	"	"	"	.882	5.6	"	"	479	286
"	"	76.4	"	"	"	.882	6.0	"	"	593	312
"	"	97	"	"	"	.882	6.4	"	"	753	338
"	"	115	"	"	"	.892	6.8	"	"	890	365
"	"	138	"	"	"	.901	7.6	"	"	1073	419
"	"	26	"	"	"	.931	7.0	"	"	202	182

Area (cm^2)	Atmospheric Pressure (mm Hg)	RPM	H_2O Flow (cc/min)	T in (^oC)	T out (^oC)	O_2 in (PPM)	O_2 out (PPM)	Sc	Re_z	Ta	Sh
636.4	775.6	32	1020	20	20	.882	4.4	969	61	248	210
"	"	40	"	"	"	.833	4.8	"	"	311	238
"	"	52	"	"	"	.804	5.1	"	"	402	258
"	"	62	"	"	"	.813	5.6	"	"	479	290
"	"	76	"	"	"	.823	6.1	"	"	593	322
"	"	96	"	"	"	.823	6.5	"	"	742	349
"	"	112	"	"	"	.853	7.0	"	"	867	380
"	"	26	"	"	"	.882	4.0	"	"	202	185
"	"	32	"	"	"	.833	4.4	"	"	248	212
"	"	41.2	"	"	"	.804	4.7	"	"	319	233
"	"	51.7	"	"	"	.804	5.1	"	"	402	258
"	"	61.7	"	"	"	.794	5.6	"	"	479	291
"	"	77.6	"	"	"	.784	6.0	"	"	602	318
"	"	94	"	"	"	.813	6.4	"	"	730	342
"	"	112	"	"	"	.882	7.1	"	"	867	386

4.7 Experimental Results

Oxygenation of Concentrated (21 wt %) Sucrose Solution

Area cm^2	Atmospheric Pressure (mm Hg)	RPM	H_2O Flow (cc/min)	T in (°C)	T out (°C)	O_2 in (PPM)	O_2 out (PPM)	Sc	Re_z	Ta	Sh
636.4	747	26	1090	17	17	.81	3.3	1962	47.4	147	227
"	"	32	1090	"	"	.80	3.6	"	47.5	181	257
"	"	43	1120	"	"	.72	3.7	"	48.8	240	281
"	"	52	1120	"	"	.71	3.9	"	48.8	293	301
"	"	62	1120	"	"	.72	4.1	"	48.8	349	320
"	"	76	1020	"	"	.69	4.5	"	44.4	432	330
"	"	94	1020	"	"	.67	4.9	"	44.4	532	369
"	"	114	1060	"	"	.71	5.2	"	46.2	641	409
"	"	138	1060	"	"	.75	5.6	"	46.2	781	444
"	"	26	1060	"	"	.82	3.4	"	46.2	147	229
"	"	33	1060	"	"	.71	3.6	"	46.2	187	257
"	"	42.3	1060	"	"	.68	3.8	"	46.2	239	278

Area (cm^2)	Atmospheric Pressure (mm Hg)	RPM	H_2O Flow (cc/min)	T in (^oC)	T out (^oC)	O_2 in (PPM)	O_2 out (PPM)	Sc	Re_z	Ta	Sh
636.4	747	51	1060	17	17	.65	4.0	1962	46.2	289	290
"	"	62	1070	"	"	.66	4.2	"	46.6	357	320
"	"	77	1070	"	"	.67	4.5	"	46.6	436	348
"	"	94.6	1040	"	"	.68	4.85	"	45.3	535	370
"	"	112	1030	"	"	.71	5.2	"	44.9	635	397
"	"	138	1030	"	"	.78	5.7	"	44.9	781	439
"	"	26	1040	"	"	.81	3.4	"	45.3	147	226
"	"	32	1040	"	"	.75	3.55	"	45.3	181	244
"	"	41.5	1040	"	"	.70	3.7	"	45.3	235	262
"	"	51.8	1060	"	"	.68	3.95	"	46.2	293	292
"	"	63	1060	"	"	.68	4.15	"	46.2	356	311
"	"	76	1060	"	"	.69	4.5	"	46.2	439	343
"	"	94	1060	"	"	.70	4.8	"	46.2	532	371
"	"	112	1070	"	"	.75	5.1	"	46.6	635	404
"	"	138	1070	"	"	.80	5.65	"	46.6	781	449

Area (cm^2)	Atmospheric Pressure (mm Hg)	RPM	H_2O Flow (cc/min)	T in (°C)	T out (°C)	O_2 in (PPM)	O_2 out (PPM)	Sc	Re_z	Ta	Sh
636.4	747	88	1020	17	17	1.0	5.0	1962	44.4	499	351
"	"	112	1020	"	"	1.0	5.45	"	44.4	632	393
"	"	141	1020	"	"	1.0	5.8	"	44.4	798	426
"	"	176	1050	"	"	1.0	6.3	"	44.4	997	474
"	"	220	1030	"	"	1.1	6.8	"	45.7	1262	529
"	"	265	1030	"	"	1.17	7.5	"	45	1496	583
"	"	323	1020	"	"	1.3	8.1	"	44.9	1829	633
"	"	394	1000	"	"	1.4	8.8	"	44.4	2228	691
"	"	476	1020	"	"	1.49	9.9	"	43.6	2693	784
"	760.4	88	1000	"	"	1.5	5.65	"	44.4	499	363
"	"	112	1000	"	"	1.34	5.85	"	43.6	632	374
"	"	144	1000	"	"	1.25	6.2	"	43.6	814	426
"	"	177	1000	"	"	1.21	6.55	"	43.6	997	462
"	"	220	1000	"	"	1.20	7.1	"	43.6	1247	514
"	"	270	1000	"	"	1.20	7.55	"	43.6	1529	557

Area (cm^2)	Atmospheric Pressure (mm Hg)	RPM	H_2O Flow (cc/min)	T in (^oC)	T out (^oC)	O_2 in (PPM)	O_2 out (PPM)	Sc	Re_z	Ta	Sh
636.4	760.7	323	1000	17	17	1.26	8.2	1962	43.6	1829	616
"	"	397	1000	"	"	1.40	8.8	"	43.6	2244	664
"	"	477	1000	"	"	1.50	9.7	"	43.6	2697	747
"	"	88	1020	"	"	1.65	5.6	"	44.4	498.7	346
"	"	118	1040	"	"	1.48	5.8	"	45.3	632	385
"	"	141	1040	"	"	1.31	6.1	"	45.3	798	429
"	"	176	1040	"	"	1.26	6.35	"	45.3	997	457
"	"	220	1040	"	"	1.22	6.8	"	45.3	1247	504
"	"	265	1040	"	"	1.22	7.3	"	45.3	1496	553
"	"	323	1040	"	"	1.25	8.0	"	45.3	1829	621
"	"	397	1060	"	"	1.40	8.7	"	46.2	2244	693
"	"	482	1060	"	"	1.52	9.7	"	46.2	2724	790
"	"	0	1060	"	"	1.1	2.55	"	46.2	0	126

4.8 Experimental Data for Transfer of Ethyl Salicylate from an Irregular Rotor into a Stream of Water.

ρ = .9988 gm/cc, μ = .01083 poise,

D_{AB} = 6.15 x 10^{-6} cm^2/sec, Cs = 2.48 x 10^{-4} gm/cc,

Sc = 1762 at 17°C. Height of "rib"/$_b$ = .28

Ri = 1.95 cm, Ro = 2.5 cm,

A = 551.6 cm^2, L = 45 cm,

RPM	T in (°C)	T out (°C)	Conc.gm ES/cc	Re_z	Ta	Sh
40	17	17	6.67	38	193	268
40	"	"	6.96	"	193	282
40	"	"	7.0	"	193	284
60	"	"	7.61	"	290	314
60	"	"	7.54	"	290	310
60	"	"	7.8	"	290	323
80	"	"	8.54	"	386	361
80	"	"	8.45	"	386	357
80	"	"	8.38	"	386	353
100	"	"	8.84	"	483	377
100	"	"	8.9	"	483	381
100	"	"	9.0	"	483	386
120	"	"	9.16	"	580	395
120	"	"	9.16	"	580	395
120	"	"	9.23	"	580	399

RPM	T in (^{o}C)	T out (^{o}C)	Conc.gm ES/cc	Re_z	Ta	Sh
50	17	17	6.67	38	241	268
50	"	"	6.61	"	241	265
50	"	"	6.74	"	241	271
70	"	"	7.45	"	338	306
70	"	"	7.9	"	338	328
70	"	"	7.74	"	338	320
90	"	"	8.1	"	435	339
90	"	"	8.23	"	435	345
90	"	"	8.25	"	435	346
110	"	"	8.58	"	532	364
110	"	"	8.68	"	532	369
110	"	"	8.68	"	532	369
150	"	"	9.22	"	725	398
150	"	"	9.16	"	725	395
150	"	"	9.16	"	725	395

4.9 Blood Experiments

4.9.1 Properties of Experimental Blood

Hematocrit - 40% ± 5%, normal value for cattle (15).

Hemolysis - Initial value - 40 mg %.

Several samples were thereafter collected at different points in the circuit; Max. concentration of hemoglobin in plasma - 98 mg %.

Blood O_2 capacity - gm Hb x 1.36.

∴ for 40% hematocrit blood, the concentration of hemoglobin is 11.5 gm/100 cc, and the O_2 capacity of blood is 15.64 cc O_2/100 cc.

The relative viscosity of ox blood is 4.6 (15); or at 17°C the viscosity of blood would be approximately .05 poise.

The specific gravity at 17°C is 1.05.

pH=6.8

4.9.2 Sample Calculation

Measured values: O_2 tension, inlet - 24.23 mm Hg.

O_2 tension, outlet - 27.26 mm Hg.

From the oxyhemoglobin dissociation curve the corresponding oxygen saturations are:

inlet - 47%

outlet - 53%

therefore OT cc/min m^2 $= \frac{Q}{A}\left(\frac{15.64 \text{ cc } O_2}{100 \text{ cc}}\right)(Co-Ci)$

$= \frac{300}{.06364}\left(\frac{15.64}{100}\right)(.53 - .47)$

$= 44.23$ cc O_2/min m^2.

4.9.3 Experimental Data

Fluid	Area (cm^2)	Atm.Pressure (mm Hg)	RPM	H_2O Flow (cc/min)	T in (^oC)	T out (^oC)	O_2 in (mm Hg)	% O_2 Sat.	O_2 out (mm Hg)	% O_2 Sat.	Sc	Re_z	Ta	Sh	OT (cc/min m^2)
Water	636.4	757.25	88.2	550	19	19	29.53	-	143.9	-	471	46	958	134	-
Water	"	"	126.5	550	19	19	22.7	-	155.23	-	471	46	1373	157	-
Water	"	"	176.4	550	19	19	21.2	-	165.8	-	471	46	1916	173	-
Water	"	"	264.6	550	18	18	18.93	-	186.3	-	499	45	2802	209	-
Water	"	"	88.2	550	18	18	16.66	-	136.3	-	499	45	934	144	-
Blood	"	"	88.2	300	17	17	24.23	47	27.26	53	4596	5.47	209	109.9	44.23
Water	"	"	126.5	440	"	"	51.5	-	174.2	-	528	35	1306	129	-
Blood	"	"	126.5	300	"	"	22.7	42	28.0	58	4596	5.47	299	295	117.96
Water	"	"	176.4	360	"	"	94.65	-	219.6	-	529	29	1823	115	-
Blood	"	"	176.4	300	"	"	22.7	42	30.3	60	4596	5.47	417	340	132.7
Water	"	"	264.6	350	"	"	66.63	-	249.9	-	529	28	2735	165	-
Blood	"	"	264.6	300	"	"	22.7	42	32.56	63	4596	5.47	626	411	154.83
Water	"	"	88.2	430	"	"	31.04	-	159	-	529	34	911	127	-
Blood	"	"	88.2	300	"	"	22.7	42	25.74	49	4596	5.47	208	209	51.61
Water	"	"	126.5	970	"	"	22.7	-	136.3	-	529	77	1307	251	-
Blood	"	"	126.5	300	"	"	22.7	42	27.26	53	4596	5.47	299	299	81.1
Water	"	"	176.4	620	"	"	83.3	-	166.6	-	528	49	1823	125	-
Blood	"	"	176.4	300	"	"	26.5	50	34.07	69	4596	5.47	417	437	140.1

References

1. Peirce, E.C.II — Trans.Asaio 15 33, 1969.

2. Lee, W.H., Jr.; Krumbaar, D.; Derry, G.; Sachs, D.; Laurence, S.H.; Clowes, J.H.; Maloney, J.V., — Surg.Forum 12 200, 1961.

3. Lee, W.H., Jr.; Krumbaar, D.; Fonkalsrud, E.W.; Maloney, J.V.; Schjeide, D.A., — Surgery 50 29, 1961.

4. Lee, W.H., Jr.; Hairston, P., — Fed.Proceedings 30 No.5 1615, Sept.-Oct. 1971.

5. Discussion — Fed.Proceedings 30 No.5 1621, Sept.-Oct. 1971.

6. Lyman, D.J.; Kim, S.W., — Fed.Proceedings 30 No.5 1658, Sept.-Oct. 1971

7. Falb, R.D.; Grode, G.A., — Fed.Proceedings 30 No.5, 1688, Sept.-Oct. 1971.

8. Baier, R.E.; Dutton, R.C., — J.Biomedical Mater.Res. 3 191, 1969.

9. Melrose, D.G. — Personal Communication.

10. Mountcastle, V.B. ed. — "Medical Physiology", Vol.1, C.V. Mosby Company, St.Louis, 1968.

11. Dow, P.; Hamilton, W.F., (eds) — "Handbook of Physiology" Section 2, Circulation 1. American Physiological Society, Washington D.C., 1962.

12. Dittmer, D.S.; Grebe, R.M., (eds) — "Handbook of Respiration", W.B. Saunders Company, Philadelphia 1958.

13. Ruch, T.C.; Patton, H.D., — "Physiology and Biophysics", 19th ed. W.B. Saunders Co. Philadelphia, 1966.

14. Galletti, P.M.; Brecher, G.A. — "Heart-Lung Bypass, Principles and Techniques of Extracorporeal Circulation", Grune & Stratton, New York, 1962.

15. Albritton, E.C., "Standard Values in Blood", W.B. Saunders Co, Philadelphia, 1952.

16. Madras, P.N., Morton, W.A., Pelschek, H.E., Fed.Proceedings, 30 No. 5 1665, Sept.-Oct. 1971.

17. Stormorken, H., Fed.Proceedings, 30 No.5 1551, Sept.-Oct. 1971.

18. Salzman, E.W., Fed.Proceedings, 30 No.5 1503, Sept.-Oct. 1971.

19. Blackshear, P.L., Jr., Dorman, F.D. Steinbach, J.H., Maybach, E.J., Singh, A., Collingham, R.E., Trans.Asaio 12 113, 1966.

20. Nevaril, C.G., Hellums, J.D., Alfrey, C.P., Lynch, E.C., AICHE Journal 15 707, 1969.

21. Croce, P.A., "Hemolysis of Erythrocytes in Laminar and Turbulent Shear Flows", Ph.D. Thesis, Washington Univ., 1972.

22. Leverett L.B. Hellums, J.D., Alfrey, C.P., Lynch, E.C., Biophysical J. 12 257, 1972.

23. Bernstein, E.F. Fed.Proceedings, 30 No.5 1510, Sept.-Oct. 1971.

24. Blackshear, P.L., Forstrom, R.J., Dorman, F.D., Voss, G.O., Fed.Proceedings, 30 No.5, 1600, Sept.-Oct. 1971.

25. Hochmut, R.N., Mohandas, N., Spaeth, E.E., Williamson, J.R., Blackshear, P.L., Johnson, D.W., Trans. Asaio 18 325, 1972.

26. Mason, R.G., Scarborough, D.E., Saba, S.R. Brinkhous, K.M., Ikenberry, L.D., Kearney, J.J., Clark, H.G., J.Biomedical Mat.Res. 3 615, 1969.

27. Gibbon, J.H. Jr., Arch.Surgery 34 1105, 1937.

28. Gibbon, J.H. Jr., Chairman's Address Trans.Asaio 1 158, 1955.

29. Ludwig, C., Schmidt, A., Leipzig Berichte 20 12, 1868.

30. Von Frey, M., Gruber, M., Virchow's Arch.f.Physiol. 9 519, 1885.

31. Jacobi, C., Arch.Exp.Path. (Leipzig) 31 330, 1895.

32. Brodie, T.G., J.Physiol. (London) 29 266, 1903.

33. Rygg, I.H., Kyusgaard, E., Acta Chir. Scand. 112 433, 1956.

34. Oxygenation Catalog, Travenol Laboratories, Deerfield, Ill., U.S.A.

35. Kay, E.B., Cross, F.S., Surg.Gynec.Obstet. 104 701, 1957.

36. Esmond, W.G., Cowley, R.A., Am.Surgeon 24 685, 1958.

37. Kolff, W.J., J. of Extracorporeal Technology 3 No.2 1969.

38. Marx, T.I., Snider, W.E., St. John, A.O., Moeller, C.E., J.App.Physiol. 15 1123, 1960.

39. Galletti, P.M., Richardson, P.D., Snider, M.T., Friedman, L.I., Trans. Asaio 18 359, 1972.

40. Clowes, G.H. Jr., Neville, W.E., Trans. Asaio 3 52, 1957.

41. Clowes, G.H. Jr., Neville, W.E., Sagba, G., Shibota, Y., Surgery 44 220, 1958.

42. Peirce, E.C. II, J.Thor.Cardiovasc.Surgery 39 438, 1960.

43. Gentsch, T.O., Boff, R.K., Siegel, J.H., Cev, M., Glenn, M.W., — Surgery 47 301, 1960.

44. Kolff, W.J., Eppler, D.B. Groves, L.K., Peereboom, G., Moraca, P.P., — Cleveland Clinical Quarterly 23 69, 1956a.

45. Hofstra, P.C., Crescenzi, A.A., Sudon, F., Cooper, P., — Trans.ASAIO 6 62, 1960.

46. Kylstra, J.A., Moulopoulos, S.D., Kolff, W.J., — Trans.ASAIO 7 355, 1961.

47. Kiil, F. Glover, J.F.Jr., — Trans.ASAIO 8 43, 1962.

48. Galletti, P.M. Hopf, M.A., Peirce, E.C. II, — Trans.ASAIO 8 47, 1962.

49. Day, S.W., Crystal, D.K., Wagner, C.L., Loreski, W.R., Kranz, J.M., — Trans.ASAIO 10 69, 1964.

50. Firme, C.N., Roland, A., Anthone, S., McNeill, A.E., — J.Thor.Cardiovasc.Surgery 40 253, 1960.

51. Crystal, P.K., Day, S.W., Wagner, C.L., Martinis, A.J., Owen, J.J., Walker, P.E.A., — Arch.Surgery 88 122, 1964.

52. Bodell, B.R., Head, J.M., Head, L.R., Formale, A.J., Head, J.R., — J.Thor.Cardiovasc.Surgery 46 639, 1963.

53. Zingg, W., Trans.ASAIO 13 334, 1967.

54. De Fillippi, R.P., Tompkins, F.C., Porter, J.H., Timmins, R.S., Buckley, M.J., Trans.ASAIO 14 236, 1968.

55. Gille, J.P. Trudell, L., Snider, M.T., Borsanyi, A.S., Galletti, P.M., Trans.ASAIO 16 365, 1970.

56. Dorson, W.Jr., Baker, E., Cohen, M.L., Meyer, B., Maltham, M., Trump. D., Elgas, R., Trans.ASAIO 15 155, 1969.

57. Dorson, W.Jr., Baker, E., Cohen, M.L., Meyer, B., Maltham, M., Trump, D., Trans.ASAIO 16 345, 1970.

58. Dutton, R.C., Mather, F.W., Walker, S.N., Lipps, B.J., Rudy, L.W., Severinghaus, J.W., Edmunds, L.H.Jr., Trans.ASAIO 17 331, 1971.

59. Dantowitz, P., Borsanyi, A.S., Deibert, M.C., Snider, M.T., Scherler, M., Lipsky, M.H., Galletti, P.M., Trans.ASAIO 15 138, 1969.

60. Rush, B.F. Jr., Boone, R., Mallette, W., Trans.ASAIO 15, 178 1969.

61. Marx, G.H., Trans.ASAIO 16 381, 1970.

62. Ratan, R.S., Bennett, G.F., Bollin, P.L., McAlpine, W.A., Selman, M.W., — J. of Thor. Cardiovasc.Surgery 53 519, 1967.

63. Galletti, P.M., — Fed.Proceedings 30 No.5 1491, Sept.-Oct. 1971.

64. Friedman, L.I., Richardson, P.D., Galletti, P.M., — Trans.ASAIO 17 369,1971.

65. Clevert, H.D., Mohnhaupt, R., Appelt, K., Wallener, F., Buchertl, E.S., — Trans.ASAIO 18 391, 1972.

66. Kolobow, T., Zapol, W., Sigman, R.L., — in "Blood Oxygenation", Ed. Daniel Hershey, Plenum Press, New York, 1970.

67. Frantz, S.L. Chopra, P., Goldenberg, A.L., Brown, L., Miller, F.M., Dennis, C., — Trans.ASAIO 14 233, 1968.

68. Bellhouse, B.J., Bellhouse, F.H., Curl, C.M., MacMillan, T.T., — Trans.ASAIO 19 72 1973.

69. Melrose, D.G., Burns, N.E., Singh, M.P., Elliot, P.L., Read, R., Williams, F.E., Becket, J., Lamb, M.P., Adams, J.S., — Biomed.Eng. 7 60, 1972.

70. Benn, J.A. Drinker, P.A., Mikic, B., Schutts, M.C., Lacava, E.J., Kopf, G.S., Bartlett, R.H., Hanson, E.L., — Trans.ASAIO 17 317, 1971.

71. Murphy, D.A., Morris, K., Martin, M., — Trans.ASAIO 17 337, 1971.

72. Lande, A.J., Das, S.J., Carlson, R.G., Perschau, R.A., Large, R.P., Sanstegaard, L.J., Lillehei, C.W., — Surg.Clin.North.Amer. 47 1461, 1967.

73. Lande, A.J., Parker, B., Subramanian, V., Carlson, R.G., Lillehei, C.W., — Trans.ASAIO 14 227, 1968.

74. Lande, A.J., Edwards, L., Bloch, J.H., Carlson, R.G., Subramanian, V., Ascheim, R.S., Scheidt, S., Fillmore, S., Killin, T. Lillehei, C.W. — Trans.ASAIO 16 352, 1970.

75. Bramson, M.L., Hill, J.D., Osborn, J.J., Tyson, W., Kahn, P., — Trans.ASAIO 18 395, 1972.

76. — GE DuaLung Data Sheets and Instruction Manual General Electric Company, Medical Division, Schenectady, New York, U.S.A.

77. Peirce, E.C.II, — Trans.ASAIO 16 358, 1970.

78. Spaeth, E.E., Ehmsen, R.J., — Trans.ASAIO 18 384, 1972.

79. Pitzele, S., Sze, S., Dobell, A.R.C., — Trans.ASAIO 18 375, 1972.

80. Melrose, D.G., Osborn, J.J., Bramson, M.L., Gerbode, F., — The Lancet 1050, May 17, 1958.

81. Galletti, P.M., Snider, M.T., Silbert-Aiden, D., — Med.Research Eng. 2nd Quarter 20, 1966.

82. Peirce, E.C.II, Dibelius, N.R., — Trans.ASAIO 14 220, 1968.

83. McCaughan, J.S., Weader, R., Schuder, J.C., Blakemore, W.S., — J. Thor.Cardiovasc.Surgery 40 574, 1960.

84. Lautier, A., Rey, P., Bizot, J., Faure, A., Sausse, A., Laurent, D., — Trans.ASAIO 15 144, 1969.

85. Lyman, D.J., Muir, W.M., Lee, I.J., — Trans.ASAIO 11 301, 1965.

86. Srinivasan, S., Sawyer, P.N., — Jour. of Colloid and Interface Science, 32 No.3 456, 1970.

87. Gott, V.L., Furuse, A., — Fed.Proceedings 30 No.5 1679, Sept.-Oct. 1971.

88. Bradley, S.A. Jr. — Trans.ASAIO 10 240, 1964.

89. Atsumi, K., Sakurai, Y., Atsumi, E., Narasauwa, S., Kunisawa, S., Okikura, M., Kimoto, S., — Trans.ASAIO 9 324, 1963.

90. Mirkovitch, V., Akutsu, T., Kolff, W.J., — Trans.ASAIO 8 79, 1962.

91. Spaeth, E.E. — in "Blood Oxygenation", p.276, ed. Daniel Hershey, Plenum Press, New York, 1970.

92. Buckles, R.G., Merrill, E.W., Gilliland, E.R., AIChE J. 14 703, 1968.

93. Weissman, M.H., Mockros, L.F., Jour. of the Eng.Mech.Div. 93(2) 225, 1967.

94. Villaroel, F., "Gas Transport to Blood Flowing in Semi-Permeable Tubes Under Steady and Pulsatile Flow Conditions", Ph.D. Thesis, University of Maryland, 1970.

95. Lautier, A., Grossin, R., Laurent, D., Trans.ASAIO 17 303, 1971.

96. Bennett, C.O., Myers, J.E., "Momentum, Heat and Mass Transfer", McGraw-Hill, New York, 1962.

97. Chang, H.K., Mockros, L.F., AIChE J. 17 397, 1971.

98. Lightfoot, E.N., AIChE J. 14 669, 1968.

99. Melrose, D.G. Personal Communication.

100. Alami, M.A., Ph.D. Thesis, in preparation, University of Edinburgh.

101. Sutera, S.P., Croce, P.A., Mehrjardi, M., Trans.ASAIO 18 335, 1972.

102. Trinkle, J.K., Surgery 68 1074, 1970.

103. West, F.B., Taylor, A.T., Chem.Eng.Progress 48 39, 1952.

104. Fagela-Alabastro, E.B., Hellums, J.D., AIChE J. 15 164, 1969.

105. Fagela-Alabastro, E.B., Hellums, J.D., AIChE J. 15 803, 1969.

106. Weissman, M.H., Mockros, L.F., Proc.ASCE, J. of the Eng.Mech.Dov. 94(1) 857, 1968.

107. Taylor, G.I., Phil.Trans.Roy.Soc. A223 289, 1923.

108.(a)	Flower, J.R., Macleod, N., Shahbenderian, A.P.,	Chem.Eng.Science 24 637,1969.
(b)	Flower, J.R., Macleod, N.,	Chem.Eng.Science 24 651, 1969.
109.	Kaye, J., Elgar, E.C.,	Trans.Am.Soc.Mech.Eng. 80 753, 1958.
110.	Flower, J.R.	"Fluid Flow and Transfer Processes in the Annulus Between Rotating Concentric Cylinders", Ph.D. Thesis, University of Edinburgh, 1963.
111.	Yamada, Y.,	Trans.JSME 27 610, 1961.
112.	Tachibana, F., Fukui, S., Mitsumura, S.,	Bull.JSME 3 119, 1960.
113.	Bjorklund, I.S., Kays, W.M.,	Trans.ASME 80c 70, 1958.
114.	Haas, F.C., Nissan, A.H.,	Proc.Roy.Soc. A261 215, 1961.
115.	Kuo, H.L.,	J.Fluid Mech.10 611, 1961.
116.	Jacob, M.,	"Heat Transfer" J.Wiley, New York, 1957.
117.	Becker, K.M., Kaye, J.,	Trans.ASME 84c 97, 1962.
118.	Yamada, Y.,	Bull JSME 5 302, 1962.
119.		"Vaporization Experiments in a Rotary Column" Shell Amsterdam, 9.1.1948.
120.	Eisenberg, M., Tobias, C.W., Wilke, C.R.,	Chem.Eng.Prgrs.Symposium Series, 51 No.16 1, 1955.
121.	Mawer, D.J., Wishart, A.F.,	B.Sc. Thesis University of Edinburgh, 1960.
122.	Macleod, N., Todd, R.B.,	Int. J. of Heat and Mass Transfer, 19 516, 1973.

123. Gibbs, H.D., Phil.J.Science, 3A 357, 1908.

124. Lundberg, R.E., McCuen, P.A., Reynolds, W.C., Int.J. of Heat and Mass Transfer 6 795, 1963.

125. Sherwood, T.K., Reid, R.C., "The Properties of Gases and Liquids, Their Estimation and Correlation", 2nd ed. McGraw-Hill, New York 1968.

126. Kapur, D.N., "The Profilometric Determination of Mass Transfer Coefficients by Holographic Interferometry", Ph.D.Thesis, University of Edinburgh, 1973.

127. Taylor, G.I., Proc.Roy.Soc. AI5I 494, 1935.

128. Prandtl, L., "The Essentials of Fluid Dynamics", Blackie & Son, Glasgow, 1957.

129. Donnelly, R.J., Simon, N.J., J.of Fluid Mech. 7 401, 1960.

130. Batchelor, G.K., Appendix to 129

131. Wendt, F., Inge.Arch. 4 577, 1933.

132. Macleod, N., Matterson, K.G., Chem.Eng.Science 10 254, 1959.

133. Information Manual, W.L. Gore Associates, Inc.Newark, Delaware, U.S.A.

134. Soyer, T., Lempinen, M., Cooper, P., Norton, L., Eiseman, B., Surgery 72 864, 1972.

135. "Application of Porous Polytetrafluoroethylene to Artificial Blood Vessels", First Report: Application to the Peripheral Artery, A Report to the 9th Japan Artificial Organs Conference (Sapporo, October, 1971).

136. Birnbaum, D., Eiseman, B., J.of Thor. and Cardiovasc,Surgery 64 443, 1972.

137. Harris, G.W., Tompkins, F.C., de Filippi, R.P., Porter, J.H., Buckley, M.J., in "Blood Oxygenation", ed. Daniel Hershey, Plenum Press, New York, 1970.

138. National Research Council, "International Critical Tables", McGraw-Hill Book Co., New York, 1926.

139. Sherwood, T.K., Ryan, J.M., Chem.Engng.Science, 11 81, 1959.

140. Gaylor, J.D.S., Murphy, J.F., Caprini, J.A., Zuckerman, L., Mockros, L.F., Trans. ASAIO, 19 516, 1973.

141. Hopf, G., Thesis, Harvard Medical School, 1970.

Chemical Engineering Science, 1975, Vol. 30, pp. 235–242. Pergamon Press. Printed in Great Britain

THE RADIAL TRANSFER OF MASS TO AN AXIAL STREAM OF LIQUID BETWEEN COAXIAL ROTATING CYLINDERS

N. MACLEOD and T. RUESS

Department of Chemical Engineering, University of Edinburgh, Edinburgh, Scotland

(*Received* 29 *May* 1974; *accepted* 5 *August* 1974)

Abstract—Measurements have been made of overall rates of mass transfer from the surfaces of a rotating cylinder and a surrounding stationary concentric tube to an axial stream of water in laminar + vortex flow in the long annular channel between them. The transfer process at the walls, characterised by a Schmidt number of about 1260, was the elution of ethyl salicylate from coatings of silicone rubber, applied to one or both surfaces, and initially swollen to equilibrium with the ester. The transfer rate was determined by spectrophotometric analysis of the effluent liquid. The physical data required for deriving absolute dimensionless transfer coefficients from these measurements were determined, and the limitations of the experimental technique were investigated.

The influence of rotor speed on transfer rate from either surface was found to be the same as that reported for transfer from rotating coaxial cylinders to a stagnant fluid at similar (high) Schmidt numbers, and significantly different from that found in our previous experiments with air at much lower Schmidt numbers (≈ 2). Axial flow rate had an insignificant effect over the range examined, as in the low Schmidt number case. The transfer rate at the outer stationary surface was significantly higher than that from the inner surface, and no evidence was found of any interaction between the two in simultaneous transfer.

These results are of practical interest in connection with the design of rotary coaxial cylinder blood oxygenators, in which the Schmidt number is of the same order as for this system.

INTRODUCTION

The present work extends to higher Schmidt numbers the investigations of Flower, Macleod and Shahbenderian [1, 2] on the rate of mass transfer to a fluid stream from the walls of an annular channel between an inner rotating cylinder and a stationary coaxial tube. In the flow situation studied both here and in the earlier experiments, laminar secondary vortex flow created by the rotation of the inner cylinder is superimposed on the laminar axial flow; and the annulus was long enough compared with its width to render end-effects insignificant.

In the previous work [1, 2], although the ranges of Ta and Re studied were fairly wide (0–2600, 200–8000 respectively), all the data were obtained with air as the experimental fluid, for Schmidt numbers extending only from 0·6 to 1·9. In connection with work in progress here and elsewhere on the development of a rotary coaxial cylinder oxygenator for blood [3], it was desired to estimate rates of physical transfer of oxygen from rotating coaxial cylindrical surfaces to blood plasma, a system for which $Sc \approx 2{,}000$. Direct measurement of such oxygen transfer rates, necessitating the provision of suitably permeable cylindrical surfaces, is inconvenient; on the other hand, the extrapolation of our previous data to a system having a Schmidt number three orders of magnitude greater would have been unjustifiable in the absence of any clear theoretical or experimental indication of the influence of molecular diffusivity on transfer rate in this system. The present experiments were therefore undertaken on the elution by a stream of water of ethyl salicylate absorbed in saturated surface-coatings of rubber, a system convenient for experimental measurement, for which $Sc = 1260$ at 20°C.

PRINCIPLES OF EXPERIMENTAL METHOD

The method used for determining the mass transfer coefficient to a liquid stream in these experiments is a novel modification of the shrinking plasticized polymer technique developed in this laboratory for the determination of mass transfer rates to air [4].

The surface of interest was coated with a permanent layer of insoluble elastomer which, at the commencement of each experiment, was swollen to equilibrium with a swelling agent sparingly soluble in water. Upon exposure of the prepared surface to the experimental stream of water, the swelling agent is eluted from the solid phase. The rate of elution may be determined from measurements of the concentration of swelling agent in the water leaving the apparatus at a known flow rate. If the swelling agent is suitably chosen, the effluent concentration is conveniently determined by ultraviolet spectrophotometry.

Under conditions which may in principle be predicted

and chosen by an extension of the theory given in [4], the activity of the swelling agent in the liquid layer immediately adjacent to, and in equilibrium with, the swollen coating surface remains within, say, 5 per cent of its initial value for a period of time sufficiently long to perform an experiment. Within this 'constant rate' period the rate of elution of the swelling agent remains sensibly constant if the flow rate is fixed. This elution rate per unit area of the interface may then be shown to be equal to the product of the concentration driving force within the water phase and the mass transfer coefficient effective over the area of transfer. The interfacial transfer area being known and the elution rate being known from measurements of the effluent composition and flow rate, the spatially averaged mass transfer coefficient can be found if the concentration driving force is known.

The concentration driving force initially, and effectively throughout the constant rate period, is equal to the solubility of the swelling agent at the experimental temperature, if the bulk concentration of the fluid stream is effectively zero and the coating is initially swollen to equilibrium; for the aqueous layer adjacent to the coating will then clearly be saturated with swelling agent if equilibrium prevails at the interface.

The constant rate period terminates when the coating has been so depleted that its surface composition corresponds to equilibrium with an aqueous solution having 95% the solute concentration at saturation. If the aqueous solution behaved ideally, in the sense that the concentration of the solute were proportional to its partial pressure, it would follow that the terminal composition of the surface of the (initially saturated) coating would be such that the vapour pressure is 95 per cent that of the pure swelling agent. This is also the condition of the swollen coating at the conclusion of the period of 'constant rate' transfer to a gas stream. The time taken to reach this state could thus be determined from the computed charts given in [4] when the mass flux from the coating, the composition of the coating at equilibrium swelling and the diffusivity of the swelling agent within the swollen polymer are known.

The constant rate period estimated by the methods of [4], which were designed for gaseous systems, will however be in error when the swelling agent/water system is not ideal. In particular, the true constant rate period will be shorter than the estimate if, as is generally to be expected, aqueous solutions of the esters used as swelling agents show positive deviations from Raoult's law; for in that case, the solute concentration at the interface will fall below 95 per cent saturation while its partial pressure is still within 5 per cent of that of the pure component. Nevertheless, in the absence of published equilibrium data for such solutions, the ideal solution estimate provides a useful rough guide for the choice of experimental conditions, as a preliminary to an experimental determination of the constant rate period.

It will be evident from the foregoing that the implementation of this method of determining liquid phase mass transfer coefficients requires knowledge of (a) the relationship between concentration of swelling agent in water and U.V. absorption of the solution, and (b) the solubility of swelling agent in water at experimental temperatures. To generalize the mass transfer results on a dimensionless basis, it is also necessary to know (c) the diffusivity of the swelling agent in the water used as the experimental fluid.

To estimate the duration of the 'constant rate' period under given experimental conditions it is further necessary to know (d) the degree of equilibrium swelling of the polymer film, and (e) the diffusivity of the swelling agent in the swollen coating. Finally, in the case of a liquid phase mass-transfer system for which the requisite vapour–liquid equilibrium data are not accurately known, it is necessary to check by direct measurement the estimated duration of the 'constant rate' period, the allowable time-span of an experiment.

EXPERIMENTAL

Apparatus

The outer cylinder of the experimental apparatus used to study mass transfer from one or both walls of an annular channel was a vertical glass tube 57 cm long and 5 cm i.d. with a water inlet at the lower end and an outlet at the top. The rotor was an aluminium alloy tube of 3·81 cm o.d. fitted with end plugs, of which that at the base was sealed to avoid inward seepage of fluid under the considerable external hydrostatic head. The driving shaft, integral with the top plug, was journalled in a ball race. It was driven through a flexible coupling from a coaxial pulley journalled in independent bearings, belt driven from a constant speed motor and variable gear. The lower plug of the rotor turned upon a 9 mm. stainless steel ball which engaged a central conical recess in the fixed brass pedestal which supported, centralized and closed the lower end of the glass tube.

The outer tube was supported and centralized at the upper end by means such that the rotor could be taken out for reactivation of the mass transferring coating leaving the glass tube in position.

The apparatus was mounted on a 15 cm wide steel column of channel section, set vertically and anchored to the roof structure and floor of the building to ensure rigidity and minimize vibration. Distilled water used as the experimental fluid was supplied from a head tank and reservoir. The water flow rate was measured with a rotameter, and its temperature was monitored with thermometers at the inlet and outlet of the experimental

annulus. The rotor speed was found by stopwatch timing of revolutions counted visually or mechanically.

Materials used

The mass transferring surface, which in these experiments was virtually the entire curved surface of one or both cylinders, was coated with Silcoloid 201 silicone rubber (ICI Ltd., Stevenston, Ayrshire). The surface was treated with the recommended primer and a solution of the rubber and curing agent, dissolved in toluene, applied either by spraying (in the case of the rotor, which was slowly turned in the lathe during this operation), or by rinsing the surface with a small quantity of the coating solution (in the case of the tube). The coatings thus obtained were $0{\cdot}04 \pm 0{\cdot}01$ cm thick. After curing, the coated cylinders were immersed in a bath of ethyl salicylate for approximately 1 hr, in which time equilibrium swelling was effectively attained.

The range of esters known to swell silicone rubber to a small extent, thereby avoiding excessive deformation of the polymer coating, was narrowed to methyl and ethyl salicylates in consideration of their low solubility in water, which is at the same time readily measureable by ultraviolet spectrophotometry. Ethyl salicylate was favoured because it appeared from previous observations that its stability in aqueous solutions is better than that of methyl salicylate.

Calibration of the spectrophotometric method of ethyl salicylate estimation

Aqueous solutions of known concentrations of ethyl salicylate, from 5–25 per cent of saturation, were prepared by weighing. Over this range the U.V. absorption at 262 nm was found to vary linearly with concentration within the limits of experimental error. The fifty sample points were all within ± 7 per cent of the absorption vs concentration line of best fit, with the majority of points clustered within ± 2 per cent of the line. Errors in weighing and handling the very small amounts of ethyl salicylate used and 'noise' in the spectrophotometer would account for these errors.

Determination of solubility of ethyl salicylate in water

In the absence of published solubility data the following method of measurement was used, developed in this laboratory by Dr. D. N. Kapur[8]. Discs of Silcoloid 201 rubber, swollen to equilibrium in a bath of ethyl salicylate, were weighed and placed in a sealed stirred flask containing a measured quantity of water and supported in a thermostat bath. After a suitable period the rubber discs were removed, dried with absorbent paper and weighed; the total weight loss corresponded to the ethyl salicylate transferred to the known volume of water.

The time required for a satisfactory approximation to equilibrium was determined by trial, as was the minimum number of discs for which the total weight loss was sensibly independent of the number of discs. These limits were then exceeded to ensure that the surface of the rubber remained virtually saturated throughout the experiment, in which the water then effectively attained a concentration corresponding to saturation with the pure ester.

Most values obtained fell within ± 7 per cent of the equilibrium concentration vs temperature curve best fitting the data (Fig. 1). This curve agrees well with solubility data for the same ester obtained independently by Kapur by the same method[8].

The major source of error was probably imperfect temperature control. The thermostat was found to have a maximum temperature variation of $\pm 0{\cdot}5$°C, sufficient to account for most of the data scatter. A further probable source of error was the difficulty of drying the disc surfaces thoroughly before weighing.

Subsequent experiments performed with methyl salicylate to test the reliability of the method gave results agreeing very closely with the solubility value $7{\cdot}7 \times 10^{-4}$ g/cm^3 at 30°C reported in the literature[5]—a most satisfactory verification of this technique.

Determination of diffusivity of ethyl salicylate in water

The diffusion coefficient of ethyl salicylate in water was determined from measurements of the rate of transfer of the ester to a laminar stream of water flowing through the stationary experimental annular channel with the inner wall transferring. Measured values of the effluent concentration at known flow rates and temperatures, together with the experimental values of the solubility obtained above, were substituted into an expression analogous to the analytical solution for the corresponding heat transfer system ([6], Case II).

The experimental diffusivity values thus obtained are

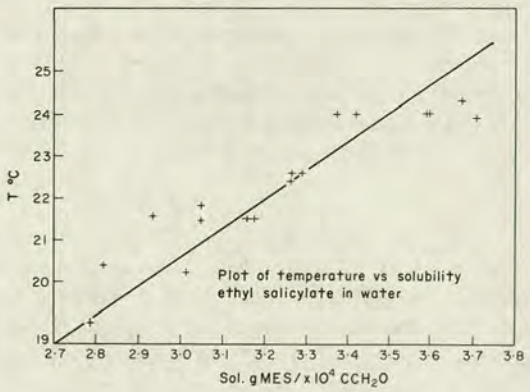

Fig. 1. Solubility results for ethyl salicylate in water as a function of temperature.

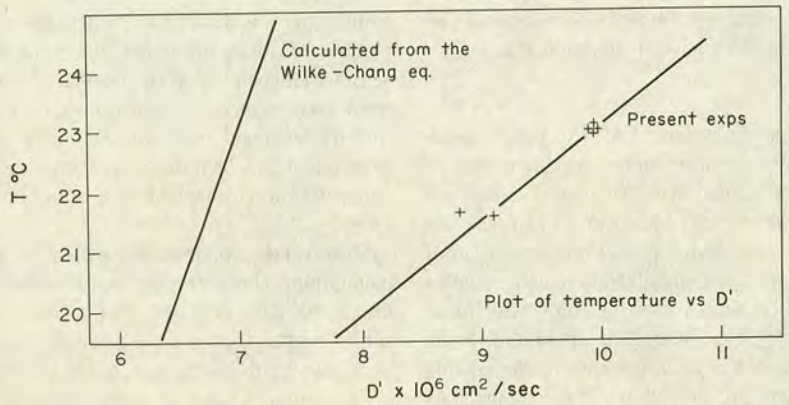

Fig. 2. Experimental and Wilke–Chang diffusivity values for ethyl salicylate in water as a function of temperature.

plotted as a function of temperature in Fig. 2, in which values estimated from the Wilke–Chang equation are also presented for comparison. The difference between the measurements and theoretical estimates is considerable (20–25 per cent), but not exceptional[7].

Errors in the determination of the solubility are reflected in the determination of the diffusion coefficient, as are errors in the measurement of the concentration of ester in the outlet stream. Assuming uncertainties of ±7 per cent in each of these factors, and assuming temperature variations and flow rate errors to be insignificant here, the maximum error in the dimensionless cup-mean concentration will be approximately ±8 per cent at these low concentrations of ester, giving a possible maximum error of ± 12 per cent in the diffusivity estimation. The consistency of the data suggests that random errors incurred are much smaller.

Determination of diffusivity of ethyl salicylate in polymer

This solid-phase diffusivity was found on the provisional assumption that it is not concentration dependent, by measuring the uptake of pure swelling agent by weighed polymer discs of known thickness as a function of time. The diffusion coefficient of ethyl salicylate in the silicone rubber was thus calculated as $1{\cdot}76\times 10^{-6}$ cm^2/sec ± 5 per cent. The diffusion coefficient adjusted to account for the increasing volume of the rubber samples as swelling progresses is;

$$D = D_{AB}(1-\phi)^{-3}$$

Where $\phi = U_s/1 - U_s$, the volume fraction of solvent penetrating the polymer. At equilibrium, ϕ was found to be 0·140 for the present polymer-solvent system. D has accordingly the value $2{\cdot}29\times 10^{-6}$ cm^2/sec.

Estimated constant rate period

χ for this system, calculated from the equilibrium value

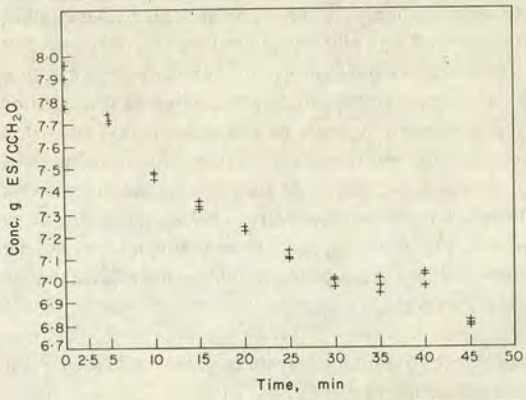

Fig. 3. Effluent concentration of ethyl salicylate as a function of time in a 'constant rate' period determination.

of ϕ using the Flory–Huggins equation, has the value 1·50. Using Figs 3 and 4a of Macleod and Todd[4], extended by Kapur[8] to cover the low values of f_1 and ϕ_E in this system, the maximum permissible fractional recession of the film, $\delta'/\delta_1 = 0{\cdot}016$ for the highest mass flux obtained in the mass transfer experiments, which was

$$F_s = kC_s = 3{\cdot}87\times 10^{-7}\ \text{g/cm}^2\ \text{sec}.$$

The allowable recession of the film, δ' is

$$(\delta'/\delta_1)\delta_1 = 6\times 10^{-4}\ \text{cm}.$$

and the 'constant rate' period t'

$$t' = \frac{\rho_R \delta'}{F_s} \approx 25\ \text{min}$$

EXPERIMENTAL RESULTS

Duration of constant rate period

The estimated 'constant rate' period was checked

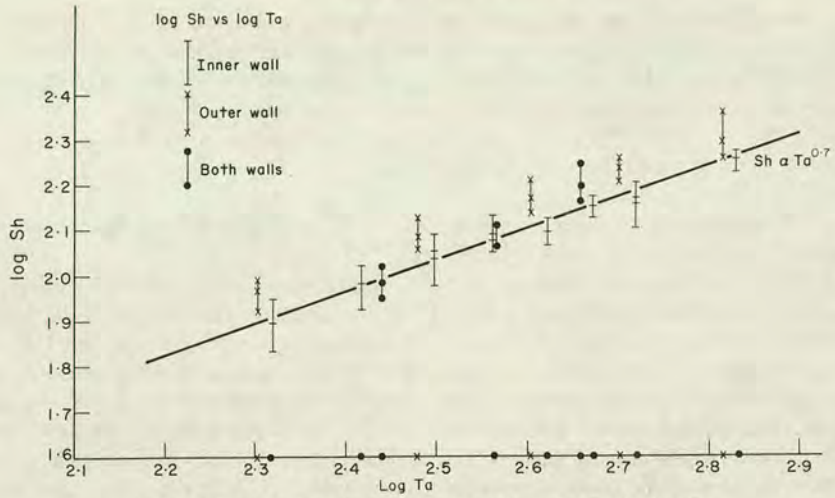

Fig. 4. *Sh* vs *Ta* for transfer from (a) inner (b) outer and (c) both walls.

experimentally for the maximum attainable transfer rate from the inner cylinder of the apparatus. The outlet concentration of ester, measured with the ultraviolet spectrophotometer, was determined at intervals so that the period for which it remained within 95 per cent of its initial value could be found. The experimental results are shown in Fig. 3. t' as given by the point where the outlet concentration is 95 per cent of the initial value was found to be approximately 9 min—approximately 1/3 the estimated period obtained from the calculations of the previous Section.

The large discrepancy between the calculated and experimental values of the constant rate period is most probably due, as explained above, to the non-ideality of the ethyl salicylate/water system. This solution might indeed be expected to show a positive deviation from Raoult's Law in view of the difference of polarity and degree of association of the components. At the end of the constant rate period as given by the computations of [4], the coating will be in equilibrium with an ethyl salicylate solution having a solute partial vapour pressure 95 per cent that of the pure ester. If the solution deviates positively from Raoult's law its concentration will then be less than 95 per cent of saturation, and the concentration driving force in the liquid phase will have fallen by more than 5 per cent. As a corollary, it follows that the 'constant rate' period for liquid phase transfer will in this case be less than that for gas phase transfer as estimated by the methods of [4].

Another source of error in the estimation of the 'constant rate' period is the uncertainty in the value of the diffusivity of the swelling agent in the rubber phase arising from the assumption of concentration-independence implicit in the method used in its determination. This is not likely to have been a major cause of the over-estimate of the 'constant rate' period, however. Inasmuch as the diffusivity of the ester in the polymer varies with composition, it probably increases with concentration; the concentration-averaged value obtained here would then lead to a low estimate of the 'constant rate' period, not to the exaggerated value observed.

All the results reported below were obtained within the actual measured 'constant rate' period following the commencement of transfer from a freshly swollen coating.

Effect of axial flow upon mass transfer rate

In the laminar + vortex regime, no significant influence of axial fluid velocity upon mass transfer rate could be detected over the range of variables investigated, either for transfer from the inner (moving) or the outer (stationary) wall of the annulus. The range of water flow rates used in these experiments was from 18 to 57 cm sec^{-1} corresponding to a Reynolds number range 33–100, for each of several rotor speeds in the range 40–130 rev/min, i.e. Taylor numbers in the range 209–680. Over the Reynolds number range examined, mass transfer measurements at a fixed rotor speed for various flow rates are irregularly scattered about their mean, and show no significant trend with Reynolds number.

A similarly weak, perhaps non-monotonic, influence of axial Reynolds number on wall transfer rate is reported in [1] for a rotating coaxial cylinder system operating at Schmidt numbers three orders of magnitude lower.

Variation of mass transfer rate with rotor speed

As no regular influence of axial fluid velocity on mass transfer rate was discernible in these laminar + vortex flow experiments, the effect of rotor speed on transfer coefficient was investigated by comparing mass transfer

results averaged irrespective of Reynolds number for each speed of rotation used. The results are presented in Fig. 4, plotted as Sh vs Ta for transfer from (a) the inner wall, (b) the outer wall and (c) both walls of the annular channel simultaneously.

The most notable features of these results, as disclosed by this plot, are:

1. The mass transfer coefficient at the outer cylinder is significantly higher than that at the inner cylinder throughout the Taylor number range examined.
2. The overall coefficient for simultaneous mass transfer from both walls of the annulus is intermediate between the coefficients at the inner and outer walls measured separately. There is thus no evidence in the present case of any significant interaction between the transfer processes at different walls of the channel, such as that suggested by certain features of the results for similar systems of much lower Schmidt numbers, discussed in [2].
3. The dependence of mass transfer rate upon rotor speed, apparently about the same for transfer from inner and outer annular surfaces, is significantly greater in this case than for the low Schmidt number systems investigated in [1]. The present results, obtained at high Schmidt number, do not follow the relation $Sh \propto Ta^{0.52}$ proposed in [1].

Our data for the inner cylinder are, on the other hand, consistent with the expression $Sh = 1{\cdot}91\ Ta^{0.7}$, which closely approximates (at the particular Sc and relatively small gap/radius ratio of our apparatus) to the correlation obtained by Eisenberg, Tobias and Wilke[9] for mass transfer at high Schmidt numbers from a rotating cylinder to a fluid contained in a stationary coaxial cylindrical outer vessel in the absence of axial flow, as discussed below.

DISCUSSION

Generalisation of results

The state of motion of a fluid flowing axially in a relatively narrow annulus ($0 < b/r_2 < 0{\cdot}4$) between a rotating inner cylinder and an outer fixed concentric tube, both being long in relation to the radius, is completely specified by the two dimensionless groups Ta and Re [1], at least if the flow is in the laminar + vortex regime, as in the present experiments. It follows that the concentration distribution, and hence the mass transfer behaviour, of flow systems of this kind is fully characterised by the three dinsionless groups Ta, Re and Sc, together with the wall flux conditions.

We may therefore write, for the laminar + vortex flow regime:

$$Sh = f(Ta, Re, Sc, \text{mass fluxes at boundaries}) \qquad (1)$$

This reasoning provides the justification for generalising the results of experiments in which only the rotor speed and the axial flow rate are varied in an apparatus of fixed dimensions by presenting them as plots of Sh vs Ta and Sh vs Re for constant specified Sc and wall-fluxes.

As (1) is not necessarily of such a functional type as to allow separation of the variables, such plots, obtained for given values of Sc and wall-flux, are not in principle necessarily of the same form for other values of these parameters. It now appears, from comparison of the present results with those reported in [1], that a large change of Sc (of three orders of magnitude) does not in fact significantly alter the (small) dependence of Sh on Re, but does on the other hand influence that of Sh on Ta.

Comparison with results for a stagnant fluid

The feeble dependence of mass-transfer coefficient upon axial flow rate observed here and in [1] suggests that the strong influence of rotor speed on the mass-transfer behaviour of this system would remain essentially the same in the limit where Re tends to zero; and hence, that the form of the Sh-Ta variation should be very similar to that found for a stagnant fluid between rotating coaxial cylinders for the same Sc and wall-flux conditions. The most extensive mass transfer results available for such a comparison are those obtained by Eisenberg, Tobias and Wilke[9] for rotating coaxial cylinder systems with no axial flow at Sc values similar to that of the present work. Unfortunately, only a few of their results were obtained at b/r_2 values sufficiently small to justify the use of Ta to characterise the state of the fluid motion. Furthermore, their wall-flux conditions were, in the narrow-gap experiments, anti-symmetric, in the sense defined in[2], whereas those of the present work were asymmetric (with one non-transferring wall) or symmetric (with both walls transferring to the stream). The comparison of the results of [9] with ours must therefore be made with caution.†

Eisenberg *et al.* correlated all their results by means of an expression substantially simpler than Eq. (1). For different cylinder dimensions, speeds of rotation and Schmidt numbers their mass transfer data fitted the expression.

$$\frac{k}{u} Sc^{0.644} = 0{\cdot}0791 \left(\frac{2\Omega r_1^2}{\nu} \right)^{-0.3} \qquad (2)$$

†The apparatus of [9] also differed from ours in that the cylinders were much shorter. However, the results of [9] for the smaller gap/radius ratios of interest here accord with those from similar experiments carried out in this laboratory using cylinders of greater length in relation to the annular gap[13]. At the smaller values of b/r_2, the cylinders used in [9] apparently behaved as 'long', therefore, and from this point of view it is legitimate to compare our system with this.
(Compare note below).

The choice of variables in Eq. (2) reflects their surprising finding that variation of the annular gap width over the range $0{\cdot}17 < b/r_2 < 0{\cdot}91$ has no significant influence on the mass transfer coefficient. Our correlation for $b/r_2 = 0{\cdot}238$ & $Sc = 1260$

$$\frac{k, 2b}{D'} \propto \left(\frac{\Omega r_1 b}{\nu}\sqrt{\left[\frac{b}{r_2}\right]}\right)^{0{\cdot}7} \tag{3}$$

gives

$$\frac{k}{u} \propto \left(\frac{\Omega r_1 b}{\nu}\right)^{-0{\cdot}3}\left(\frac{b}{r_2}\right)^{0{\cdot}35}$$

or

$$\frac{k}{u} \propto \left(\frac{2\Omega r_1^2}{\nu}\right)^{-0{\cdot}3}\left(\frac{r_1}{r_2}\right)^{0{\cdot}3}\left(\frac{b}{r_2}\right)^{0{\cdot}05} \tag{3a}$$

Equation (3a) yields the same dependence of mass transfer coefficient on rotor speed as Eq. (2) and likewise implies a relatively small influence of annular gap width on mass transfer coefficient over the b/r_2 range for which Eq. (1) is expected to hold. The smallest b/r_2 value used in [9] was 0·173; the largest for which the fluid motion is characterised by Ta as defined here is about $b/r_2 = 0{\cdot}4$. Over this range of b/r_2 variation, Eisenberg *et al*'s correlation, Eq. (2), gives no change in k for fixed r_1, whereas our correlation Eq. (3), predicts a change of about 6 per cent. Such a change would not have appeared significant in Eisenberg *et al.*'s experiments in view of the scatter of the data and the small number of measurements made by them in this range of b/r_2. Eq. (3) is thus consistent with the relevant experimental observations of Eisenberg *et al.* concerning the influence of the mechanical variables on k, but has the advantage over Eq. (2) (for relatively small gap widths) of consistency with the known dependence of the state of the fluid motion on the group Ta rather than on rotor Reynolds number alone.*

The close agreement between our results for transfer from a rotor contained in a stationary glass tube and the correlation of Eisenberg *et al.*, based largely on data for anti-symmetric wall-flux conditions different from ours, indicates that the mass flux situation at one boundary has little influence on the transfer rate at the other, at least in this high Schmidt number case. The insignificance of 'far boundary' effects here is borne out by the concordance of Eisenberg *et al.*'s electrochemical mass transfer measurements at rotating cylindrical electrodes (for which the wall-flux conditions were antisymmetric) with their determinations of the rate of solution of benzoic acid from rotating cylinders (where the situation was asymmetric, as in our experiments). The fact that the mass transfer rate in these high Sc systems is affected only by the situation in the immediate neighbourhood of the transferring surface is confirmed by our finding, on the basis of Fig. 4, that simultaneous transfers from the two walls of the annulus are additive.

Dissimilarity between mass and momentum transport

The independence of mass transfer effects at the walls of the annulus contrasts with the interdependence of the corresponding momentum fluxes, or wall shear stresses, necessitated (for steady motion) by Newton's Third Law. This law requires that, in the absence of axial flow, the torque on the inner and outer cylinders should be the same. In our axial flow system, inasmuch as the fluid enters the annulus with virtually zero angular momentum, the same principle ensures that the torque on the outer cylinder cannot exceed that on the rotor. As the radius and perimeter of the outer cylinder are greater than those of the rotor, it follows that the shear stress, or momentum flux, at the outer cylinder must be less than that at the rotor surface. Our results show, on the other hand, that the mass flux is greater at the outer than at the inner surface in the present system.

It therefore appears that there is no uniform relation between momentum and mass transfer rates at the different walls of the annulus in the present case. This suggests that momentum and mass are here transported by different mechanisms, a conclusion consistent with the different influences of rotor speed on torque and on mass transfer coefficient. There seems little doubt that angular momentum is transported in such systems, at least at high Taylor numbers, by a mechanism involving the secondary vortices in the fluid; and that this mechanism would lead to the observed variation of friction factor with $Ta^{-1/2}$ [10] and to the proportionality of Sh with $Ta^{1/2}$ observed in our low Sc experiments [1] but not found here. Accordingly, it seems reasonable to suppose that in the present high Sc system, on the other hand, the concentration boundary layer is too thin to be penetrated to a significant degree by the closed streamlines of the vortices spanning the greater part of the annulus width and effective as agents of momentum transfer.

CONCLUSIONS

The supposition that the concentration boundary layer might at the high Schmidt number values obtaining here be so thin as to lie effectively outside the vortical 'core' of

*These considerations, of course, in no way qualify or explain the success of Eq. (2) in correlating that (major) part of Eisenberg *et al.*'s data obtained at $b/r_2 > 0{\cdot}4$. For these large gaps the form of the dimensionless group corresponding to Ta, characterising the fluid motion, is as yet unknown. An additional unknown function of a further dimensionless group (e.g. b/r_2) would appear on the right hand side of Eq(1) in this case. It is also worth noting that, in their experiments with larger gaps, Eisenberg *et al.*'s annuli presumably cannot be considered long (as ours can) and that gap/length ratio variations may thus also have affected their results.

the annular stream is consistent with published measurements of velocity and temperature profiles in rotating coaxial cylinder systems[11], and is supported by the three salient features of Fig. 4 listed above. Thus: 1. Channel wall layers are in general more disturbed at concave than at convex surfaces[12], so that the higher transfer rate at the outer wall is to be expected if it is a boundary-layer process in the classical sense; 2. The non-interaction of the transfer processes at opposite walls is likewise consistent with their association with thin, independent boundary layers; 3. The effect of rotor speed on transfer rate, here supposedly reflecting the influence on boundary layer resistance, is likely to be different from the effects of increased vortex convection, which supposedly control the transfer of momentum and that of mass at low *Sc* [2].

From the practical standpoint of the designer of rotary coaxial cylinder blood oxygenators or other similar mass transfer equipment operating in the same *Sc* range, an important feature of these results is their close agreement with those of Eisenberg Tobias and Wilke for the case of zero axial flow. The latter workers established their correlation over a much wider range of the variables Ω, b/r_2 and *Sc* than we were able to examine; their results thus furnish a basis for extrapolating our results to apparatus configurations not directly covered by our measurements.

Acknowledgments—One of us (T.R.) was financially supported by an Edinburgh University Postgraduate Studentship during this research.

NOTATION

- b annular gap, cm
- C_s saturation concentration of ethyl salicylate in water, g/cm^3
- D diffusion coefficient of ester in the polymer coating adjusted to account for the increase in volume as swelling proceeds, cm^2/sec
- D_{AB} average diffusion coefficient in polymer, cm^2/sec
- D' diffusion coefficient of swelling agent in water, cm^2/sec
- k mass transfer coefficient, cm/sec
- F_s mass flux of swelling agent across polymer–fluid interface, g/cm^2 sec
- f_1 function of Φ *and* χ defined in [4]
- t' constant rate period, sec
- r_1 radius of inner cylinder, cm
- r_2 radius of outer cylinder, cm
- U_s volume ratio of ethyl salicylate to dry rubber
- u rotor surface velocity Ωr_1, cm/sec
- δ_1 initial coating thickness, cm
- δ' coating recession at the end of the 'constant rate' period, cm
- χ constant in Flory-Huggins equation, defined in [4]
- ν kinematic viscosity of experimental fluid, cm^2/sec
- ρ_R density of rubber phase, g/cm^3
- Φ volume fraction of swelling agent
- Φ_E equilibrium volume fraction of swelling agent
- Ω angular velocity of rotor, radians/sec
- *Re* axial Reynolds number
- *Sc* Schmidt number, $= \equiv \nu/D'$
- *Sh* Sherwood number $\equiv k.2b/D'$
- *Ta* Taylor number $\equiv (\Omega r_1 b/\nu)\sqrt{(b/r_2)}$

REFERENCES

[1] Flower J. R., Macleod N. and Shahbenderian A. P., *Chem. Engng Sci.* 1969 **24** 637.
[2] Flower J. R. and Macleod N., *Chem. Engng Sci.* 1969 **24** 651.
[3] Gaylor J. D. S., Murphy J. F., Caprini J. A., Luckerman L. and Mokros L. F., *Trans. Am. Soc. Art. Int. Organs* 1973 **19** 516.
[4] Macleod N. and Todd R. B., *Int. J. Heat and Mass Transfer* 1973 **19** 516.
[5] Gibbs H. D., *Phil. J. Sci.* 1908 **3A** 357.
[6] Lundberg R. E., McCuen P. A. and Reynolds W. C., *Int. J. Heat and Mass Transfer* 1963 **6** 795.
[7] Sherwood T. K. and Reid R. C., *The Properties of Gases and Liquids, Their Estimation and Correlation*, (2nd ed.) 1966 McGraw-Hill, New York.
[8] Kapur D. N., The Profilometric Determination of Mass Transfer Coefficients by Holographic Interferometry. Ph.D. Thesis, University of Edinburgh 1973.
[9] Eisenberg M., Tobias C. W. and Wilke C. R., *Chem. Engng Prog. Symp. Ser.* No. 16 1955 **51** 1.
[10] Batchelor G. R., *J. Fluid Mech.* 1960 **7** 401.
[11] Taylor G. I., *Proc. Roy. Soc.* 1935 **A151** 494.
[12] Prandtl L., *The Essentials of Fluid Dynamics* p. 132 1957. Blackie & Son, Glasgow.
[13] Mawer D. J. and Wishart A. F., Mass Transfer from Rotating Cylinders. Research Project Report, University of Edinburgh, (Department of Chemical Technology), 1960.